[Abstract]

Pareiasaurs were important medium- to large-sized herbivores in the Middle and Late Permian, some 268-252 million years (Myr) ago. They are best known from abundant remains of several taxa each in South Africa and Russia, with isolated finds from other parts of the world. Six genera and species of pareiasaurs have been described from China, and yet they have not been reviewed. Of these six, *Tsiyuania* may be a synonym of *Honania*, but this taxon is not further considered here. The other four, which were named for separate finds from the Sunjiagou Formation (Changhsingian, 254-252 Myr) show considerable similarities. Despite earlier suggestions, there are no convincing anatomical characters to distinguish *Shihtienfenia*, *Shansisaurus*, and *Huanghesaurus*, and these three genera are synonymised as *Shihtienfenia permica* Young & Yeh, 1963. The fourth taxon, *Sanchuansaurus pygmaeus* Gao, 1989, shows distinctly different teeth from those of *Huanghesaurus* (= *Shihtienfenia*), and was about one-third of the size, so it is retained as a second valid pareiasaur from the Chinese latest Permian. Phylogenetic analysis confirms the validity of these two taxa, with *Sanchuansaurus* belonging among the basal forms, and *Shihtienfenia* being a member of the derived clades Velosauria and Therischia, part of the new clade Sinopareiasauria, sister to the derived Elginiidae and *Scutosaurus*.

ADDITIONAL KEYWORDS: Permian, amniotes, Parareptilia, Changhsingian, Sunjiagou Formation.

INTRODUCTION

Pareiasaurs were a significant and unusual clade of Middle and Late Permian parareptiles, having been key herbivores in many faunas. In certain locations in the Russian and South African Permo-Triassic, pareiasaurs were the dominant animals, representing for example at the upper Middle Permian (upper Capitanian) site of Kotel'nich in Russia some 52% of all tetrapod skeletons recovered (Benton *et al.* 2012). They flourished from the Wordian to Changhsingian, but died out during the Permo-Triassic mass extinction. Pareiasaurs are best known from the Middle and Late Permian of South Africa (Lee *et al.* 1997) and Russia (Lee 2000; Tsuji 2013), with several forms reported from China (Young & Yeh 1963; Gao 1983, 1989; Li & Liu 2013; Xu *et al*. 2015), and isolated taxa from Morocco (Jalil & Janvier 2005), Niger (Tsuji *et al*. 2013), Brazil (Araújo 1985), Germany (Tsuji & Müller 2008), and Scotland (Newton 1893). Pareiasaurs ranged in size from little more than 1 m to 3 m in body length, and the larger animals were massively constructed and perhaps weighed a tonne in life. These massive, sprawling herbivores, with bony armour plates in their skin, were probably preyed on by sabre-toothed gorgonopsians, but otherwise presumably had few predators. Although interpreted as largely aquatic by some authors, finds of fossil footprints, and the taphonomy of their burial, suggests a primarily terrestrial lifestyle (Benton *et al.* 2012), a suggestion confirmed by stable isotope studies of pareiasaur teeth and bones (Canoville *et al*. 2014).

An unusual aspect of pareiasaurs is that they were identified as an outgroup, even the sister group, of turtles by Lee (1993, 1995, 1996, 1997), based on their shared characters of a rigid covering of dermal armour over the entire dorsal region, expanded flattened ribs, a cylindrical scapula blade, great reduction in humeral torsion (to 25°), a greatly developed trochanter major, an offset femoral head, and a reduced cnemial crest of the tibia. This was disputed by other morphological phylogenetic analyses (e.g. Rieppel & deBraga 1996; deBraga & Rieppel 1997; Rieppel & Reisz 1999; Li *et al.* 2009) that indicated a pairing of turtles and lepidosauromorphs among the diapsids, and by molecular phylogenetic studies of modern reptiles that repeatedly placed turtles among the Diapsida, and the Archosauromorpha in particular (e.g. Hedges and Poling 1999; Field *et al*. 2014). New finds of the Triassic proto-turtles *Pappochelys* and *Odontochelys* show close links to the Middle Permian *Eunotosaurus*, and turtles are confirmed as archosauromorphs on the basis of fossil and molecular data, and not related to pareiasaurs (Joyce 2015; Schoch and Sues 2015).

Pareiasaurs have been reported from the Late Permian of China in several papers, with six genera and species so far named from two geological formations, the Shihezhi Formation of Henan Province (*Honania complicidentata*, *Tsiyuania simpicidentata*), and the Sunjiagou Formation of Shanxi Province (*Shihtienfenia permica*, *Shansisaurus xuecunensis*, *Huanghesaurus liulinensis*, *Sanchuansaurus pygmaeus*). The aims of this paper are to present comprehensive descriptions of all the Chinese pareiasaurs so far described, to determine the likely validity of the various named taxa, and to consider their phylogenetic position in comparison with pareiasaurs from other parts of the world. A final aim is to review their stratigraphic occurrences, and compare these with pareiasaurs from elsewhere in the world.

INSTITUTIONAL ABBREVIATIONS

CAGS, Chinese Academy of Geological Sciences, Beijing, China; IVPP, Institute of Vertebrate Paleontology and Paleoanthropology, Beijing, China.

GEOGRAPHIC AND STRATIGRAPHIC DISTRIBUTION OF THE CHINESE PAREIASAURS

The localities for the Shihezi Formation pareiasaurs from Henan are described by Liu *et al*. (2014) and Xu *et al*. (2015), and so will not be further discussed. The Sunjiagou Formation pareiasaurs come from two sections along the banks of the Yellow River (Huanghe) and its tributary, the Sanchuan River (Fig. 1), namely Baode and Liulin Counties, parts respectively of Xinzhou City and Lüliang Prefectures, in the Province of Shanxi, to the west of Beijing, China.

The type material of *Shihtienfenia permica* Young & Yeh, 1963 came from the 'Upper Permian from the vicinity of Lishenglen, Paote, N. W. Shansi, near the banks of the Huangho (= Yellow) River'. In modern pinyin transliteration of the Chinese characters, these latter names become Baode, Shanxi, and Huanghe. The stratigraphic section, including the find spot of the fossils (Young & Yeh 1963: fig. 1), extends from Baode to Huayuan, 'along the south bank of the Huangho'. The place name 'Lishenglen' cannot be found on Google-Maps, but Baode is located in Baode County, near Xinzhou City, on the east bank of Huanghe, at coordinates 39.032N, 111.114E (Fig. 1).

The other three Shanxi pareiasaurs are from Liulin County, near Xuecunzhen (= Xuecun town). *Shansisaurus xuecunensis* is from Tianjialing village, near Xuecun (Cheng 1980: 115), and *Sanchuansaurus pygmaeus* and the other pareiasaur bones reported by Gao (1989: 1234) are also 'from a locality near Tianjialing village, Liulin County'. The find site of *Huanghesaurus liulinensis* seemed less clear from Gao's (1983) description, but Li and Liu (2013: 199–200) state that it was from the same location. It turns out that Tianjialing village no longer exists – it was a former habitation of the Tian family (Tianjialing means 'Tian family hill'), located at coordinates 37.410N, 110.811E, but the fossil site (37.412757N, 110.815922E), as confirmed by Li and Liu (2013: 200), lies at the top of the cliff on the south bank of the Sanchuan River, opposite the G307 road, east of the bridge leading to Beigou village, and to the west of the G20 expressway bridge that crosses the Sanchuan valley, and just above a water tank for Beigou village, which carries the label 'Tianjialing' (as noted during fieldwork in July 2015).

Fossil vertebrates have been identified at several levels from the terrestrial Permian of north China, but the finds are sporadic and the stratigraphy not well confirmed. Key levels are those of the Dashankou and Jiyaun faunas, dated as Roadian and Wuchiapingian respectively (Fig. 2). The Jiyuan fauna, with *Honania* and *Tsiyuania*, comes from the Upper Shihezhi (formerly Shihhotse) Formation, of Henan Province in northern China (Fig. 2), which dates from the lower Capitanian to upper Wuchiapingian, based primarily on magnetostratigraphy (Embleton *et* al. 1996; Stevens *et al.* 2011). The Jiyuan Fauna is from near the top of the unit, and is dated as late Wuchiapingian (Liu *et al.* 2014).

The other pareiasaurs come from the Sunjiagou (formerly Shiqianfeng or Shihtienfeng) Formation, part of the Shiqianfeng Group (reviewed by Mueller *et al.* 1991; Stevens *et al.* 2011), a succession of more than 1000 m of red, brown, and purple claystones and sandstones, interpreted as generally deposited in arid conditions, which is confirmed by the occurrence of gypsum in lower units and fine-grained aeolian sandstones in the upper 700 m (Norin 1922; Wang & Wang 1986; Wang & Chen 2001). Fossils are rare throughout, with plant fossils in upper parts, suggesting reductions in wetland floras towards the Permo-Triassic boundary (Wang 1993; Wang & Chen 2001; Stevens *et al.* 2011).

Earlier Chinese authors could compare their tetrapod finds with the Russian and South African (Karoo) sequences, which themselves lacked any independent age control. For example, Young & Yeh (1963: 211-212) compared *Shihtienfenia* with *Scutosaurus* from Russia and *Propappus* and *Pareiasaurus* from South Africa, equivalent respectively to the Russian lower Vyatkian (Zone IV) and the *Cistecephalus* Zone of the Karroo (Fig. 2). Cheng

(1980) confirmed these comparisons with respect to his *Shansisaurus* material, as did Gao (1983) with respect to *Huanghesaurus*. In more detail, Gao (1989:1239-1240) developed these ideas, splitting the Sunjiagou pareiasaurs into two geological age categories: *Sanchuansaurus* from the lowest part of the Shanxi redbed sequence, was 'at the same evolutionary stage as *Pareiasuchus*', and so this unit correlated best with the *Cistecephalus* Zone of South Africa. The other three Chinese pareiasaurs came from higher in the Sunjiagou Formation, and showed greatest similarity with *Scutosaurus* from the upper part of Zone IV in Russia, and the *Daptocephalus* Zone (= now, *Dicynodon* Zone) of South Africa. If these correlations were correct, the Sunjiagou Formation would span from mid Wuchiapingian (*Cistecephalus* Assemblage Zone) to Changhsingian (*Daptocephalus* = *Dicynodon* Assemblage Zone), and a similar age range for upper parts of the old Russian Zone IV (= Sokolki; Vyatkian) (Fig. 2; Benton 2012; Benton *et al.* 2012).

The pareiasaurs occurred at different levels in the Sunjiagou Formation. *Shihtienfenia* was located in the lower part of the formation, at the top of Unit II, a 40 m thick unit of intercalated red mudstones and sandstones (Young & Yeh 1963). *Huanghesaurus* was reported from 'the topmost part of the Shihtienfeng Formation' (Gao 1983. Gao (1989: 1239) noted that the fossiliferous lens with *Sanchuansaurus* occurred in the 'lowest part' of the Shihtienfeng (= Sunjiagou) Formation, and he is clear that this was below the levels at which *Shihtienfenia*, *Shansisaurus*, and *Huanghesaurus* had been found. These uppermost and lower levels are confirmed by Li and Liu (2013: 199–200). The three levels are discriminated in the summary stratigraphic chart (Fig. 2), but their exact horizons are uncertain.

Debates about the relative ages of the tetrapods can be resolved only by independent dating. Palaeobotanists and palynologists date the Sunjiagou Formation as late Late Permian, and the overlying Liujiaggou and Heshanggou Formations as Early Triassic (Wang & Wang 1986; Hou & Ouyang 2000; Wang & Chen 2001; Stevens *et al*. 2001; Zhang *et al*. 2012). For example, Zhang *et al*. (2012) describe the Sunjiagou Formation as about 200 m thick, and correlated with the entirety of the Changhsingian stage, with roughly equal Lower, Middle, and Upper divisions. Stevens *et al*. (2011) concur, and show the underlying Upper Shihezhi Formation as extending from the base of the Capitanian to the top of the Capitanian or to the late Wuchiapingian; in either interpretation, there is a hiatus below the Sunjiagou Formation. The Lower Shihezhi (= Xiashihezhi) Formation lies below, extending from late Kungurian to the end of the Wordian, and the Shanxi Formation lies below that (Fig. 2). Stevens *et al*. (2011) note that palynology is a good guide to dating the Lower Permian terrestrial units, but not for the Middle or Upper Permian units. Magnetostratigraphy provides some confirmation

of ages (Embleton *et al*. 1996; Menning and Jin 1998), with the Illawarra Reversal located in the lower part of the Upper Shihezhi Formation, so dating that horizon as uppermost Wordian or lowest Capitanian (Fig. 2). Intense reversals throughout the Upper Shihezhi and Sunjiagou formations confirm they are all Illawarra in age (i.e. Capitanian to Changhsingian). Matching of the Illawarra magnetostratigraphic signature gives two models for the ages of these units, implying a larger or smaller gap between the Upper Shihezhi Formation and the Sunjiagou Formation, and making the former unit either 5 or 10 Myr in duration. The overlying Sunjiagou Formation has been dated as entirely Changhsingian, terminating arbitrarily at the Permo-Triassic boundary (Embleton *et al.* 1996; Stevens *et al.* 2011). Even so, the Changhsingian lasted about 2 Myr (254.1-252.2 Myr; Shen *et al.* 2011), perhaps time for some moderate differentiation among amniote faunas.

THE UPPER SHIHEZHI FORMATION PAREIASAURS

The pareiasaur taxa from the Upper Shihezi Formation of Henan, *Honania complicidentata* and *Tsiyuania simplicidentata*, are presented briefly, as they have been redescribed and their materials augmented by Xu et al. (2015).

The three original specimens of *Honania* are isolated teeth, each consisting of the crown and part of the root (Fig. 3; Table 1). A fourth specimen tabulated by Young (1979:103) is currently missing. IVPP V4015.1 (Fig. 3A, C; Young 1979: fig. 4, left) is well preserved, and shows the cingulum and serrations clearly. The tooth is 25 mm long in all. The root measures 6 x 7 mm in section, and it is not exactly circular, being slightly twisted and with rather flat antero-posterior sides. The cingulum (Fig. 3A, ci) carries about 12 small serrations, but they are abraded, and the margin of the crown carries eight very distinct serrations up each side, making a total of 16. The crown portion, as delimited by the cingulum, measures 13 mm dorsoventrally high and 10 mm anteroposteriorly wide. IVPP V4015.2 (Fig. 3C; Young 1979: fig. 4, centre) is still in the rock, a deep purple-coloured coarse sandstone containing bone and scale fragments, and is visible only in external (lateral/ labial) view. The root is missing, and the crown shows eight denticles on one margin, six on the other, suggesting a total of 15-17. The third specimen, IVPP V4015.3 (Fig. 3B, C; Young 1979: fig. 4, right) is smaller than the other two, being 18 mm long in all, and has a shorter root that is waisted at mid-height, and appears roughly circular in cross section, measuring about 7 x 8 mm. The cingulum and marginal denticles are partly abraded, but there seem to be

about 12 small denticles on the cingulum, and 5-7 denticles on each crown margin. Each of the marginal denticles is at the end of a distinct longitudinal ridge that may be seen traversing the lingual and labial faces of the tooth.

The original materials of *Tsiyuania* (IVPP V4016; Fig. 3D) are currently missing, but Young (1979: 103, fig. 5) shows two specimens out of five whose measurements he tabulates. These two teeth are much larger than the teeth of *Honania*, apparently measuring 13 and 16 mm anteroposteriorly wide, and 21 and 25 mm dorsoventrally tall. In both illustrated examples, the margins are badly damaged, and the full height and width of the crowns cannot be measured accurately (Table 1). Further, it is hard to estimate the numbers of cingular and marginal denticles. Young (1979:103) included some much smaller, but unillustrated, teeth in this taxon, with total heights of 15, ?9, and 8 mm, and it is not clear how the nine pareiasaur teeth in all were divided between two taxa, nor what their diagnostic characters are.

These two pareiasaur taxa have rarely been mentioned in the literature. Lee (1997: 287) suggested they were upper (*Tsiyuania*) and lower (*Honania*) teeth of the same taxon, but most authors either ignored the two genera, or declared they were *nomina nuda* (e.g. Li 2001). Liu *et al*. (2014), in brief, and then Xu *et al*. (2015), in more detail, proposed that *Honania complicidentata* was indeed valid, and synonymized *Tsiyuania simplicidentata* with it. They identified additional pareiasaurian teeth among the other fossils described by Young (1979), and also assigned additional elements collected in 2010 to this taxon, including a maxilla and dentary, some other skull bones, vertebrae, ribs, and limb and girdle elements.

Xu *et al*. (2015) argue that the expanded materials of *Honania* confirm that it is a distinctive taxon. They characterize it as having 'maxillary teeth with high crowns, dentary teeth slightly posteriorly inclined compared to the dentary dorsal margin, nearly all preserved marginal teeth have a cusped cingulum on the lingual surface, and humerus without an ectepicondylar foramen'. The tooth characters are general to all or most pareiasaurs, but the absence of an ectepicondylar foramen, if confirmed, would distinguish *Honania* from all other pareiasaurs. However, in their discussion, Xu *et al*. (2015) do not compare their *Honania* material with *Sanchuansaurus*, regarding this genus as a synonym of *Huanghesaurus* and *Shansisaurus*, a view not taken here. The only comparable elements are the maxilla and femur: the maxilla and teeth of *Honania* seem identical to those of *Sanchuansaurus*, and both femurs are similar enough, but both are incomplete, so a final view on synonymy cannot be given.

HOW MANY SUNJIAGOU FORMATION PAREIASAURS?

BACKGROUND

The pareiasaurs of the Sunjiagou Formation of Shanxi are: *Shihtienfenia permica*, named by Young & Yeh (1963) on the basis of a partial postcranial skeleton (IVPP V2717) and a second specimen consisting of 11 vertebrae and other fragments (IVPP V2718); *Shansisaurus xuecunensis*, named by Cheng (1980) for some isolated vertebrae, a scapulocoracoid, humerus, and femur (CAGS V301); *Huanghesaurus liulinensis*, established by Gao (1983) for an incomplete skeleton, comprising a right lower jaw and a large number of vertebrae and limb bones (IVPP V6722); and *Sanchuansaurus pygmaeus* named by Gao (1989) for a maxilla and isolated postcranial remains (IVPP V6723-5).

There are three viewpoints on the taxonomic validity of these four taxa: (1) to synonymise them all with *Shihtienfenia permica* Young & Yeh, 1963, the first-named taxon, on the basis that the other three species show no distinguishing characters; (2) to accept three taxa as valid, by synonymising *Huanghesaurus* with *Shansisaurus*; or (3) to accept two taxa as valid, by synonymising *Huanghesaurus* and *Sanchuansaurus* with *Shansisaurus*, and retaining *Shihtienfenia*.

The first view, in which all taxa are synonymised, was presented by Sun *et al.* (1992) and Lucas (2001). These authors noted that Cheng (1980) distinguished his new genus and species *Shansisaurus xuecunensis* from *Shihtienfenia* by its supposedly more robust humerus, a view they disputed. Further, they noted that Gao (1983) did not mention any diagnostic characters to differentiate his new genus and species *Huanghesaurus liulinensis* from the two earlier named taxa. Accordingly, Sun *et al.* (1992) synonymised *Shansisaurus xuecunensis* and *Huanghesaurus liulinensis* with *Shihtienfenia permica*, a view with which Lucas (2001) agreed. These authors did not comment on the fourth taxon, *Sanchuansaurus pygmaeus*.

Sanchuansaurus pygmaeus was named by Gao (1989), in his description of a variety of pareiasaur materials from a single locality. He assigned a maxilla, a femur, and a fibula to the new species *Sanchuansaurus pygmaeus* (IVPP V6723-5), and other postcranial remains to *Shansisaurus* sp. (IVPP V6726-7) and to 'Pareiasauride gen. et sp. indet.' (IVPP V8533-5). The only reasons given for not associating all these specimens into a single taxon, despite the fact that they were all found within a single sandstone lens, is 'the striking difference in size and thickness of the bones, as well as their disarticulation' and the fact that some, such as the maxilla, are in very good condition, whereas some of the postcranial bones show signs of

abrasion and transport. Here, and in line with earlier work by Lee (1997) and others, all the materials described by Gao (1989) as from the same sedimentary lens are treated tentatively as associated with the type maxilla of *Sanchuansaurus*.

The second view was presented by Lee (1997: 209), who regarded *Shihtienfenia*, *Shansisaurus*, and *Sanchuansaurus* as valid, and synonymised *Huanghesaurus* with *Shansisaurus*. These he characterised as follows:

1. *Shihtienfenia permica*. "Monophyletic. Autapomorphies: there is a rounded expansion on the anterior margin of the scapula blade, near the dorsal end; and the acromion process is a smoothly contoured, semicircular flange. Material: IVPP V2717 (Type), IVPP V8533."
2. *Shansisaurus xuecunensis*. "Metaspecies. This species... differs from *Shihtienfenia* in lacking the autapomorphies of the latter, and in possessing an ectepicondylar foramen. Material: CAGS V301 (Type); IVPP V6722."
3. *Sanchuansaurus pygmaeus*. "Monophyletic. Autapomorphies: the two exits for the infraorbital canal are very far apart; and every tooth has a cusped cingulum on the lingual surface. Material: IVPP V6723 (Type)."

This view was accepted by Jalil & Janvier (2005), Tsuji & Müller (2008), Tsuji (2013), and Tsuji *et al*. (2013), who retained these three as separate taxa for cladistic coding, and found close phylogenetic links between the first two and *Pareiasuchus*, but that *Sanchuansaurus* formed part of a more derived clade, with *Scutosaurus* and *Elginia*, characterised by a single synapomorphy, a cusped cingulum, a horizontal ridge that bears a row of small cusps on the medial surface of some teeth (Character 64).

The third view was presented by Li & Liu (2013), who described new material from the Sunjiagou Formation, and synonymised *Sanchuansaurus* and *Huanghesaurus* with *Shansisaurus xuecunensis* based on supposed identity of the teeth of the first two.

COMMENTARY ON SUPPOSED DISTINGUISHING FEATURES

The one synonymy agreed generally is that *Huanghesaurus* is the same as *Shansisaurus*. The only element preserved for both taxa, the scapulocoracoid, is identical in *Shansisaurus* (Cheng 1980: fig. 19) and *Huanghesaurus* (Gao 1983: fig. 4), in terms of size, overall shape, relative proportions, and anatomical details.

The question then is whether *Shansisaurus* (incl. *Huanghesaurus*) could be the same as *Shihtienfenia* or not. Lee (1997: 209) noted that *Shansisaurus* 'differs from *Shihtienfenia* in

lacking the autapomorphies of the latter, and in possessing an ectepicondylar foramen'. There is no *Shansisaurus* humerus, so the reference is to *Huanghesaurus*, but it has no ectepicondylar foramen, but in fact a possible entepicondylar foramen (this was a misprint, and is presented correctly by Lee, 1997: 255). In any case, an ectepicondylar foramen is said to be 'universally present in pareiasaurs' (Lee 1997: 237), whereas an entepicondylar foramen is present in basal amniotes, and is retained by many pareiasaurs, but it 'is an open groove in *Pareiasuchus peringueyi* and *Shihtienfenia*' (Lee 1997: 237). This is a dubious character upon which to differentiate *Shansisaurus* and *Shihtienfenia* because the purported entepicondylar foramen on the left humerus of *Huanghesaurus* (IVPP V6722-26) is superficial in location, being bridged by the thinnest of arches, and indeed this region has been substantially repaired, and most of the 'bone' bridge is plaster.

Close comparison of the two most complete Chinese pareiasaur individuals, the holotypes of *Shihtienfenia permica* (IVPP V2717) and *Huanghesaurus liulinensis* (IVPP V6722), reveals four possible differentiating characters: (1) in posterior dorsal vertebrae of *Shihtienfenia* there are ventral facets that each occupy one third of the vertebral length formed from deeply overturned articular faces, and these are not seen in *Huanghesaurus*; (2) the rib attachment facets in middle and posterior dorsal vertebrae of *Shihtienfenia* are shorter and more massive; (3) the right scapula has an elongate, almost cylindrical blade ending in a rounded, spoon-shaped distal end which expands especially on the anterior margin; and, (4) the humerus is of conservative design and lacks the flared proximal end seen in *Huanghesaurus*. The first two characters are hard to confirm because the numbering of presacral vertebrae is debatable in both taxa, and those differential features might be minor variations or size-related phenomena. The scapula characters, the basis of the two autapomorphies of *Shihtienfenia* cited by Lee (1997: 209), namely the 'rounded expansion on the anterior margin of the scapula blade, near the dorsal end' and 'the acromion process is a smoothly contoured, semicircular flange', certainly occur in the figured right scapula (Young & Yeh 1963: fig. 6), but they are absent in the left scapula, which is indistinguishable from that of *Shansisaurus*, *Huanghesaurus*, and many other pareiasaurs – the blade has no rounded distal portion, and the acromion process is of normal shape. However, the left scapula (IVPP V2717) is incomplete distally and so the 'rounded expansion' cannot be considered. These 'autapomorphies' apply to the right scapula only, and there is little doubt, both from Young & Yeh's (1963) description of the circumstances of discovery, and the nature of the specimens, that these are parts of the body of a single individual. The two scapular autapomorphies of *Shihtienfenia* (Lee 1997: 209) reflect morphological variation between left and right sides

within a single individual, and so must be discarded. The fourth character, the flared proximal end of the humerus in *Huanghesaurus*, may be exaggerated by the mode of preservation, and so is not a reliable difference.

So far, the balance of evidence favours the view of Sun *et al.* (1992) and Lucas (2001) that *Shansisaurus* and *Huanghesaurus* are junior synonyms of *Shihtienfenia*. This leaves the fourth taxon, *Sanchuansaurus pygmaeus* to be considered.

SANCHUANSAURUS, DISTINCTIVE TOOTH MORPHOLOGY

The suggestion will be made here, in support of the view presented by Gao (1989), but against Li & Liu (2013), that *Sanchuansaurus*, limited to the three specimens he assigned to the taxon (IVPP V6723, V6724, V6725), is a distinct pareiasaur genus and species. Key evidence is the lower number of marginal cusps in tooth crowns (9-11), and less significant evidence is the smaller size of the animal and its greater stratigraphic age. These points will be considered in turn. First, we consider other potential distinguishing characters.

One of the two autapomorphies of *Sanchuansaurus* noted by Lee (1997: 209), 'the two exits for the infraorbital canal [on the maxilla] are very far apart', may be distinct from other pareiasaurs with maxillae preserved, but it cannot be checked in the other Chinese pareiasaurs because they lack this element. Gao (1989: 1234) distinguished *Sanchuansaurus* from all other pareiasaurs based on the following combination of characters: "Maxillary short and deep, with robust antorbital process and palatal flange. Teeth closely and firmly implanted in maxillary; roots curved medially. Tooth crowns slightly compressed transversely, markedly overlapping with each other; cusps, numbering 9-11, arranged as 3-4 anteriorly, 3 in middle, and 3-4 posteriorly." In fact, these characters occur in nearly all pareiasaurs.

There is a key difference in the teeth, in terms of the number of tooth cusps, a phylogenetically important character (Lee 1997), 'and every tooth has a cusped cingulum on the lingual surface' in *Sanchuansaurus*. In addition, Gao (1989: 1238) had noted that the maxillary teeth of *Sanchuansaurus* have fewer serrations in total (10-12) than the dentary teeth of *Huanghesaurus* (14-17). In all cladistic analyses so far (Lee 1997; Jalil & Janvier 2005; Tsuji & Müller 2008; Tsuji 2013; Tsuji *et al*. 2013), *Sanchuansaurus* is separated phylogenetically from *Shihtienfenia* and *Shansisaurus*, partly as a result of the difference in marginal cusp numbers in the teeth. Including all teeth, the figures are 9-12 denticles in *Sanchuansaurus* and 13-17 in *Huanghesaurus* (Table 1). Li & Liu (2013) describe a tooth

(IVPP V18614) with 17 cusps, seemingly then an example of *Huanghesaurus*, but they note it was found in association with the holotype of *Sanchuansaurus*, from the lower part of the Sunjiagou Formation, and so synonymise the two genera, and those two with *Shansisaurus*. However, this tooth cannot be unequivocally identified as *Sanchuansaurus*, and not *Huanghesaurus*, and so does not prove a synonymy.

A second dental apomorphy is less clear. In the cladistic analyses (Lee 1997; Jalil & Janvier 2005; Tsuji & Müller 2008; Tsuji 2013; Tsuji *et al*. 2013), *Sanchuansaurus* and *Scutosaurus* are paired by possession of the unique apomorphy of a cusped cingulum, and thereby distinguished from the other Chinese pareiasaurs. However, the possession of a cingulum and of cingular denticles by *Sanchuansaurus* is not unique among the Chinese pareiasaurs. All dentary teeth of *Huanghesaurus* also show a clear cingulum, and it bears several denticles in the marginal portions, as noted also by Li & Liu (2013: 202). These features are presented in more detail below, and re-coded for the revised cladistic analysis.

It could be countered that there is a danger in these comparisons, because *Sanchuansaurus* and *Huanghesaurus* are distinguished on differences between maxillary and dentary teeth, and that pareiasaurs show differences in the size and shape of upper and lower dentitions (Lee 1997: 215). For example, in *Pareiasuchus nasicornis*, the single dentary tooth that can be seen differs in shape from the maxillary and premaxillary teeth in being taller, possessing more cusps, having cusps that face somewhat anteriorly and posteriorly, and a crown that is not recurved lingually, differential features seen also in *Pareiasuchus peringueyi* and *Scutosaurus karpinskii*. However, such variation does not occur in all pareiasaurs: *Deltavjatia* shows similar-sized teeth in both upper and lower dentitions (Tsuji 2013). Further, these variations between upper and lower dentitions do not extend to cusp numbers.

Less significant is body size. The *Sanchuansaurus* maxilla and *Huanghesaurus* dentary could hardly come from the same animal: the first possesses 15 teeth within a tooth-row length of 135 mm, the latter possesses 19 teeth in a tooth-row length of 200 mm, suggesting that, if upper and lower tooth row lengths should be comparable, and these two tooth rows are more or less complete, that the *Sanchuansaurus* individual was about two-thirds the linear dimensions of the *Huanghesaurus* animal, which could scale to one-third of the body mass, assuming isometry (0.67 x 0.67 x 0.67 = 0.3).

The postcranial bones assigned to *Sanchuansaurus* by Gao (1989) include a partial left femur (IVPP V6724) and a left fibula (IVPP V6725). The femur, although relatively featureless, and indistinguishable from that of *Shansisaurus* (Cheng 1980: fig. 20), is considerably shorter (270 mm, compared to 430 mm for a similar portion of the bone in

Shansisaurus). Likewise the left fibula is smaller than expected, some 236 mm long, and in proportion to the femur, although no fibula of the larger Chinese pareiasaurs is known, for comparison. The other elements from the same bone-bearing lens, including a dorsal vertebra, a right scapulocoracoid, a partial scapula blade, and the now lost left humerus and right tibia, assigned variously by Gao (1989: 1238-1239) to *Shansisaurus* sp. and Pareiasaur indet., come from larger animals, perhaps one-third larger, and similar in size to *Shihtienfenia.* Size is a poor criterion for taxon discrimination, as is stratigraphic age, but Gao (1989: 1239) and Li and Liu (2013: 199–200) note that *Sanchuansaurus* was older than the other Sunjiagou Formation pareiasaurs.

SYSTEMATIC DESCRIPTIONS

ORDER PARAREPTILIA OLSON, 1947

SUBORDER PAREIASAURIA SEELEY, 1888

FAMILY PAREIASAURIDAE COPE, 1896

Comments: Here, we describe the two valid Sunjiagou Formation pareiasaurs, *Sanchuansaurus pygmaeus* and *Shihtienfenia permica.* Several specimens were found to be missing (May 2012), namely IVPP V2718 (paratype of *Shihtienfenia*, 11 dorsal vertebrae and fragments, badly weathered; Young & Yeh 1963: 207); IVPP V4016 (holotype teeth of *Tsiyuania simplicidentata* Young, 1979: 103-104, fig. 5); IVPP V8535 (pareiasaurid right tibia in Gao 1989: 1239); CAGS V301 and V302 (holotype and paratypes of *Shansisaurus xuecunensis* Cheng, 1980, scapulocoracoid, humerus, vertebrae, ribs, isolated teeth).

SANCHUANSAURUS GAO, 1989

Type species: Sanchuansaurus pugmaeus Gao, 1989.

Diagnosis: As for the type species.

Distribution: Shanxi Province, China; Upper Permian (Changhsingian).

SANCHUANSAURUS PYGMAEUS GAO, 1989

Sanchuansaurus pygmaeus Gao; Gao 1989: 1234-1238, fig. 1, pl. 1

Sanchuansaurus pygmaeus Gao; Lee 1997: 210

Sanchuansaurus pygmaeus Gao; Jalil & Janvier 2005: 115

Sanchuansaurus pygmaeus Gao; Tsuji & Müller 2008: 1118

Holotype - IVPP V6723, a right maxilla.

Paratypes - IVPP V6724, a left femur, and IVPP V6725, a left fibula.

Type locality and horizon - Beigou village, near Weicun town, Liulin County, Shanxi Province, China; lowest part of the Sunjiagou Formation, Upper Permian (Changhsingian).

Revised diagnosis - A pareiasaur, about one-third the body mass, and two-thirds the length, of the other Sunjiagou Formation pareiasaurs, with 9-12 marginal cusps on maxillary teeth; the two exits for the infraorbital canal [on the maxilla] are very far apart (Lee 1997: 209).

Maxilla - The holotype of *Sanchuansaurus pygmaeus* Gao, 1989 (IVPP V6723; Fig. 4) is 135 mm anteroposteriorly long and 85 mm dorsoventrally deep, and it is cracked and lacks the most anterior and most posterior portions. The anterior end is massive and terminates in a vertical portion, probably representing more or less the orientation of the premaxillary contact. The narial margin of the maxilla is elongate and sweeps up and back into the antorbital process (Fig. 4A, B, a.p.), which appears to be more or less complete, lacking perhaps the dorsalmost portion. This process broadens into a distinct lateral boss, located above maxillary teeth 5-7, an unusual feature among pareiasaurs, as noted by Gao (1989: 1235). The posterodorsal margin of the maxilla, which presumably contacted the lacrimal in life, again lacks the thinner portions, but sweeps back and down to the relatively narrow posterior portion of the maxilla, which would have met the jugal with a narrow process. The ventral margin is more or less straight in lateral view (Fig. 4A), and bears the remains of 15 marginal teeth. These sit in distinct sockets which crowd closely, and somewhat irregularly on the ventral margin. Around the teeth, and above them, is a zone, some 7-12 mm deep, of somewhat porous-looking, unfinished bone surface that might represent actively replacing bone tissue associated with the continuing tooth replacement.

The medial view of the maxilla (Fig. 4B) shows a substantial palatal shelf (Fig. 4B, C, p.s.) running nearly horizontally, and more or less parallel to the ventral tooth-bearing margin. The medial faces of the maxilla that lie above and below the palatal shelf are somewhat

concave. The shelf is located halfway between the dorsal point of the antorbital process and the ventral margin of the maxilla (80 mm), and it projects medially. The maxilla is about 15 mm thick above the tooth-bearing area, and with the shelf its overall thickness varies from 25-30 mm and up to 35 mm at the position of the antorbital boss. The antorbital process (Fig. 4B, a.p.) projects above, and below is the deep tooth-bearing area. Three replacement teeth have been exposed in this zone, located above teeth 3-4, 6, and 8 respectively. The somewhat irregular arrangement of the marginal teeth is clear in medial view (Fig. 4B), with numbers 3, 5, and 7 projecting more laterally than the others. In this area, teeth 3-7 are relatively large, and there is insufficient space for them to form a uniform row, so presumably several were forced out of line as they emerged into their final positions. As on the dorsal face, there is a distinct zone, some 17-25 mm deep, above and round the functioning and the replacement teeth, where the bone surface texture is porous or irregular. In places it shows vertically oriented striations, which contrast with the more horizontal striation pattern in the finished bone surface above.

The bone shows surprisingly few vessel openings, and no trace of the often abundant small canals in the snout and gum region of other amniotes. The infraorbital canal is very clear in medial view (Fig. 4B, io.c.), entering the maxilla above the palatine shelf, and just behind the antorbital process, and perhaps exiting through two large openings on the lateral face (Fig. 4A, io.c.). This canal presumably carried the infraorbital nerve, the anterior portion of the maxillary branch of the trigeminal nerve (cranial nerve V_2) as well as presumably the infraorbital artery.

The teeth are of normal pareiasaur shape (Table 1), with a broad, somewhat diamond-shaped crown and a narrower, smooth shaft. Each tooth emerges from the maxilla, expands into the crown, and curves medially and slightly posteriorly. This gives the lateral (labial) face of each tooth a distinct convex shape, with a definite medial bend at the transition from shaft to crown. Tooth 2 is broken at the level of the maxillary margin, and it shows a more or less circular cross section (Fig. 4C, 2), measuring 9 mm in the antero-posterior axis, and 8 mm medio-laterally. The outer dentine wall is 2 mm wide, leaving a 4-5 mm wide central dentine core. This central shaft of younger dentine is seen clearly in tooth 1, which has been partly prepared out (Fig. 4B, 1). The tooth crown measures 7-12 mm in the antero-posterior axis, compared to a shaft of 5-7 mm in the same orientation. The teeth vary slightly in size, becoming slightly larger from front to back (Table 1). The crown extends to the distal margin smoothly in lateral view (Fig. 4A), but there is a distinct cingulum and occlusal surface on the medial (lingual) face (Fig. 4B). This medial crown surface bears no lingual ridge (Lee 1997:

fig. 11). The cingulum at the proximal margin of the occlusal surface is gently curved, whereas the distal margin of the tooth is somewhat pointed, although most marginal teeth in this specimen have been damaged. The cingulum bears 10-12 tiny serrations on the edge of the occlusal surface (2.5 per mm), and at the outer edges, these serrations expand into the most proximal of the major serrations that surround the biting edge of the tooth. Each tooth bears 9-12 such marginal denticles, or cusps, each typically 1 mm wide, but some proximal ones 1.5 mm wide, and separated by deep grooves on labial and lingual tooth faces; each marginal serration then is 1-3 mm long, if the grooves are included. These marginal cusps point essentially ventrally, parallel to the longitudinal axis of the tooth.

The anterodorsal margin of the maxilla indicates that *Sanchuansaurus* had an elongate external naris (Lee 1997, character 23; Tsuji 2013, character 20); the maxilla shows a prominent maxillary boss (Lee 1997, character 25; Tsuji 2013, character 26); the maxillary dentition is inflected towards the palate, and the teeth are oriented ventromedially (Lee 1997, character 27; Tsuji 2013, character 50); the number of maxillary teeth in each maxilla is more than or equal to 10 (Lee 1997, character 55; Tsuji 2013, character 51); the teeth are labiolingually compressed, leaf-shaped, and with small denticles on the tooth crown (Lee 1997, character 58; Tsuji 2013, character 52); cusps are regularly spaced along the tooth crown (Lee 1997, character 61; Tsuji 2013, character 53); there are 9-11 marginal cusps on each maxillary tooth (Lee 1997, character 59; Tsuji 2013, character 54); there is a cingulum present, with small cuspules (Lee 1997, character 64; Tsuji 2013, character 57); and there is no caniniform region in the tooth row (Tsuji 2013, character 120).

Femur - An incomplete left femur was assigned to *Sanchuansaurus* by Gao (1989: 1235-1238, fig. 2, pl. 2A, B). The specimen (IVPP V6724) is 270 mm long at most (not 300 mm, as stated by Gao 1989: 1235), and it lacks both articular ends, these being represented by irregular broken faces and red sandstone infill (Fig. 5A-D). The irregular termination of the element at both ends suggests that the epiphyses fell off before fossilisation, and even that the exposed diaphyseal ends were somewhat damaged; perhaps the element comes from a young animal in which the epiphyses had not fused. This femur may have been 290 mm or more in length when complete. As in other pareiasaurs (Seeley 1892, figs. 8-11), this is a relatively short element, with short diaphysis and expanded ends. The maximum width of the anterior end is 112 mm, of the posterior end 115 mm, and minimum breadth of the shaft is 55 mm (excluding the postaxial flange), all measured in dorsal view (Fig. 5A). The shaft is strong, and it expands proximally as a convex face in dorsal view (Fig. 5A), extending posteriorly

into a sizable postaxial flange (Fig. 5A, p.f.) that diminishes to a minimum thickness of 18 mm near the margin. Distally, the shaft expands to form a concave intercondylar sulcus (Fig. 5A, i.s.) towards the distal end. The intercondylar foramen in this sulcus is not seen, the preserved bone terminating before that point. The distal condyles are missing, but the preserved bone extends somewhat further on the anterior side, forming the proximal part of the tibial condyle (Fig. 5A, ti.c.). In ventral/ medial view (Fig. 5B), the proximal intertrochanteric fossa is broad and nearly symmetrical, and extends from the anterior margin across the postaxial flange. The distal end is too incomplete to see the popliteal fossa or any foramen in the fibular condyle, as indicated by Gao (1989: 1235, fig. 2B).

The proximal head of this femur is curved slightly anteriorly (preaxially) (Lee 1997, character 107; Tsuji 2013, character 95); the postaxial flange is present, and extends the entire length of the femur, but is narrower in the middle, so the femur looks concave in dorsal or ventral view (Lee 1997, character 112; Tsuji 2013, character 97).

Fibula - A complete left fibula was also referred to *Sanchuansaurus pygmaeus* by Gao (1989: 1235), but not illustrated. This element (IVPP V6725) is a straight bone, 236 mm long, and with expanded proximal and distal ends, some 86 and 75 mm at their greatest widths respectively (Fig. 5E–H). The shaft narrows to 30 x 38 mm. The proximal end is massive, oval in shape in proximal view and measuring 62 x 85 mm. The shaft is roughly straight, with minimal twisting so that the long axes of the articular ends are set at 30 degrees to each other. The distal articular end is narrower, measuring 30 x 72 mm. The bone is broadest in extensor (dorsal) and flexor (ventral) views (Fig. 5E, G), and it shows a clear anterior trochanter in flexor and anterior views (Fig. 5G, H, a.t.), some 30 mm long, located entirely within the proximal half of the bone. The anterior fibular ridge is slightly marked, but other muscle attachment sites are less clearly demarcated. At the distal end, the facets for articulation with the fibulare and intermedium (Fig. 5E, fib., int.) are separated by an angulation, and there is a depressed area above these on the extensor face of the shaft. It seems that Gao (1989: 1235) confused the proximal and distal articular ends in giving measurements.

SHIHTIENFENIA YOUNG & YEH, 1963

Type species - *Shihtienfenia permica* Young & Yeh, 1963

Diagnosis - As for the type species.

Distribution - Shanxi Province, China; Upper Permian (Changhsingian).

SHIHTIENFENIA PERMICA YOUNG & YEH, 1963

Shihtienfenia permica Young & Yeh; Young & Yeh 1963: 195-212, figs. 1-9, pls. 1, 2
Shansisaurus xuecunensis Cheng; Cheng, 1980: 115-119, figs. 18-20, pls. 127, 128; subjective synonym
Shihtienfenia Young & Yeh; Gao 1983: 201
Shansisaurus Cheng; Gao 1983: 201
Huanghesaurus liulinensis Gao; Gao, 1983: 193-203, figs. 1-7, pls. 1, 2; subjective synonym
Shansisaurus xuecunesis Cheng; Gao 1989: 1238-1239, fig. 3
Huanghesaurus liulinensis Gao; Gao 1989: 1238
Shihtienfenia Young & Yeh; Lee 1995: 503
Shihtienfenia permica Young & Yeh; Lee 1997: 209
Shansisaurus xuecunensis Cheng, 1980; Lee 1997: 209
Shihtienfenia permica Young & Yeh; Lucas 2001: 79-80, fig. 6-8
Syn. *Shansisaurus xuecunensis* Cheng; Lucas 2001: 79
Syn. *Huanghesaurus liulinensis* Gao; Lucas 2001: 79-80
Shihtienfenia permica Young & Yeh; Jalil & Janvier 2005: 115
Shansisaurus xuecunesis Cheng; Jalil & Janvier 2005: 115
Shihtienfenia permica Young & Yeh; Tsuji & Müller 2008: 1118
Shansisaurus xuecunesis Cheng; Tsuji & Müller 2008: 1118

Holotype - IVPP V2717, a partial skeleton, consisting of about 20 vertebrae, ribs, and elements of the pectoral girdle (scapulocoracoids, dermal pectoral elements), both humeri, and both pelvic plates (ilium, pubis, ischium).

Paratypes - CAGS V301, isolated vertebrae, a complete left scapulocoracoid, a left femur, and some rib fragments, the type material of *Shansisaurus xuecunensis* Cheng, 1980; CAGS V302, vertebrae, assigned to *Shansisaurus xuecunensis* Cheng, 1980; IVPP 6722-1 to 29, an incomplete skeleton, consisting of a left lower jaw, a possible jugal, part of the right lower jaw, conjoined splenials, 13 vertebrae, the left scapulocoracoid, clavicles, interclavicle, and the left humerus, ulna, and radius, the type specimen of *Huanghesaurus liulinensis* Gao, 1983.

Type locality and horizon - Lishenglen, Baode town, Baode County, Shanxi Province, China; Sunjiagou Formation, Upper Permian (Changhsingian).

Revised diagnosis - A pareiasaur, about three times the body mass, and 1.5 times the length, of *Sanchuansaurus*, with 13-17 marginal cusps on maxillary teeth. Entepicondylar foramen of humerus situated on the side of the epicondyle and feebly exposed in dorsal view, foramen has migrated around the edge of the humerus (coded in *Shihtienfenia* and *Huanghesaurus*). Possibly also intercondylar depression on the dorsal surface of the distal end of the humerus with a transverse ridge present on the distal surface, defined dorsally by the ulnar articular surface (seen in *Shihtienfenia*, but not codable in *Shansisaurus* or *Huanghesaurus*).

SKULL AND LOWER JAW

POSSIBLE JUGAL

An isolated element, IVPP V6722-3, was identified by Gao (1983: 195, pl. 1, figs. 3, 4) as an angular of *Huanghesaurus*, the descending boss from the left side of the lower jaw. This identification, however, cannot be correct because the narrow process that is supposed to be the descending boss, and so free of all contact with other bones, bears an articulating facet. This specimen (Fig. 6) is reinterpreted here very tentatively as a left jugal. It is roughly-L-shaped, with a long narrow process and, more or less at right angles, a wider process. These two outline a curved margin on the inside of the L-shape that did not suture with anything, and could then be the postero-ventral margin of the orbit. If this is the case, then the narrower process is the anterior process that contacts the lacrimal with its anterior tip, and the maxilla along most of the ventral margin. The broader process at right angles would then contact the postorbital dorsally on the broad upper margin. The posterior margin of the element has an upper portion that describes a distinctly concave surface in medial view (Fig. 6B), with a slot or groove below. If correctly interpreted, these faces would mark contacts with the squamosal above, and the quadratojugal below. An objection to this revised interpretation is that the element bears little if any sculpture externally (Fig. 6A), whereas the jugal is liberally sculpted in most pareiasaurs. However, there is a raised portion and a groove in the middle of the lower portion of the broader process, and the distal region of this process is damaged, so the external surface cannot be assessed.

MANDIBLE

The lower jaw is represented by three specimens, IVPP V6722-1 and 2, both ascribed to *Huanghesaurus* by Gao (1983: fig. 1, pl. 1, figs. 1, 2, 5), and an unnumbered piece.

Mandible - IVPP V6722-1 (Fig. 7A–C) is a huge right lower jaw of a pareiasaur, seemingly much larger than any of the associated remains. It appears to be complete except for the splenial. The specimen is undistorted and preservation quality is excellent. In lateral view (Fig. 7A), the jaw is remarkably equal in depth from front to back. The whole specimen measures 364 mm in maximum length, along its ventral region from the posterior expansion of the angular to the anterior symphyseal point. The dorsal margin, from articular to anterior teeth insertions measures 273 mm. Depth of the jaw is 62 mm below tooth 2, 53 mm below tooth 3, 81 mm at the back of the tooth row, and 96 mm measured vertically from the high point in front of the articular facet. The specimen evidently broke in two, and this has been repaired by IVPP technicians, so the specimen can be displayed. Close inspection suggests that this line of break roughly marks the posterior margin of the dentary in lateral and medial views.

The dentary is by far the largest element of the lower jaw, comprising 60% of its length ventrally and nearly 90% dorsally. In lateral view (Fig. 7A), the dentary is a broad strap-like plate that curves slightly from the symphyseal portion, and its ventral margin sweeps back in a straight line. Here the edge is very thin, tapering to nothing where it would have overlapped the absent splenial. This ventral margin angles slightly upwards posteriorly, exposing the anterior process of the angular in lateral view, and it then bends more dorsally into its posterior margin, also presumably wafer-thin, but obscured by repair medium, and presumably running to a point at the postero-dorsal angle. The dorsal margin of the dentary is closely lined with teeth from its most medial point above the symphysis, back some 200 mm, leaving only 45 mm or so of toothless dorsal margin behind (exact distance obscured by repair medium). In the space of 200 mm are 19 teeth, numbers 1-15 more or less complete (3 is a pit), and 16-18 represented by broken-off roots, and tooth 19 by a pit (Fig. 7A–C). Gao (1983: 203) noted 20 teeth. Tooth 3 is represented by a pit, as if it had been shed, and not replaced, just before death. Tooth 11 is set lower than the others, and is perhaps just emerging from the jaw line and moving into place. Otherwise, the intact teeth form a regular palisade, all reaching the same level dorsally, and so providing a uniform cutting blade. There are three

large vessel openings (Fig. 7A, v.o.) at mid-height on the lateral face of the dentary, measuring 8, 10, and 7 mm respectively in maximum antero-posterior length respectively fromfront to back. These canal openings lie below tooth positions 3, 7, and 9, and they presumably housed exiting mental nerves and blood vessels.

The dentary forms part of the symphysis (Fig. 7B, sy.), on a flattened vertical face that consists of the lateral plate and a medial plate below the tooth row, each at most 12 mm thick medio-laterally. The lateral plate descends 65 mm below the first tooth, whereas the medial plate descends 50 mm, diverging from the lateral plate, and leaving a shallow roofed channel beneath, the anteriormost portion of the Meckelian fossa. In medial view posterior to the symphysis (Fig. 7B), the ventral margin of the medial plate runs back for some 90 mm above an open Meckelian fossa (Fig. 7B, me.f.) below which would have been covered by the splenial in life. The ventral margin of the dentary slopes gradually upwards, partially obscured by the repair medium, and its depth below the dental lamina zone diminishes from some 40 mm below teeth 1-3, to 34 mm below teeth 0-11, and presumably further diminishing in depth more posteriorly. There is a large opening, measuring 32 x 18 mm, located below teeth 7-9 on this medial portion of the dentary, but it is uncertain whether this is a real structure or a result of enthusiastic preparation work. It does not match any such opening in other basal tetrapods.

Above this medial dentary plate is a deep dental lamina zone (Fig. 7B, d.l.), varying from 20 mm deep below tooth 7 to 10 mm deep below tooth 15. This zone lies above a clearly demarcated rounded margin of the dentary bone, and the bone texture switches from relatively smooth and longitudinally striated below the demarcation to irregular and vertically striated in the dental lamina zone. Further, this zone contains many circular-topped erosion hollows where teeth were presumably in the process of being implanted into the dentary bone from the soft-tissue dental lamina. Three such replacement teeth are in place, in order of advancement of eruption, beneath marginal teeth 17 and 14, and tooth 11, which has expelled its precursor and is moving up into place in the marginal tooth row. The equal spacing (three teeth apart) could suggest a Zahnreihe, a wave of tooth replacement running from back to front of the tooth row (DeMar 1972). There is a trace of a replacement tooth in a small pit beneath tooth 1. Further, there are irregular erosion pits in the dental lamina beneath teeth 15, 12, 8-10, 7, and 5. The status of teeth 3-4 is hard to determine: tooth 4 is complete, but has been exposed, broken off, and re-inserted into the jaw bone partially reversed by a preparator, whereas the position of tooth 3 is marked by a deep depression in the jaw margin, possibly from original jaw damage or from over-preparation.

There is no sign of a coronoid bone, and the splenial is apparently entirely missing, leaving the ventral margin of the dentary exposed as a wafer-thin bone plate, and showing the anterior process of the angular in medial view.

The sutures among the post-dentary elements are not clear. The angular forms most of the lower margin of the jaw, being presumably at least 250 mm long as seen in medial view (Fig. 7B, an.). The anterior tip is broken off, so it would have been longer. The lateral portion of the angular lies beneath the dentary, in a longitudinal facet on the medial side of the lateral plate of the dentary about 11 mm deep. The ventral margin of the angular is narrow, ranging from 10-20 mm in medio-lateral width, but the medial side of the hemimandible suggests there may have been some crushing and a partial collapse of the Meckelian fossa. On the medial face, the dorsal contacts of the angular with the prearticular and articular cannot be seen with certainty, but some possible indications are shown (Fig. 7A, sa?). In lateral view (Fig. 7A, ma.f.), the ventral margin of the mandibular fenestra at least seems genuine, and the dorsal extent might be also, or perhaps slightly enlarged. In any case, the mandibular fenestra appears to measure 32 x 16 mm. The contact between angular and surangular seems to begin just above and behind the mandibular foramen, and then it becomes obscure posteriorly. The angular boss, a substantial vertical extension of the bone seen in most pareiasaurs, is at best only modest here, represented by a slight downwards expansion of the posterior portion of the mandible when the dentary tooth row is held horizontal. Gao (1983: pl. 1, figs. 3,4) identified IVPP V6722-3 as the angular boss, and suggested the structure lay far forward, essentially below its current anterior termination (Gao 1983: fig. 1). However, this very anterior location is impossible as that portion of the angular was demonstrably covered by the splenial in life. Present evidence suggests that *Shihtienfenia* had only a modest ventral angular boss, and IVPP V6722-3 is identified here as a possible jugal (see above).

The surangular is presumably bordered by the dentary anteriorly, and the contact is lost in the zone of repair medium, the angular ventrally, as noted, and it sweeps round the pediment of the articular facet of the jaw. The prearticular is similarly of uncertain extent (Fig. 7B, pa?), its anterior contact with the dentary obscured beneath repair medium, and its ventral contact with the angular only seen incompletely. Finally, the articular is presumably largely restricted to the articular facet, which is 70 mm in antero-posterior length and 50 mm in medio-lateral width. The articular face (Fig. 7C, ar) consists of an elongate lateral portion that curves around the medial face, and descends substantially ventrally in the posterior portion. The smaller medial portion of the articular facet is 36 mm in antero-posterior length

and 23 mm in medio-lateral width, and it sits at an angle of 60° above horizontal, facing mainly medially.

Splenials - IVPP V6772-2 consists of much of the two splenials of a pareiasaur (Fig. 7D, E), and the size is about right for these to match IVPP V6772-1, which lacks the splenials. Indeed, the proportions of the missing splenial in IVPP V6772-1, the curvature of the jaw line, and the shape of the ventral margins of the dentary all make a very good match to IVPP V6772-2. However, the preservation is rather different, the latter specimen being somewhat 'rougher' in appearance, and bearing patches of a deeper red colour, whereas the corresponding portions of IVPP V6772-1 are preserved with a better bone surface texture and the predominant colour is grey. However, the postdentary portion of IVPP V6772-1 is similar in texture and colour to IVPP V6772-2, so the two may have been disarticulated before death, and they might conceivably have come from the same individual. As preserved, the left splenial is 205 mm long, measured round the curve, and the right splenial 230 mm long. The symphysis is thick, and measures 48 mm antero-posteriorly at the midline, compared to 28 mm at the narrowest point of the anterior portion. This midline thickening is seen also in other pareiasaurs, such as *Pareiasuchus* (Lee *et al.* 1997: fig. 7C). There is a distinct channel running the entire length of each splenial, beginning as a depression that is open posteriorly at the front, and then the medial thin wall rises some 40 mm behind the symphysis to a height of 25 mm, where the wall bounds the base of the medial flange of the dentary. The lateral wall of the splenial longitudinal groove begins low and broad, and rises to a height of 20 mm above the base of the groove. These medial and lateral splenial walls are incomplete, but would have bounded the anterior part of the Meckelian fossa (Fig. 7C, me.f.). The base of the canal is somewhat irregular, and it is hard to identify a step where the anterior process of the angular inserted. In ventral view (Fig. 7E), the splenial expands to an approximate medio-lateral breadth of 32 mm on the left and 35 mm on the right, perhaps indicating the true original breadth of the lower portion of each hemimandible, and perhaps confirming the suggestion above that IVPP V6722-1 might have been gently medio-laterally compressed.

The external surface of both specimens is sculpted with a subtle, and low pattern of small bosses, 1-2 mm in diameter, and thin ridges, each less than 1 mm wide. If anything, the ventral face of the splenials seem more sculpted than the dentary and post-dentary elements in IVPP V6722-1.

Right dentary - The unnumbered specimen, in a box of uncatalogued fragments and scraps of bone associated with IVPP V6722, is a roughly prepared anterior right hemimandible, exactly matching IVPP 6722-1, and fitting neatly on the midline symphysis. The specimen (Fig. 8A, B) carries 17 teeth, some complete and others rather broken, and it shows the dental lamina and the medial face of the dentary that roofs the anterior portion of the Meckelian cartilage. The lateral surface is rough and poorly preserved, and it terminates above the point at which it would have contacted the splenial.

Dentition - The teeth of IVPP V6772-1 (Figs. 7A–C, 8C, D) individually have cylindrical roots, nearly perfectly circular in cross section, measuring 7-9 mm across (Table 1). These expand into the slightly flattened, rhomb-shaped crown, which is typically 14-20 mm dorso-ventrally high and 11-12 mm antero-posteriorly wide. With 19 teeth in 200 mm, this means the crowns overlap slightly, the anterior margin of each tooth at its widest part being located medially of the posterior margin of the tooth in front. The teeth individually vary in length and breadth (Table 1), but there is no sign of a regular pattern of increasing or diminishing size from front to back – tooth size is difficult to measure because many teeth have partly damaged edges. The teeth are curved convex-laterally from ventral root to dorsal crown. The dorsal margin of the dentigerous portion of the maxilla is little more than 10 mm thick medio-laterally, and so the teeth form the bulk of this element, being separated by thin inserts of bone. The root slopes dorso-laterally, and emerges at the very lateral edge of the dentary with which the lateral (lingual) face of the tooth crown is more or less parallel, each rising near-vertically. In medial (labial) view (Fig. 8D), the tooth crowns are somewhat concave medially. Each crown is an asymmetrical rhomb, with the shorter edges ventrally, and the longer edges dorsally, above a marked cingulum (Fig. 8E, ci). Above the cingulum, in fully erupted teeth, a midline bulge ascends the medial face of the crown, demarcated by two ridges (Fig. 8E, ri) that curve from the cingulum to the denticles on either side of the middle two denticles at the dorsalmost point of the tooth.

A series of seven or eight well-marked, pointed denticles or cusps extends along each margin of the tooth crown, giving a total of 13-17 on each tooth crown (Fig. 8C–E; Table 1). Unlike the more longitudinally oriented cusps in the maxillary teeth of *Sanchuansaurus* (see above), these cusps point more to the sides, in other words anteriorly and posteriorly, as seen also in species of *Pareiasuchus* and *Scutosaurus* (Lee *et al.* 1997: 325).

Despite previous assertions about *Huanghesaurus* (coded as '*Shansisaurus*' by Lee 1997: 231; Jalil & Janvier 2005: 192), this taxon shows a distinct cingulum (Fig. 8E, ci),

demarcating the somewhat hollowed, or spoon-shaped labial crown face. The cingulum traverses the entire width of the tooth, and bears two or three denticles on either side of a substantial midline lingual ridge that bears two distinct longitudinal ridges close to the midline, and divides the crown

Comparison - The lower jaw specimens allow coding of several phylogenetically informative characters: the splenial forms the ventral portion of the mandibular symphysis (Lee 1997, character 51; Tsuji 2013, character 46); the ventral surface of the angular is smooth and with no boss (Lee 1997, character 52; Tsuji 2013, character 47); there is a small dorsal projection on the retroarticular process (Lee 1997, character 54; Tsuji 2013, character 48); there is no lateral shelf on the articular (Tsuji 2013, character 49); the teeth are labiolingually compressed, leaf-shaped, and with small denticles on the tooth crown (Lee 1997, character 58; Tsuji 2013, character 52); cusps are regularly spaced along the tooth crown (Lee 1997, character 61; Tsuji 2013, character 53); there are more than 11 marginal cusps on each dentary tooth (Lee 1997, character 60; Tsuji 2013, character 55); the mandibular teeth show a distinct, triangular ridge, narrowing towards the crown of the tooth (Lee 1997, character 63; Tsuji 2013, character 56); there is a cingulum present, with small cuspules (Lee 1997, character 64; Tsuji 2013, character 57); and there is no caniniform region in the tooth row (Tsuji 2013, character 120).

AXIAL SKELETON

INTRODUCTION

The original materials of *Shihtienfenia* included ‘about 20 vertebrae’ in the holotype (IVPP V2717) and ‘11 more or less well preserved dorsal vertebrae and some fragments of the same’ in the paratype (IVPP V2718, specimen now missing). Young & Yeh (1963: 207-208) described four isolated possible cervical vertebrae, four isolated anterior dorsals, a block containing four posterior dorsals, perhaps numbers 16-20, near to, but not quite contacting the sacrum, a block of five sacral vertebrae, and two isolated caudal vertebrae, one of which belongs to IVPP V2717. The specimens are somewhat distorted, and some are incomplete, but the articulated series, the appropriate sizes of all materials (Table 2), and the apparently

close proximity of all specimens, is strong evidence that the holotype (IVPP V2717) is a single specimen.

The *Huanghesaurus* holotype includes 13 vertebrae (IVPP V6722-4 to 16) and six partial ribs (IVPP V6722-17 to 22) and, as ever, these are hard to assign to their exact locations in the vertebral column. Pareiasaurs typically have 17-21 presacral vertebrae, the lower numbers being found in more basal taxa (Lee 1997). It is likely the 13 vertebrae of *Huanghesaurus* come from a single individual, as they were all found together in one spot (Gao 1983), they appear to match in overall dimensions, and they show subtly changing morphology from one to the next. Clearly, several vertebrae are missing, and the present materials do not permit any estimate of total presacral vertebral numbers (Lee 1997, character 67).

The first vertebrae (IVPP V6722-4 to 7) appear to form an articulating sequence (Gao 1983: fig. 2, pl. 1, fig. 6), and they are quite different in morphology from the others (IVPP V6722-8 to 16). The first four are identified as posterior cervical vertebrae on the basis of three characters: the parapophysis and diapophysis are entirely distinct from each other, the transverse processes are located far anteriorly (Jalil & Janvier 2005: 76), and the neural spine, most unusually, slopes forwards. Of the further two criteria given by Jalil & Janvier (2005: 76), we see some compression of the centra, but not 'the very pronounced compression' they note, nor do the specimens bear the longitudinal, median ridge on the ventral surface seen in the Moroccan pareiasaur. The other vertebrae (IVPP V6722-8 to 16) are identified as dorsals, and probably posterior dorsals, on the basis of their short centra, fused rib attachments located less anteriorly, near-vertical neural spine, and the massive transverse processes, resembling in many ways the middle to posterior dorsals of the Moroccan pareiasaur (Jalil & Janvier 2005, figs. 32, 33).

Few phylogenetically informative characters of the axial skeleton can be coded with confidence. In that all putative presacral vertebrae of both *Shihtienfenia* and *Huanghesaurus* show transverse processes with rib attachments, there is no evidence that either specimen had ribless lumbar vertebrae (Lee 1997, character 68; Tsuji 2013, character 62). *Shihtienfenia* has five sacral vertebrae (Lee 1997, character 93; Tsuji 2013, character 63). Further, *Shihtienfenia* shows the primitive amniote morphology of the second and third sacral ribs showing only slight dorsoventral compression (Lee 1997, character 94; Tsuji 2013, character 84).

POSTERIOR CERVICAL VERTEBRAE

Young & Yeh (1963:207) refer to 'four isolated neck vertebrae' of *Shihtienfenia*, of which three are incomplete centra, and cannot be further described, and the fourth is more complete. It presents an unusual shape, showing the somewhat crushed and incomplete centrum and the right-hand lateral portion of the vertebra. The centrum (IVPP V2717) is tall and narrow (Table 2) and the paired axially oriented bases of the neural arch (Fig. 9A, n.a.) are clear, spaced some 30 mm apart. The lateral portion of the vertebra includes the prezygapophysis, projected far laterally, up to 140 mm from the midline, and with an articular facet 80 mm mediolaterally long and 35 mm anteroposteriorly deep. Beneath the prezygapophysis, a wall of bone descends vertically, and expands forward into the flared transverse process (Fig. 9A, t.p.) with a facet some 110 mm long at most. This vertical lamina beneath the prezygapophyseal articular facet also flares backwards as a separate process, but the detail is unclear because the posterior part of the vertebra is incomplete. Such broad posterior cervical vertebrae, with a wall-like flange connecting the laterally projected prezygapophysis and transverse process, are typical of pareiasaurs (e.g. Jalil & Janvier 2005; Tsuji & Müller 2008; Tsuji 2013).

The four posterior cervicals of *Huanghesaurus* are two rather incomplete specimens, consisting of centrum and base of the neural arch only (IVPP V6722-4 and 5) and two rather more complete specimens (IVPP V6722-6 and 7). The description is based primarily on the latter two specimens, with comparative remarks for the others (Table 3). In these, the centrum is more or less square when viewed laterally (Fig. 9B), with a slightly emarginated ventral margin, and broadly overturned articular faces. The mid-central pinching is more marked when viewed ventrally, but there is no clear mid-ventral ridge. The articular faces are roughly circular in shape, with a slight ventral prolongation associated with the ventral lateral pinching of the centrum. Both faces are deeply amphicoelous, with a deep, centrally located pit, which is much deeper on the posterior than the anterior face. In lateral view, the diapophysis and parapophysis are pronounced (Fig. 9B, dp., pp.), each standing well proud of the centrum surface, and located about midway between the two articular ends. These two rib facets are of about equal size in three of these vertebrae, each measuring about 20 x 33 mm, but the diapophysis is somewhat narrower in IVPP V6722-4, measuring 14 x 32 mm. They are oval, and each slopes back and down. Their diagonal arrangement means that the diapophysis is set slightly more posteriorly, the parapophysis more anteriorly, implying that the ribs canted substantially backwards.

The contact between centrum and neural arch is hard to detect, partly because it may have been fused in life, but also because of the rather coarse preservation. Presumably the line

of contact ran along the base of the neural canal, and then between diapophysis (on the neural arch) and parapophysis (on the centrum). The base of the neural arch surrounds a narrow neural canal, 27 mm wide and 14 mm high, and beneath the rather modestly sized prezygapophyses, the whole neural arch is only 50 mm wide, just over half the width of the centrum. The prezygapophyses, best seen in IVPP V6722-4 (Fig. 9B, prz.), are set back and do not project in front of the line of the anterior articular face of the centrum. The articular faces are oval, measuring 45 x 24 mm, and with the long axis oriented nearly parasagittally. They are tilted up at about 35° from medial to lateral. The postzygapophyses, best seen in IVPP V6722-6 (Fig. 9B, poz.), have an articular face that measures 50 x 28 mm, with the long axis oriented parasagittally. The postzygapophyses are set far back, and project entirely beyond the posterior margin of the centrum.

The neural spine is most unusual, sloping substantially forwards (Fig. 9B, n.sp.). Its base is set well back, emerging above the proximal portions of the postzygapophyses. It then slopes forwards, with the posterior margin beginning above the posterior margin of the centrum, and running upwards and forwards, with a gentle concave curve, and the anterior margin more or less straight. The neural spine is 85 mm long on the anterior margin, and 80 mm along the posterior margin from the dorsal root of the postzygapophysis to the tip. The spine is somewhat oval in cross section, with modest anterior and posterior midline ridges, The distal tip of the spine broadens laterally, with a maximum width of 50 mm, and maximum antero-posterior depth of 24 mm. The distal end bears two broad bosses, one on each side, forming a symmetrical, C-shaped curved head in dorsal view, with the concave face anteriorly, and the convex surface posteriorly.

ANTERIOR DORSAL VERTEBRAE

Three incomplete and laterally compressed vertebrae of the holotype of *Shihtienfenia* (IVPP V2717) are identified as anterior dorsals (Young & Yeh 1963: 207-208, fig. 5). The centra are tall and narrow (Table 2), doubtless much exaggerated by lateral crushing. The articular faces of the centra show deep central excavations, and broadly overturned lips. The anterior face of the vertebra identified as 11 (Fig. 9C) shows a concave articular face of the centrum, surmounted by distorted transverse processes, one pointing up and the other down, and the neural spine twisted round to the side. On the left sides of vertebrae identified as 11 and 12 (Fig. 9D) an extensive bone lamina descends on the lateral face of the centrum, providing the diapophyseal articulation at just above mid-height of the centrum, and the parapophyseal

articulation 60 mm or so higher on the transverse process, although this portion is not preserved. Vertebra 13 (Young & Yeh 1963: fig. 5) is incomplete and retains little to describe (Fig. 9E), whereas vertebra ?14 is more complete, with the anterior view (Fig. 9F) showing the massive zygapophyses, a circular neural canal measuring 25 x 27 mm, and the base of the anteriorly located neural spine. The hypantrum noted by Young & Yeh (1963: fig. 5, top right) cannot be seen.

A single vertebra that formed part of the holotype of *Shansisaurus xuecunensis* (Cheng 1980: fig. 18; CAGS V301) appears to be a partial anterior or middle dorsal. The anterior articular face is slightly taller than wide and deeply excavated. It is surmounted by a tiny neural canal, and expands substantially laterally in the preserved right-hand side, which shows a large prezygapophysis projected up to 85 mm from the midline. Beneath it, and projecting only slightly less far is the transverse process, apparently with a single diapophyseal head.

POSTERIOR DORSAL VERTEBRAE

The five articulated posterior dorsal vertebrae of *Shihtienfenia* (Fig. 10A–C) are all incomplete, lacking the neural spine in all cases, the prezygapophyses in numbers 16, 17 and 20, the postzygapophyses in numbers 16 and 20, and much of the posterior part of the centrum in 20. Note that the numbering comes from Young and Yeh (1963, fig. 2), based on context of discovery. These vertebrae all share similar dimensions, so far as can be measured (Table 2). The centrum is narrow, taller than broad, with deeply concave sides. The articular faces are deeply concave, with the deepest portion penetrating in the centre. The marginal lips of the articular faces are substantially turned over, and ventrally, these overturned portions of the articular faces extend considerably. In ventral view (Fig. 10C), where the vertebrae meet, the anterior and posterior overturned articular faces form a substantial diamond-shaped facet between each pair of vertebrae, some 60 mm measured axially. Thus, the ventral portion of each centrum, which typically measures 90 mm long (Table 2; Fig. 10C), is composed of three equal-length portions, the anterior articular facet and the posterior articular facet, separated by only 30 mm of ventral centrum which forms a narrow ridge between. This extreme articular foldover and ventral facet is not seen in dorsal vertebrae of *Huanghesaurus*.

In all five vertebrae, the rib attachment is projected on a short transverse process (Fig. 10A, B, t.p.) which projects laterally little more than the prezygapophysis. The rib facet, representing the fused diapophysis and parapophysis, is broad and rounded, not as elongate as

in *Huanghesaurus*, with the long axis, 50-55 mm long, slanting at 45° from posterodorsal to anteroventral, and 30 mm measured orthogonally. In lateral view (Fig. 10B, prez., poz.), the prezygapophyses project far forward of the anterior margin of the centrum, and this is matched by the anterior location of the neural spine and postzygapophyses which, although huge (the postzygapophyseal facet of presacral 19 measures 95 x 55 mm), do not extend behind the posterior articular face of the centrum.

The posterior dorsal vertebrae of *Huanghesaurus* (Table 3) include several more or less complete specimens (IVPP V6772-8, 12, 13, 15), and others (IVPP V6772-9, 11, 14) missing most of the neural arch and transverse processes, and one lacking the centrum (IVPP V6772-16). The most complete example (IVPP V6722-15) is a massive vertebra, with a short centrum, and massive zygapophyses and transverse processes (Fig. 10D–F). In lateral view (Fig. 10E), the centrum is substantially constricted from side to side, reduced to half the width of the articular faces, but the ventral emargination, although pronounced, is less substantial. The articular faces lie roughly at the same level with no vertical offset, but the centrum is distorted moderately laterally. The articular faces are similar in shape, being somewhat circular, but wider than high, and the anterior face is slightly larger than the posterior (Table 3). The centrum is deeply amphicoelous, with a narrow, but very deep hollow in the centre of each articular face (Fig. 10D, F).

The anterior view of the neural arch consists of massive, flat lateral laminae on either side of a tiny neural canal (Fig. 10D, n.c.), about 18 mm wide and tall (it is up to 25 mm wide in other dorsal vertebrae). These lateral laminae rise to the base of the prezygapophyses, which are missing, but presumably had articular faces tilting down and back, to judge from the postzygapophyses. The transverse process sprouts from immediately below the base of the prezygapophysis (Fig. 10D, t.p., prz.), and runs up and slightly backwards, terminating in a broad distal tip. The rib facet, clear on the right-hand side, is a single structure, oriented at 45° anteroventrally, and shaped like an extended, pinched oval, some 80 mm long, 25 mm deep in the anterior part and 23 mm in the posterior, and narrowing to 12 mm wide in the middle (Fig. 10E, r.f.). The articular face of this facet is concave. In other dorsals (e.g. IVPP V6722-8), the transverse process is at most 50 mm wide antero-posteriorly. The lamina beneath the transverse process runs from its distal end to the rib facet located anterodorsally on the side of the centrum; this lamina is from 15 to 25 mm thick anteroposteriorly. In posterior view (Fig. 10F), the transverse process proper stands distinctly apart from the lamina beneath, the division being marked by a substantial depression in the whole ventral part of the lamina. The

depth of the lamina varies from substantial in IVPP V6722-8 to more shallow in IVPP V6722-15.

The postzygapophyses are massive, each extending some 120 mm from the midline, and so similar in length to the transverse processes below. Each postzygapophysis (Fig. 10D–F, poz.) extends more or less horizontally from the midline, and the articular face is canted at an angle of some 20°, facing ventro-anteriorly. The facet is not flat, but curved from front to back and from distally to proximally, and it sweeps down to meet the dorsal margin of the transverse process, in posterior view (Fig. 10F). There is a deep space between the postzygapophyses in the midline, and the tiny (17 x 17 mm) neural canal lies some distance below, and partly behind the raised margin of the posterior articular face.

The neural spine stands nearly vertical, unlike that of the cervicals, but it is similarly massive and carries a similar expanded double-bossed distal end. The neural spine emerges from the top of the massive postzygapophyses, and because of the way they sweep downwards to the upper margin of the transverse process, and because the shortening of the whole vertebra, a Λ-shaped cavity is formed beneath the base of the neural spine when seen in anterior view (Fig. 10D). The neural spine is 105 mm tall, broadening from a minimum width of 30 mm to 52 mm at the massively expanded and heavy dorsal tip. In life, these massive boss-like neural spines probably articulated with each other, forming a basis for some of the massive dorsal armour, as shown by Seeley (1892: pl. 17) for *Pareiasaurus*. The shaft of the neural spine is deeper antero-posteriorly than wide laterally, and it has a somewhat triangular anterior face, coming to a ridge that extends in the midline from base to tip of the neural spine. In posterior view (Fig. 10F), the neural spine bears a midline ridge proximally, but this splits into two narrow ridges that diverge dorsally. The distal end of the neural spine in posterior view carries a broad boss at each side, and is slightly hollowed between; the diverging ridges each run to the base of the lateral distal bosses.

Specimen IVPP V6722-15 is illustrated by Gao (1983: fig. 3), but the posterior view is labelled as ‘anterior’, and the details of the vertebra are slightly stylised, with an inaccurate rendition of the posterior depression beneath the transverse process. The ‘figure of eight’ rib facet terminating the transverse process seen in this specimen (Fig. 10E, r.f.) is very similar to that shown by the Pareiasauria gen. et sp. indet., from the Upper Permian of Morocco (Jalil & Janvier 2005: 80).

Accessory articulations between dorsal vertebrae, the hypantrum and hyposphene, were noted in dorsal vertebrae of *Shihtienfenia* by Young & Yeh 1963: 207, fig. 5) and in dorsal vertebrae of *Huanghesaurus* by Gao (1983: 196), but these identifications seem to be

incorrect. The structures labelled by Young & Yeh (1963: fig. 5) are sketchy and hard to match with the specimens. Young & Yeh (1963: 207) describe these structures as follows: 'In the anterior view the "hypantrum" is weakly indicated. Between it and the neural canal there is a weakly developed pyramid-like development which [is] not found in any of the related forms. This structure is, however, missing in the fourth isolated vertebra." Further, in describing *Huanghesaurus*, Gao (1983: 196) reports that "The hypantrum and hyposphene are all pronounced" in the dorsal vertebrae, although they are not marked in the figures or further described. In *Shihtienfenia*, these appear to be singular midline structures, and little more than the hollow between the base of the flaring postzygapophyses ('hyposphene') and an irregular single, midline projection above the neural canal ('hypantrum'). In *Huanghesaurus*, for example the dorsal vertebrae IVPP V6722-8, 10 and 15 show a slight expansion of the lamina below the location of the (missing) prezygapophyses, on either side and close to the midline, just above the neural canal (Fig. 10D), and these angular structures are seen also in IVPP V6722-10, but these do not show any facet, and there is no matching structure beneath the postzygapophyses. Further, these putative facets are tiny when compared to the rather substantial zygapophyses, and are presumably just small projections that perhaps carried intervertebral muscles or ligaments and no more.

Such additional articulations are well known in trunk vertebrae of sauropodomorph dinosaurs (Apesteguia 2005) and theropods, and might be a saurischian synapomorphy, as they are absent in ornithischians (Gauthier 1986; Langer & Benton 2006). In addition, these accessory articulations have been identified in some basal archosaurs (notably, large rauisuchids), basal sauropterygians (Rieppel 1994), placodonts (Rieppel 2000), and diadectids (KIssel & Lehman 2002). In these taxa, the hyposphenes and hypantra are paired structures lying between, and slightly below the zygapophyses, and with definite facets for contact when the vertebrae are articulated. The hypantra and hyposphenes described in the Chinese pareiasaurs appear to be illusory.

SACRAL AND CAUDAL VERTEBRAE

The only sacrum so far reported is a substantial specimen in the type of *Shihtienfenia* (IVPP V2717) showing five vertebrae in articulation (Fig. 11). Young & Yeh (1963: 208) note that the first of the series is broken, and they speculate that there might have been a further sacral in front, making six in all. This is a high figure, in view of the fact that pareiasaurs generally had four or five sacral vertebrae; Lee (1995, 1997: 239-240) prefers to regard the putative

sixth sacral of *Shihtienfenia* as the first caudal. These statements may sound confusing, in that the first authors refer to an additional anterior sacral, and Lee refers to a putative additional posterior one. Young & Yeh (1963) are right that the first sacral is represented by a substantial sacral rib on the left side, but Lee (1995, 1997) is correct that the posteriormost of the six vertebrae in the block is likely the anteriomost caudal.

The block of six vertebrae is fused, and the centra of vertebrae 2-5 form a dorsally convex curve, running smoothly from one to the next (Fig. 11A; Table 2). Despite distortion in many specimens, this arch seems so smooth and regular that it may be original. As noted, the first vertebra in the series is incomplete, missing most of the centrum. The postzygapophyses are present, but the neural spine is missing.

The divisions between centra 2 to 4 are hard to make out because of the close association of these vertebrae, and the absence of extreme broadening or overturn at the articular faces. Sacral 5 shows a more spool-shaped centrum, with slightly expanded articular ends, and this is more marked in caudal 1. Sacral centra 2-4 then show little lateral narrowing, and no sign of a ventral ridge (Fig. 11D). Sacral 5 and caudal 1 do show some lateral pinching, but the ventral view shows no sign of a narrow ridge. All centra are of roughly equal length (Table 2), but observations on the articular faces and dorsal regions of the centra are impossible because of the way the specimens are so closely associated. The anterior face of sacral centrum 1 is partly obscured, but the posterior face of caudal centrum 1 appears deeply excavated.

In the more complete sacrals 2-4, the neural spine is near vertical, and located well forward (Fig. 11A, B, n.sp.), as in the dorsals. The distal tips of the sacral neural spines are missing, but the remainder of the three spines is a laterally compressed rod, 55 mm long anteroposteriorly at the base and 45 mm at the distal end, as preserved, and from 25 mm wide mediolaterally at the base and 12 mm distally. The neural spine flares ventrally into the postzygapophyses: these diminish substantially from a length of 80 mm in sacral 1, to 45 mm in sacrals 2 and 3, and 40 mm in sacral 4. At the same time they become narrower, and directed much more dorsally than in the dorsal vertebrae, where they are massive laterally directed elements. The angle of the midline of the postzygapophyses in dorsal vertebrae was some 10^{o} posterior to lateral, whereas these sacral postzygapophyses are oriented at some 60^{o} posterior to lateral. The prezygapophyses are less clear, but can be seen firmly adhering below the narrow postzygapophyses of sacrals 3 and 4 (Fig. 11A–C, poz., prz.). Presumably the substantial fusion of the sacral centra and ribs reduces the need for strengthening of the vertebral column by substantial zygapophyses.

The lower neural arch expands anterior to the postzygapophysis to form a short transverse process that extends nearly vertically, but slightly posteriorly ventrally over the upper lateral face of the centrum. Sacral ribs are seen on both sides, but the first and second are best on the left. The first sacral rib appears largest, and it runs diagonally backwards from a massive near-vertical medial attachment to the neural arch of sacral vertebra 1 (Fig. 11A, D, s.r.1). The first sacral rib on the left measures 180 mm long on its dorsal margin, and tapers from a dorsoventral height of 115 mm proximally to 65 mm distally. At this distal end, it appears to be firmly fused to the second sacral rib of the left side, a shorter element, 105 mm along the dorsal margin. The joint lateral facet measures 65 mm dorsoventrally high by 70 mm anteroposteriorly wide at the dorsal margin, and 45 mm at the ventral margin. Young & Yeh (1963: fig. 3) show a putative portion of left sacral rib 3 forming part of this complex, but this cannot be seen in the specimen. Sacral ribs are seen on all vertebrae on the right side, but they are compressed to the midline, and lack their distal portions. The transverse processes and sacral ribs extend smoothly beneath and behind the prezygapophyses, and the junction between transverse process and rib is not clear. As preserved, these sacral ribs project posteriorly and ventrally, narrowing substantially distally, but their original length and orientation cannot be determined because of distortion and breakage.

The first caudal vertebra in this block (Fig. 11), identified as a putative sixth sacral by Young & Yeh (1963: 208), but as a first caudal by Lee (1997: 240), is similar in overall shape to the fifth sacral, showing the same shape of centrum, much diminished zygapophyses, the prezygapophyses spanning little more than 55 mm in all measured mediolaterally, a tiny fraction of the span of the zygapophyses of the dorsal vertebrae. The transverse process and presumed fused rib appear short, but the distal end on the right side is damaged, and this structure is missing on the left. Young & Yeh (1963: 208-209) mention one other caudal vertebra of the holotype (IVPP V2717) and one of the paratype (IVPP V2718, missing), but they ‘are too imperfect for a detailed description’.

RIBS

A number of ribs and rib fragments of *Huanghesaurus* are preserved, some of them double-headed (IVPP V6722-17 to 19) and others single-headed (IVPP V6722-20 to 22). One double-headed rib, lacking its distal end (IVPP V6722-18; Fig. 12A, tu., ca.), shows the substantial tuberculum and smaller, projecting capitulum. This 188-mm long fragment measures 95 mm across the maximum spread of the articular heads and 40 mm deep. The

capitulum extends on a distinct lateral projection, some 50 mm long, extending from the side of the broader tuberculum. The single-headed ribs have elongate figure-of-eight articular facets that match the facets on transverse processes of presumed posterior dorsal vertebrae, such as IVPP V6722-20 (Fig. 12B). These articular facets vary from 71 mm along the maximum axis to 125 mm in IVPP V6722-22 (Fig. 12D). This last, most massive, of the several ribs, has a relatively straight shaft varying from 34–38 mm in maximum dimension, and showing the beginning of a deep groove on the posterior margin. This does not seem to correspond to any distal broadening of the rib, so *Shihtienfenia* did not have the derived condition of broadened ribs seen in *Pumilopareia* (Lee 1997, character 69).

The double-headed ribs presumably pertain to the cervical or anterior dorsal vertebrae, and the single-headed ribs to the mid to posterior dorsals. Judging from comparisons with articulated pareiasaur skeletons (e.g. Seeley, 1889, 1892; Tsuji 2013), the most substantial rib (IVPP V6722-19) may come from the middle region of the torso, corresponding to the largest dorsal vertebrae, and perhaps the greatest mass of the torso region.

SHOULDER GIRDLE AND FORELIMB

SCAPULOCORACOID

The scapulocoracoid of pareiasaurs is a three-part element, consisting of a scapula and two coracoid elements, often termed the anterior coracoid and coracoid (= posterior coracoid; = metacoracoid), whose homologies to the equivalent elements of turtles (Lee 1998) and mammals (Vickaryous & Hall 2006) are complex and debated. Here, we term these two elements the anterior and posterior coracoids respectively, and regard the acromion process of the scapula as equivalent to that of other basal amniotes, and not a modified anterior coracoid (Lee 1998).

The right scapula of *Shihtienfenia* (IVPP V2717) is a long slender element, seemingly more or less complete because it lacks broken edges (Fig. 13; Young & Yeh 1963: fig. 6). The element is maximally 630 mm dorsoventrally long, of which 450 mm forms the scapular blade, and 180 mm the acromion process and glenoid. The distal end of the blade apparently tapers to a rather rounded distal termination; the margins of the distal end are partly repaired with plaster, but sufficient of the edges are original to suggest the shape is about right. The distal portion of the blade is flat and slightly spoon-shaped, and the blade thickens proximally

in a mediolateral orientation from 15 mm to 20 mm, and 35 mm proximally, at which point it measures 77-80 mm wide anteroposteriorly. The lateral face of the scapular blade shows coarse longitudinal striations. On the medial face, the distal end is roughened, and the remainder shows similar coarse longitudinal striations, including a large, irregular midline ridge.

Proximally, the anterior margin of the scapular blade broadens and extends into the acromion process on the anterior margin (Fig. 13A, B, D, acr.) and an internal process seen in medial view (Fig. 13D, int.pr.). The acromion process is massive, located on the anterior scapular margin, and with a roughened boss some 55 mm dorsoventrally long and 25 mm mediolaterally wide at most. The internal process is slightly broken, but extends as a broad ridge to the coracoidal margin. The proximal portion of the scapula is 115 mm anteroposteriorly wide at the level of the acromion, and up to 60 mm mediolaterally deep. It narrows slightly to 95 mm and 55 mm respectively, and expands towards the glenoid, which is incomplete and cannot be described clearly.

The left scapula consists of a blade and a separate portion of the fused proximal scapula, anterior coracoid, and posterior coracoid (Fig. 14; Young & Yeh 1963: fig. 7, right). The scapular blade is preserved for 460 mm from acromion to distal end, which is irregularly broken. This is equivalent to the length on the right side above the acromion, so interpretations of the distal end of the former might require care. On the left side, there is no sign of thinning, nor of the apparently spoon-shaped expanded and curved distal end seen on the right. As preserved, the left scapular blade narrows from 120 mm distally to 85 mm proximally, measured anteroposteriorly. At the same time, the blade thickens from 30 mm deep mediolaterally at the distal end to 75 mm in line with the acromion. This creates a somewhat cylindrical scapular blade, especially proximally (Lee 1997). Anterior and posterior margins of the scapular blade are nearly straight. On the anterior margin, the acromion and medial internal process form roughly equal-sized processes on either side of the clavicle. The roughened distal face of the acromion measures 80 x 25 mm. Below the acromion, the scapula expands to an anteroposterior width of about 200 mm, partly by an anterior flange, but mainly through the upper portion of the glenoid facet (Fig. 14A, gl.).

Sutures between scapula, posterior coracoid, and anterior coracoid are hard to distinguish in lateral view (Fig. 14A), and they are entirely obscured in medial view. Further, the anterior, ventral, and posterior margins of the posterior coracoids are missing, so their original dimensions cannot be determined. At most, the anterior coracoid-posterior coracoid plate measures 270 mm anteroposteriorly. The glenoid (Fig. 14A, gl.) is a broad and deeply

concave articulation face with its long axis oriented at approximately 45° above horizontal. The glenoid measures 210 mm long at most along this long axis, and 105 mm wide, measured orthogonally to the long axis. A large, deep coracoid foramen (Fig. 14A, co.f.) is located just anterior to the glenoid and it penetrates the posterodorsal portion of the anterior coracoid deeply. In medial view (Fig. 14B), the scapulocoracoid presents a smooth aspect, with no evidence of the sutures dividing scapula from posterior coracoid and anterior coracoid, but the groove to the subscapular fossa and the deep foramen, which connects with the coracoid foramen are evident.

The left scapulocoracoid of *Huanghesaurus* (IVPP V6722-22) presents similar characters (Gao 1983: fig. 197), but is one-quarter again larger. The whole specimen (Fig. 15A–D) is at most 870 mm long, of which the scapular blade is about 600 mm. The distal end is incomplete, and has a maximum anteroposterior width of 190 mm. The blade is roughly straight-sided, but it narrows to a minimum anteroposterior width of 95 mm, and expands to 130 mm just above the acromion process. The blade is flattened distally, becoming more cylindrical proximally. The acromion process is set on a pedestal projecting from the anterior margin of the scapula (Fig. 15C, D, acr.), and the medial part of the scapula expands anteriorly. The glenoid is steeply angled from anterodorsal to posteroventral, and measures 210 x 105 mm, with a twist halfway along its length. In lateral view, the anterior and posterior coracoids (Fig. 15A, B, aco., pco.) have incomplete ventral margins, and they seem to have been of similar dimensions. The coracoid foramen penetrates the posterodorsal angle of the anterior coracoid in lateral view (Fig. 15B, D, co.f.), and passes upwards to emerge in the middle of the basal portion of the scapula, in medial view. The sutures between all three elements can just be discerned in lateral view, but they are invisible in medial view (Fig. 15C). The medial face is uniform and smooth, interrupted only by the substantial subscapular foramen, which measures 40 x 20 mm in diameter.

The left scapulocoracoid of *Shansisaurus xuecunensis* (CAGS V301), as illustrated (Cheng 1980: fig. 19; pl. 1, fig. 1), shows the same overall shape, size, proportions, and detail as in that of *Huanghesaurus* (Gao 1983: fig. 4). The scapular blade is long and tapers slightly, while its cross-sectional shape changes from rather flattened at the distal end, to more cylindrical proximally. The acromion is projected on a distinct square process, and has a distinct facet. The glenoid is angled at some 30° above horizontal and is distributed almost equally between scapula and posterior coracoid. The anterior coracoid is of similar dimensions to the posterior coracoid in lateral view, and it carries the exit of the coracoid foramen in its extreme posterodorsal corner, close to the junction of all three elements.

An incomplete right scapulocoracoid, IVPP V6727 (Fig. 15E, F), was assigned by Gao (1989: 1238-1239) to *Shansisaurus* sp., and he identified some diagnostic features, namely 'a long, narrow, and internally curved scapular blade; a weakly developed and low-positioned acromion; and a distinct precoracoid foramen, the internal opening of which is located entirely in the anterior coracoid'. These are, however, all features seen widely among pareiasaurs, and indeed in many basal tetrapods, and cannot distinguish *Shansisaurus* from *Shihtienfenia*. The specimen shows the proximal portion of the scapula and much of the anterior coracoid, but it lacks the margins of the latter, the posterior coracoid is missing, and the glenoid fossa is badly damaged. The coracoids are in the same plane as the scapula, and the suture between anterior coracoid and scapula is firmly fused, but still detectable laterally as a fine interdigitating suture line running from the anterior margin to the glenoid. The anterior coracoid is a broad flat plate in lateral view (Fig. 15E, aco.), and it bears a large coracoid foramen in its posterior portion, measuring 20 mm across (Fig. 15E, co.f.). The anterior coracoid thickens posterodorsally towards the glenoid, but this region is damaged and its original location and shape cannot be identified. The scapula has a massive proximal portion, 80 mm thick mediolaterally at the glenoid region. The base, as preserved, is 140 mm anteroposteriorly wide, and at most 255 mm ventrodorsally long, from the posterior coracoid-scapula suture to the broken distal end of the scapular blade. There is a massive, rectangular acromion process (Fig. 15E, F, acr.), rugose and 70 mm along its longest axis, extending substantially laterally from the scapula. In addition, the anterior, narrow margin of the lower portion of the scapula also extends as a rectangular process, with a 38 mm long rugose surface, and beginning 53 mm above the scapula-anterior coracoid suture. Above the acromion, the preserved portion of the scapular blade is of approximately equal anteroposterior width, measuring 70-75 mm, and 35 mm medio-laterally deep at the centre of the blade, which is marked by a gentle midline ridge. In medial view (Fig. 15F), the whole preserved portion of the scapulocoracoid is remarkably smooth and uniform, and the main feature is the very obvious and deep subscapular fossa (Fig. 15F, s.s.f.), which penetrates at the middle of the ventral margin of the scapula, on the faint interdigitating suture line between scapula and anterior coracoid. This fossa is at the ventral end of a slight channel down the medial face of the scapula, and the canal opening enters the anterior coracoid medially and exits as the coracoid foramen.

An isolated left scapula (IVPP V8533), assigned by Gao (1989: 1239, pl. 2K) to 'Pareiasauride gen. et sp. indet.', is a long, slender, strap-like element, 85 mm antero-posteriorly wide at the base of the blade, narrowing to 73 mm at mid-length, and expanding

distally to a maximum of 107 mm (Fig. 15G, H). The whole specimen is some 400 mm long, and it lacks the glenoid region, the contacts with the coracoids, and the distalmost parts of the blade. The scapula blade is a thin plate of bone, the primitive condition (Lee 1997, character 76), and not cylindrical as in some derived pareiasaurs. There is a modest acromion process on the anterior margin (Lee 1997, character 74), and behind it, visible in medial view (Fig. 15H), the base of another process, broken off. There is no groove on the anterior margin of the blade for a cleithrum.

These scapulocoracoids provide several phylogenetically informative characters, and they appear to be identical in all three nominal 'taxa': there is an acromion process on the anterior surface of the scapula (Lee 1997, character 74; Tsuji 2013, character 68); the scapular blade is very long, with a length at least three times the diameter of the glenoid fossa (Lee 1997, character 75; Tsuji 2013, character 69); and the dorsal edge of the posterior coracoid is almost horizontal, and meets the posterior border of the scapula at an angle of less than 135° (Lee 1997, character 77; Tsuji 2013, character 70). This last character has been coded as derived in previous studies, but it is hard to determine because it depends on the orientation of the scapulocoracoid, whether with scapular blade vertical or pointing posterodorsally. With the scapular blade vertical, as shown by Lee (1997: fig. 12), there is a distinct shift from a more or less horizontal suture line to one that runs at about 45° in a posterodorsal direction (equivalent to the 135° angle – measured from the anterior orientation - mentioned in previous character definitions). In the Chinese pareiasaurs, the sutures are hard to determine in the specimens thanks to extensive fusion. Although Cheng (1980: fig. 19) shows the posterior coracoid-scapular contact at an angle of about 30° in *Shansisaurus*, the angle is near-horizontal in *Shihtienfenia* and *Huanghesaurus* (Figs. 14, 15).

DERMAL SHOULDER GIRDLE

The dermal shoulder girdle of *Shihtienfenia* (IVPP V 2717) is represented by both clavicles, but no interclavicle. The clavicles are elongate, slender elements, each some 530 mm long and with a blade 70 mm anteroposteriorly long distally, and 80 mm proximally (Fig. 14B, 16A). The clavicle begins proximally as a flat, bladed element that fitted into the anterior facet of the (missing) interclavicle, then turns gently in line with the broadly semi-circular cross section of the whole pectoral girdle, terminating in a distal rod-like structure. As reconstructed, the posterior margin of the clavicle sits close to the anterior margin of the scapula, with the acromion process located laterally, and the medial internal process medially

(Figs. 13D, 16A, acr., int.pr.). There is no slot or distinct marking on the anterior margin of the scapula for the clavicles, so they presumably did not adhere closely in life.

This is confirmed by the dermal shoulder girdle of *Huanghesaurus*, which is represented by a pair of clavicles, but also a well-preserved interclavicle. A cleithrum occurs in the pareiasaurs *Embrithosaurus* and *Bradysaurus*, but has not been identified among the materials of *Shihtienfenia*, and the absence of a groove on the anterior margin of the scapula suggests there was no cleithrum (Lee 1997, character 79; Tsuji 2013, character 71).

The right and left clavicles of *Huanghesaurus* (IVPP V6722-23, 24) are both elongate, blade-like elements (Fig. 16B–E) that fitted tightly into the anterior groove on the interclavicle, and met each other in the midline of that element. The right clavicle is 515 mm long mediolaterally, and at most 120 mm deep anteroposteriorly at the proximal end. The clavicle narrows to 65 mm deep anteroposteriorly at mid-shaft, and the distal end is 62 mm deep. Proximally, the clavicle shows a long, narrow process on the dorsal (interior) surface (Fig. 16D, icl.pr. r.cl.) that fits snugly into the anterior groove on the interclavicle. The clavicle has a broad, rounded anterior portion, up to 50 mm deep dorsoventrally, that runs from the proximal to the distal end, and provides the structural strength of the element. The anterior portion is demarcated from the posterior flange of the clavicle, which is 15-20 mm thick dorsoventrally. The posterior flange (Fig. 16E, p.fl.) forms a deep slot at the proximal end, and the exact shape of the anterior margin of the posterior flange matches the anterior margin of the interclavicle. Distally, the posterior flange of the clavicle expands posteriorly into a short, 70 mm long mediolaterally oriented blade. This, and the middle and distal parts of the posterior flange acted as the major site of origin for the pectoralis muscle. The distal end of the clavicle is marked by the loss of the posterior flange, and a twist of the anterior margin to form a rounded tongue-like termination, covered in a sculptured region of longitudinally oriented irregular ridges, each 2-3 mm wide. The ventral (exterior) surface of the clavicle (Fig. 16C) shows a uniform, smoothly curved appearance, and a distinct tapering to the distal end.

The single, substantial interclavicle of *Huanghesaurus* (IVPP6722-25) is preserved more or less complete, lacking just the distal end of the left-hand anterior process (Fig. 16F, G). The whole element measures 345 mm wide across the anterior processes, and 310 mm anteroposteriorly, so showing the derived condition of a long anterior processes (Lee 1995; 1997, character 80). The anterior part of the interclavicle bears a deep facet for reception of the clavicles along its entire width (Fig. 16F, cl.f.). This facet has a roughened surface, and radiating ridges and grooves at the lateral ends, and there is a distinct lip at the midline

posterior margin, which overlapped the clavicles ventrally when they were in place. The posterior portion of the interclavicle is a short tongue-shaped structure, 92 mm wide at its narrowest, and 135 mm at its widest. The posterior process (Fig. 16F, G, p.pr.) is thickest in the centre, measuring 35 mm ventrodorsally. The posterior margin of the posterior process is curved around the arc of a circle, and it bears deep radial grooves, seen in both external (ventral) and internal (dorsal) views. These radial grooves are seen only along the posterior margin, and all are oriented anteroposteriorly, and they are deepest on the dorsal face. These were presumably structures for the attachment of parts of the pectoralis muscle, and were adapted to withstand substantial stresses and strains.

Together, the three dermal elements of the shoulder girdle formed a powerful supporting structure beneath the thorax, and the clavicles presumably met the anterior margin of the scapular blade at mid-length. The initial reconstruction (Fig. 16H, I), based on IVPP V2717 (Young and Sun 1963, pl. 1, 2), shows the broad thorax surrounded by clavicles below and scapulae round the sides. Here, the interclavicle is missing, but it would have bound the clavicles together into a powerful ventral cuirass that also provided the origin of the substantial pectoralis muscle.

HUMERUS

In the description of the humerus and femur, I use the terms ventral, dorsal, anterior, and posterior, assuming the limb is at rest, and in sprawling pose. Both humeri of the type specimen of *Shihtienfenia* (IVPP V2717) are preserved, the left essentially complete, and the right as a much distorted proximal portion that shows the proximal articular face, measuring 180 x 60 mm. The description is devoted to the left humerus (Fig. 17A–D), some 400 mm long, with an expanded proximal end, 295 mm wide at most, and an expanded distal end, 250 mm wide at most, and with a twist of the shaft that sets the major planes of the two articular ends at an angle of 45^{o} to each other. The proximal articular end carries the articulation for the glenoid of the scapulocoracoid, an elongate facet up to 210 mm long and 70 mm wide at the middle point (Fig. 17A–D, a.f.). The articular facet has narrow distal ends, and it rolls from proximally- to proximodorsally-facing in the anterior portion. In dorsal view, the proximal articular end of the humerus is roughly square, with the anterior dorsoventral prominent ridge that separates an anterodorsal face from the remainder of the proximal humerus. In ventral view (Fig. 17A), the proximal end of the humerus shows a flaring posterior and middle portion, and a massively thickened anterior margin that extends into the deltopectoral crest

(Fig. 17A–C, dpc.), which projects as a substantial boss about halfway down the length of the humerus. The narrow humeral shaft is oval, measuring 80 x 65 mm in diameter. The flared distal end of the humerus shows a damaged entepicondylar region, but a large and delicate ectepicondylar lamina extending on the dorsal face, for the distalmost 170 mm of the humerus (Fig. 17C, ect.). This terminates proximally as a thin lamina. Young and Yeh (1963, p. 210) noted that there is an entepicondylar groove, which runs parallel to the shaft orientation, on the anterior face of the lamina, but no ectepicondylar foramen. However, at the proximal end of the ectepicondylar groove, there is a distinct pocket or pit that has been scooped out by the preparators (Fig. 17B, ect.) – it is in the correct location to be an ectepicondylar foramen, but it is impossible to say whether this might indeed be a foramen or not. Suffice to say that all other pareiasaurs appear to possess such a foramen (Lee 1997, p. 237). In posterior view (Fig. 17D, ect., ent.), the ectepicondylar lamina provides a squared margin to the dorsal edge of the distal end of the humerus, the entepicondylar projection being less complete. The supinator process, forming part of the ectepicondylar lamina, projects (Fig. 17D, sup.). The distal end of the humerus is damaged, so the tibial and fibular condyles cannot be clearly distinguished.

The left humerus of *Huanghesaurus* (IVPP V6722-26) is a massive element, with more or less complete proximal end, but lacking the distal articular end (Fig. 17E, F). The bone is at most 350 mm long, as preserved. The massively expanded proximal portion is up to 360 mm across anteroposteriorly, and the shaft narrows to 85 mm, and the distal end expands again to 145 mm. In dorsal view (Fig. 17E), the anterior margin is marked by a massive process with a deeply roughened surface. Behind, there is a distinct and rather straight anterior dorsoventral line (Fig. 17E, a.d.v.l.) that marked areas for major dorsal musculature, the deltoid insertion on the deltopectoral crest portion, and the latissimus dorsi and triceps on the other side. This structure is a raised, broad ridge that separates the two planes of the anterior portion of the humerus. In the posterior portion is the deltopectoral crest (Fig. 17E, F, dpc.), an irregular ridge that wraps around from the posterior margin. In ventral view (Fig. 17F), the expanded proximal end of the humerus is broadly convex and apparently featureless.

The proximal articular facet is located entirely along the proximal margin of the element, with only its posteriormost portion visible in ventral view (Fig. 17F, p.a.f.). The face is elongate, 225 mm mediolaterally long in all, with a narrow anterior portion and a broader posterior portion, up to 82 mm across, which shows a distinct corkscrew twist, matching the natural rolling motion of the humerus as the forearm moves position in the typical sprawling pareiasaur posture. The humerus shows torsion, the long axis of the proximal articular head

set at about 60-70° to the distal, but the absence of the distal articular facets makes this uncertain.

The distal end of the humerus, although missing the articular condyles, shows distinct ectepicondylar and entepicondylar expansions. These lie on either side of the deep anterodorsally located intercondylar fossa (= trochlear fossa; olecranon fossa; Fig. 17E, ic.f.), the deep channel in which the substantial olecranon of the ulna could move. The entepicondyle consists of a narrow bone rod that encompasses an entepicondylar foramen (Fig. 17F, ent.f.). The proximal part of the encompassing bone rod is original, but the distal part of the rod has been remodelled in plaster, so its original dimensions are not certain. Nonetheless, the proximal portion shows that the entepicondylar foramen was entirely surrounded by bone, measured 32 x 10 mm, and angled from an antero-distal to a postero-proximal orientation. The ectepicondyle projects substantially dorsally as a broad process with an external margin that forms a helical curve that terminates with an antero-dorsally sweeping point, the supinator process (Fig. 17E, ect., sup.). The ectepicondylar foramen (Gao 1983, fig. 5) has been excavated into the bluish sediment that invests the broken distal end of the humerus, so its original dimensions, including depth, are uncertain. Indeed, the bone edges are not clear, so it cannot be claimed with certainty that this is an original structure.

A further essentially complete left humerus (IVPP V8534) was identified by Gao (1989: 1239, pl. 2L) as 'Pareiasauride gen. et sp. indet.' The element is flattened and distorted, and lacks the articular ends, so it is hard to assess the degree of torsion of the humerus: both articular ends lie in the same plane. As preserved (Fig. 17G), the humerus measures 435 mm long, and it has a hugely expanded proximal end, up to 265 mm across, and this narrows dramatically about 230 mm from the proximal margin to a distal shaft measuring 71 mm in maximum dimension at its narrowest, and expanding distally to measure 140 mm. In ventral view, the distinct facet for articulation with the scapulocoracoid measures 100 x 45 mm. The deltopectoral crest forms part of the hugely flared proximal end. The condition of preservation does not allow any consideration of entepicondylar and entepicondylar foramina, nor of the distal articulation facets.

Of the phylogenetically informative characters of the humerus, the humeri of *Shihtienfenia* and *Huanghesaurus* show: torsion such that the expanded proximal and distal ends stand at an angle of less than or equal to 45° (Lee 1997, character 81; Tsuji 2013, character 72); the ectepicondyle is expanded and forms a wide rectangular flange that projects in front (preaxially) of the radial condyle (Lee 1997, character 82; Tsuji 2013, character 73); there is no ectepicondylar foramen (Lee 1997, character 83; Tsuji 2013, character 74); the

entepicondyle is rounded, narrow, and with a reduced distal expansion (Lee 1997, character 84; Tsuji 2013, character 75); the entepicondylar foramen is present in the form of an open groove in *Shihtienfenia*, and apparently as a fully enclosed structure in *Huanghesaurus*, although the area has been much repaired (Lee 1997, character 85; Tsuji 2013, character 76); the entepicondylar foramen is situated on the side of the epicondyle and is feebly exposed in dorsal view (Lee 1997, character 86; Tsuji 2013, character 77; wrongly coded 0 by Lee 1997); the entepicondyle and ectepicondyle do not project distally beyond the epicondylar region, in *Shihtienfenia* at least (Lee 1997, character 87; Tsuji 2013, character 78); there is a transverse ridge on the intercondylar depression on the distal humerus, defined dorsally by the ulnar articular surface (Lee 1997, character 88; Tsuji 2013, character 79); the ulnar articulation surface of the humerus takes the form of a groove bordered posteriorly by a faint ridge, with no expansion (Lee 1997, character 89; Tsuji 2013, character 80); and the radial condyle of the humerus is hemispherical and located entirely on the ventral surface of the humerus (Lee 1997, character 90; Tsuji 2013, character 81). Characters 78-81 cannot be coded in *Huanghesaurus* because the distal end of the humerus is damaged.

ULNA AND RADIUS

A largely complete, but crushed, left ulna of *Huanghesaurus* (IVPP V6722-27) is striking because of the massive olecranon portion (Fig. 18A, B., ole.), the primitive condition for pareiasaurs (Lee 1997, character 91). The ulna is 535 mm long, but lacks the proximalmost and distalmost articular terminations. The proximal expanded portion of the ulna extends for nearly half its length (260 mm) and is at most 170 mm antero-posteriorly broad, which may be partially exaggerated by the flattening, and the shaft narrows to 62 mm, before expanding slightly distally to 80 mm. In lateral (external) view (Fig. 18A), the ulna shows the two sigmoid processes of similar dimensions, defining a narrow sigmoid notch (= radial notch), which in life received the head of the radius. The anterior margin of the ulna is rounded in section and describes a gentle curve, whereas the posterior margin is marked by a distinct ridge, extending distally from the olecranon for 140 mm. In medial (internal) view (Fig. 18B), the ulna shows a flat proximal portion with some longitudinal cracks suggesting crushing during fossilisation. The posterior distal flange is demarcated from the main shaft. The expanded olecranon and medially facing proximal articular surface of the ulna indicate the primitive condition for Tsuji's (2013) character 82 (= Lee's 1997 character 91).

The left radius of *Huanghesaurus* (IVPP V6722-28; Fig. 18C, D) is shorter than the ulna, measuring 385 mm long, but lacking the articular ends. The element has expanded ends, the proximal measuring 125 x 80 mm, the distal 135 x 85 mm, and the shaft narrowing to 57 x 40 mm at mid-length. The element bears a marked, but damaged, expansion on the lateral (external) face (Fig. 18C) at the proximal end, which runs into a narrow diagonal ridge extending at least halfway down the shaft, but is relatively flat on the medial (internal) face (Fig. 18D). There is also a broad ridge in the midline towards the distal end. Both ends of the radius are deeply excavated, and filled with sediment, indicating loss of the epipophyses before fossilisation.

PELVIC GIRDLE AND HINDLIMB

PELVIC GIRDLE

The pelvic girdle is represented by the fused elements of both sides in *Shihtienfenia* (IVPP V2727), of which the left side is almost complete, and the right side less so, with the lower borders of pubis and ischium being damaged. The left side of the pelvis (Fig. 19A, B) is massive and compact. The whole pelvis is firmly fused, and measures some 430 mm in dorsoventral height from the anterior tip of the iliac blade to the ventral public margin at the anterior end and 370 mm from the posterior tip of the iliac blade to the ventral ischiadic margin at the posterior. The dorsal blade of the ilium has a substantial anterior process (Fig. 19A, B, ant.pr.), and the blade slopes steeply posteroventrally, being 320 mm long in all. The dorsal margin is massive, 60 mm mediolaterally thick at the everted and horizontally oriented anterior process, but tapering to 25 mm at the posterior process. Ventrally, the ilium narrows to 125 mm wide anteroposteriorly at the neck, and expands to 150 mm at the level of the acetabulum. The whole ilium slopes well forwards with respect to the horizontal dorsal margin of the iliac blade. The acetabulum (Fig. 19A, ac.) is nearly perfectly circular, measuring about 160 mm across in every dimension from the high point of the surrounding lip. It is generally shallow, but deepens to 40 mm beneath a marked expansion, or buttress, on the dorsal iliac margin. The sutures with pubis and ischium are heavily fused, but can still be determined approximately.

In medial view (Fig. 19B), the left ilium shows a groove above the posteroventral margin of the blade. Along the dorsal blade margin is a groove sloping posteroventrally in the

anterior portion, associated with sacral ribs 1 and 2, and below it lies a ridge, the crista sacralis (Hartmann-Weinberg 1933, 1937; Lee 1997: 240; Fig. 19B, cr.sac.). There is a fragment, possibly of sacral rib 2 still adhering in the anteroventral angle. Anteriorly, and still close to the dorsal blade margin are more fragments of sacral ribs, presumably ribs 3 and 4. The fourth rib is quite substantial (Fig. 19B, s.r.4), measuring 85 mm anteroposteriorly and 52 mm dorsoventrally, and narrowing from its flared distal end to dimensions of 30 x 25 mm respectively at 75 mm medially from the medial face of the iliac blade.

In lateral view, the ilium expands more or less symmetrically around the circular acetabulum, leaving a margin of some 30 mm anteriorly and posteriorly. The somewhat fused contacts between the three pelvic elements can be discerned (Fig. 19A, il., is., pu.). The pubis and ischium are relatively modest-sized elements, the former appearing to lack its anterior and ventral margins. The pubis carries a slightly smaller portion of the ventral part of the acetabulum than the ischium, if their sutured contact is correctly identified. The ischium has a modest posteroventral process, whose distal end is missing. In medial view (Fig. 19B), the surface behind the acetabulum, and the medial faces of pubis and ischium, are relatively smooth and featureless, and the bone contacts cannot be seen. The maximum anteroposterior length of the puboischiadic plate, missing anterior and posterior projections, is 245 mm.

The right pelvic plate (Fig. 19C, D) is rather less complete, lacking the distal ends of the iliac blade and most of the pubis and ischium below the ventral margin of the acetabulum. It appears to show similar features to the left pelvic plate, measuring 280 mm anteroposteriorly along the iliac blade, and 265 mm at most across the ischiopubis. Dorsoventral heights are 420 mm anteriorly and 340 mm posteriorly, and the acetabulum is circular and 160 mm in diameter, as on the left side. The acetabulum is deepest in its dorsal portion. Most of the features in medial view (Fig. 19D) are the same as on the left pelvic plate, except that the sacral rib attachments are less clear. From the distal end of the anterior process, a deep groove runs posteroventrally on the medial face of the iliac blade. Further ventrally, below the 120 mm anteroposterior waist of the pelvic plate, there appears to be a twist, with a broad process sweeping across the posterior ventral portion of the ilium and across to the posteroventral point of the ischium. Near the anterior margin, the ilium forms a slightly overturned and flattened area and a distinct broad, vertical groove and process descends across the posterior portion of the pubis.

The pelvis of *Shihtienfenia* provides evidence about a number of phylogenetically informative characters: the crista sacralis of the ilium is a well developed ridge (Lee 1997, character 95; Tsuji 2013, character 85); the iliac shaft is inclined anterodorsally, forming an

angle with the vertical of more than 20° (Lee 1997, character 96; Tsuji 2013, character 86); the iliac blade is expanded well anterior of the iliac shaft (Lee 1997, character 97; Tsuji 2013, character 87); the anterior extent of the ilium is concave along the vertical dimension and the anteroventral margin is strongly everted, even pointed looking and oriented almost horizontally (Lee 1997, character 98; Tsuji 2013, character 88); the posterior process of the iliac blade is strongly reduced (Lee 1997, character 99; Tsuji 2013, character 89); the dorsal buttress on the acetabulum is strongly developed (Lee 1997, character 100; Tsuji 2013, character 90); and the edge of the acetabulum is anteriorly rounded or slightly oval (Lee 1997, character 101; Tsuji 2013, character 91).

HINDLIMB ELEMENTS

The only identified hindlimb element of any of the Shanxi pareiasaurs is an incomplete left femur of the *Shansisaurus xuecunesis* holotype (CAGS V301, not currently accessible; Cheng 1980: fig. 20; pl. 2, fig. 1). This element (Fig. 19E, F) was robust, and it measured 420 mm long. If complete, the proximal end would have been about 168 mm wide, narrowing to 92 mm at mid-shaft, and expanding distally to 184 mm. In dorsal view (Fig. 19E), the twist of the narrow, and somewhat flattened shaft is clear, as is the intercondylar groove between tibial and fibular facets. The ventral view of the proximal face (Fig. 19F, i.tr., tr.m.) shows the incurved internal trochanter near the posterior margin, but the anterior margin with the trochanter major is missing. Between them lies a broad, concave intetrochanteric fossa. On the expanded distal end of the femur the substantial tibial and fibular articular condyles occupy the distal end (Fig. 19F, fi.c., ti.c.), and wrap round some distance onto the ventral face of the femur, a characteristic of sprawling forms.

The proximal head of this femur of *Shansisaurus* is curved slightly anteriorly (preaxially) (Lee 1997, character 107; Tsuji 2013, character 95); the postaxial flange is present, and extends the entire length of the femur, but is narrower in the middle, so the femur looks concave in dorsal or ventral view (Lee 1997, character 112; Tsuji 2013, character 97); and the internal (minor) trochanter is long and curved in its proximal region in ventral view, with the preaxial (anterior) side concave and the postaxial (posterior) side convex (Lee 1997, character 114; Tsuji 2013, character 98).

Additional undescribed limb elements are three polygonal bones that may have been elements of the ankle or wrist. They are part of IVPP V6722, and so presumably belong with the other elements, and yet three of them (Fig. 19G–I) cannot readily be matched with ankle

or wrist elements from other pareiasaurs. The largest (Fig. 19G) is a flattened element, bearing three articular facets, two at one end, separated from each other by a narrow bone bridge, and set at an angle of about 90° to each other, and a single facet at the other end. This element measures 68 mm long, 70 mm wide across the double facets, and 56 mm wide at the other end. This could be identified as an astragalocalcaneum, in which the double facets were for contact with tibia and fibula, and the single, or broader facet at the other end, with a number of smaller distal tarsals. The second element (Fig. 19H) is 66 mm long and with terminal ends 60 mm and 50 mm wide, and is generally similar in shape. The identity of these two elements is uncertain: they look like the astragalus of the stem-amniote *Diadectes* (Schaeffer 1941: fig. 13D), and very different from the rectangular astragalocalcaneum, pierced with a foramen, seen in other pareiasaurs (e.g. Lee 1997: fig. 18; Tsuji 2013: fig. 7). The third, smaller element (Fig. 19I) is more equidimensional, with terminal facets, and a narrowed shaft between. It is 46 mm long and 45 mm and 34 mm wide across each end, and could be a distal tarsal or carpal. If correctly identified, these elements suggest *Huanghesaurus* had a fused astragalocalcaneum (Tsuji 2013, character 100; Lee, 1997, character 116), a typical feature of pareiasaurs (Lee, 1995).

DERMAL ARMOUR

Osteoderms of the Chinese pareiasaurs have not been described or illustrated, but Young & Yeh (1963: 211) noted 'There is no sure indication of the presence of the dermal scutes, although some of the fragmentary bone may be proved as such'. Gao (1983, p. 200) describes, but does not illustrate armour plates from *Huanghesaurus*. Indeed, among the un-catalogued material of *Huanghesaurus* (IVPP V6722), there are five armour plates (Fig. 19J), each saddle-shaped, with a smooth, convex internal face, and a sculpted external face, with a central boss and generally radiating sculpture. The best specimen measures 48 x 33 mm, and 23 mm thick at the boss. These are similar to the armour plates of *Scutosaurus* (Lee, 1997, fig. 20B), but more regular in outline. Presumably these plates were set in the skin of *Huanghesaurus* in regular rows, with their long axes mediolaterally oriented, as in the reconstruction of *Scutosaurus* armament (Lee, 1997: fig. 19B). An extraneous rounded structure is preserved on the radius of *Huanghesaurus*, adhering to the bone at the distal end. This rounded 45 x 25 mm bony object could be interpreted as a dermal ossification of the kind seen in *Anthodon*, but it seems to lack internal structure. Four or five similar rounded

objects occur among the uncatalogued *Huanghesaurus* material (IVPP V6722) and they may be either coprolites of some smaller animal, or inorganic nodules of some kind.

These previously undescribed armour plates allow coding of some cladistic characters, namely osteoderms present (Tsuji, 2013, character 105; Lee, 1997, character 122); dorsal surface of osteoderm possesses a distinct rounded central boss (Tsuji, 2013, character 106; Lee, 1997, character 123); osteoderm ornamentation consists of few, large, lumpy ridges, irregularly spaced (Tsuji, 2013, character 107; Lee, 1997, character 124); and osteoderms are round and small, no larger than the diameter of the centra of dorsal vertebrae (Tsuji, 2013, character 108; Lee, 1997, character 125).

RECONSTRUCTION

A detailed reconstruction of *Shihtienfenia* is not attempted because so many portions of the skeleton and skull are missing. However, the articulated shoulder girdle region confirms that this pareiasaur resembled the Russian *Scutosaurus* closely in size and proportions, so a reconstruction is attempted (Fig. 20) based on the classic sketch reconstruction of *Scutosaurus* by Helen Ziska, reproduced in Gregory (1946), with modifications based on known elements from *Shihtienfenia*. Like other derived pareiasaurs, *Shihtienfenia* was a bulky animal, with a massive torso, powerful, sprawling limbs, and a short neck and relatively small head. The teeth are those of a herbivore, and the massive torso implies substantial digestive systems, also typical of herbivores.

PHYLOGENETIC ANALYSIS

The aim is not to provide a new phylogenetic analysis of the pareiasaurs. Indeed, in a series of recent publications (Lee 1997; Jalil and Janvier 2005; Tsuji & Müller 2008; Tsuji 2013; Tsuji *et al*. 2013), with slight revisions of the data matrix, a reasonably stable phylogeny has been established. The aim here has been to code the Chinese pareiasaurs first-hand, perhaps for the first time, instead of simply from publications, and to do so in light of the thorough alpha-taxonomic review just performed. The major specimens were coded separately so that the relative positions of the synonymised taxa *Shihtienfenia*, *Shansisaurus*, and *Huanghesaurus* might be assessed. The data matrix of Tsuji (2013) was used, representing a substantial

revision of the Lee (1997) matrix, and character codings for the four putative Chinese taxa considered here, *Shihtienfenia*, *Shansisaurus*, *Huanghesaurus*, and *Sanchuansaurus*, are shown in Table 4. The evidence for the codings is presented throughout the descriptive portion of the paper. *Honania* is not included, as the author has not seen the new material first-hand.

The cladistic data matrix, comprising 30 taxa and 126 characters, with all characters run as unordered and equally weighted, was analysed in PAUP 4.0a146 for Macintosh (X86), using standard settings for a parsimony analysis by the branch-and-bound method. Six characters were parsimony uninformative, and the analysis based on the remaining 120 characters retained 11340 trees of length 219 steps (consistency index excluding uninformative characters = 0.7170, retention index = 0.8611, rescaled consistency index = 0.6252). The strict consensus tree (Fig. 21) was well resolved, except for some uncertainty in the relationships of the nycteroleterids in the outgroup, *Provelosaurus* and *Nanoparia*, and the three Chinese taxa *Shihtienfenia*, *Shansisaurus*, and *Huanghesaurus*. Bootstrap values were 100% throughout, except for the two lower values shown (Fig. 21).

The cladistic analysis confirms previous analyses in broad outline (e.g. Lee 1997; Jalil and Janvier 2005; Tsuji 2013), but differs in obtaining better resolution of the several outgroup taxa, from Millerettidae to *Macroleter*, especially in discriminating Nycteroleteridae from the other taxa, and in resolving the relationships of the basal pareiasaurs, and those of the derived clade around *Pareiasaurus* and *Arganaceras*. The analysis confirms the clades Pareiasauromorpha, Pareiasauria, Velosauria, Pumiliopareiasauria (*Provelosaurus*–*Pumilopareia*), Therischia, and the *Pareiasuchus*–*Shihtienfenia* subclades. The clade name Pareiasauria was erected by Seeley (1888), the names Velosauria, Therischia, and Pumiliopareiasauria by Lee (1994), and used first in print by deBraga and Rieppel (1997), although not by Lee (1997) himself. The clade Elginiidae was named by Cope (1896), and widely used by Russian authors in particular since then.

This leaves unnamed the *Pareiasuchus*-*Shihtienfenia* clade, which we term here the **Sinopareiasauria**, referencing the Chinese pareiasaurs in this small clade. This clade has been robust in all recent cladistic analyses (e.g. Lee 1997; Jalil and Janvier 2005; Tsuji 2013), and yet has only a single apomorphy (character 69, 1 → 2; scapular blade length: very long, with a length at least three times the diameter of the glenoid fossa).

As for the Chinese taxa, *Sanchuansaurus* is clearly separated from the other three genera and placed in a more basal position in the cladogram (Fig. 21), between *Deltavjatia* and the derived Velosauria. This confirms its distinctiveness as a separate genus from the

other Chinese taxa. Importantly, the other three taxa form an unresolved tritomy paired with the two valid species of *Pareiasuchus*, and this strongly suggests that *Shansisaurus* and *Huanghesaurus* can be reasonably synonymised with *Shihtienfenia*, as suggested earlier in the systematic and descriptive section of this paper.

The cladogram makes no indications about the palaeogeographic history of the pareiasaurs. Indeed, the 22 taxa divide into subclades that do not correspond to geographic regions, with African, Russian, and Chinese taxa occurring together within subclades, perhaps suggesting that many taxa were more-or-less worldwide in occurrence over the supercontinent Pangaea. There is an approximate stratigraphic equivalence of the cladogram, with three broad age bands represented: Middle Permian (*Bradysaurus*, *Embrithosaurus*, *Nochelesaurus*), Wuchiapingian (*Deltavjatia*, Pumiliopareiasauria, *Pareiasuchus*, *Pareiasaurus*) and Changhsingian (*Sanchuansaurus*, *Shihtienfenia*, *Scutosaurus*, Elginiidae).

CONCLUSION

The detailed redescription of the various pareiasaur fossils from the Late Permian of China has confirmed earlier suggestions that there might be only two valid taxa, *Sanchuansaurus* and *Shihtienfenia* in the Sunjiagou Formation. These are distinguished by several characters, especially those that place *Shihtienfenia* in the derived clades Velosauria and Therischia, as well as the lower number of marginal cusps in tooth crowns (9-11) in *Sanchuansaurus*, and the general points that it is of smaller size and of greater stratigraphic age. Nearly all the specimens described by Chinese authors from 1963 onwards could be examined first-hand, and these confirm the key features presented in earlier papers by Young and Yeh (1963), Gao (1983, 1989), Cheng (1980), and Young (1979).

Phylogenetic analysis confirms that pareiasaurs are related to nycteroleterids and procolophonians, but probably not to turtles. In detail, the phylogeny broadly tracks the evolution of the clade through time, with origins in the Middle Permian, and substantial diversification through the Late Permian across Russia, Africa, and China, with occasional incursions into South America and western Europe. The palaeogeographic history appears to suggest a main centre of evolution in South Africa, and with repeated excursions of taxa worldwide happening several times.

The relative completeness of the first-named Chinese pareiasaur, *Shihtienfenia permica*, suggests that complete specimens can be found in the Sunjiagou Formation. Materials collected later were less complete, and yet the individual bones appear to be

generally in good condition; this suggests that the materials may have been limited as much for logistical reasons as taphonomic. Therefore, complete skeletons, as found in Russia and South Africa, may await an expedition with sufficient lifting and transporting equipment.

ACKNOWLEDGEMENTS

I am very grateful to the Chinese Academy of Sciences for funding my visit to China in April and May 2012 as a CAS Visiting Professor, and to Fucheng Zhang for arranging the application. At the Institute of Vertebrate Paleontology and Paleoanthropology, I am grateful to Jun Liu for advice and conversations about Chinese Permian tetrapods, to Zheng Fang for making the IVPP collections available and helping in manhandling unwieldy specimens, and to my PhD student Qi Zhao for making daily arrangements and for teaching me some Chinese. Further, I thank Mike Lee and an anonymous referee for many helpful comments that helped restructure the paper.

REFERENCES

Apesteguía S. 2005. Evolution of the hyposphene–hypantrum complex within Sauropoda. In: Tidwell V, Carpenter, K, eds. *Thunder-lizards: the sauropodomorph dinosaurs*. Bloomington: University of Indiana Press, Bloomington, 248–267.

Araújo DCF. 1985. Sobre *Pareiasaurus americanus* sp. nov., do Permiano Superior do Rio Grande do Sul, Brasil. I. Diagnose especifica. *Anais Academie do Brasileira de Ciências* **57:** 63–66.

Benton MJ. 2012. No gap in the Middle Permian record of fossil vertebrates. *Geology* **40**: 339-342.

Benton MJ, Newell AJ, Khlyupin AYu, Shumov IS, Price GD, Kurkin AA. 2012. Preservation of exceptional vertebrate assemblages in Middle Permian fluviolacustrine mudstones of Kotel'nich, Russia: stratigraphy, sedimentology, and taphonomy. *Palaeogeography, Palaeoclimatology, Palaeoecology* **319-320**: 58-83.

Canoville A, Thomas DB, Chinsamy A. 2014. Insights into the habitat of Middle Permian pareiasaurs (Parareptilia) from preliminary isotopic analyses. *Lethaia* **47:** 266–274.

Cheng ZW. 1980. Mesozoic stratigraphy and paleontology of the Shaanxi-Gansu-Ningxia Basin. Vol. 2. Beijing: Publishing House of Geology, 115-119. [In Chinese.]

Cope ED. 1896. The reptilian order Cotylosauria. *Proceedings of the American Philosophical Society* **34:** 436–457.

DeBraga M, Rieppel O. 1997. Reptile phylogeny and the affinities of turtles. *Zoological Journal of the Linnean Society* **120**: 281–354.

DeMar R 1972. Evolutionary implications of Zahnreihen. *Evolution* **26**: 435–350.

Embleton BJJ, McElhinny MW, Ma XH, Zhang ZK, Li ZX. 1996. Permo-Triassic magnetostratigraphy in China: the type section near Taiyuan, Shanxi Province, North China. *Geophysical Journal International* **126**: 382–388.

Field DJ, Gauther JA, King BL, Pisani D, Lyson TR, Peterson KJ. 2014. Toward consilience in reptile phylogeny: miRNAs support an archosaur, not lepidosaur, affinity for turtles. *Evolution and Development* **16:** 189–196.

Gao KQ. 1983. A new pareiasaur from Liulin, Shanxi. *Vertebrata Palasiatica* **21:** 193–203.

Gao KQ. 1989. Pareiasaurs from the Upper Permian of north China. *Canadian Journal of Earth Sciences* **26:** 1234–1240.

Gauthier JA. 1986. Saurischian monophyly and the origin of birds. *Memoirs of the California Academy of Sciences* **8:** 1–55.

Gregory WT. 1946. Pareiasaurs versus placodonts as near ancestors to turtles. *Bulletin of the American Museum of Natural History* **86:** 276–323.

Hartmann-Weinberg A. 1933. Die Evolution der Pareiasauriden. *Trudy Paleontologicheskogo Instituta, Akademia Nauk SSSR* **3**: 3–66.

Hartmann-Weinberg A. 1937. Pareiasauriden als Leitfossilien. *Problemy Paleontologii* **2/3**: 649–712.

Hedges SB, Poling LL. 1999. A molecular phylogeny of reptiles. *Science* **283:** 998–1001.

Hou JP, Ouyang, S. 2000. Palynoflora from the Sunjiagou Formation in Liulin County, Shanxi Province. *Acta Palaeontoloica Sinica* **39:** 356–368.

Jalil N-E, Janvier P. 2005. Les pareiasaures (Amniota, Parareptilia) du Permien supérieur du Bassin d'Argana, Maroc. *Geodiversitas* **27:** 35–132.

Joyce WG. 2015. The origin of turtles: a paleontological perspective. *Journal of Experimental Zoology Part B: Molecular and Developmental Evolution* **324B:** 181–193.

Kissel RA, Lehman TM. 2002. Upper Pennsylvanian tetrapods from the Ada Formation of Seminole County, Oklahoma. *Journal of Paleontology* **76:** 529–545.

Langer MC, Benton MJ. 2006. Early dinosaurs: a phylogenetic study. *Journal of Systematic Palaeontology* **4:** 309–358.

Lee MSY. 1993. The origin of the turtle body plan: bridging a famous morphological gap. *Science* **261:** 1716–1720.

Lee MSY. 1994. *Evolutionary morphology of pareiasaurs.* PhD Thesis, University of Cambridge, UK.

Lee MSY. 1995. Historical burden in systematics and the interrelationships of 'parareptiles'. *Biological Reviews* **70:** 459–547.

Lee MSY. 1996. Correlated progression and the origin of turtles. *Nature* **379:** 812–815.

Lee MSY. 1997. Pareiasaur phylogeny and the origin of turtles. *Zoological Journal of the Linnean Society* **120:** 197–280.

Lee MSY. 1998. Similarity, parsimony and conjectures of homology: the chelonian shoulder girdle revisited. *Journal of Evolutionary Biology* **11:** 379–387.

Lee MSY. 2000. The Russian pareiasaurs. In: Benton MJ, Shishkin MA, Unwin DM, Kurochkin EN, eds. *The age of dinosaurs in Russia and Mongolia.* Cambridge: Cambridge University Press, 71–85.

Lee MSY, Gow CE, Kitching JW. 1997. Anatomy and relationships of the pareiasaur *Pareiasuchus nasicornis* from the Upper Permian of Zambia. *Palaeontology* **40:** 307–335.

Li C, Wu XC, Rieppel O, Wang LT, Zhao J. 2009. Ancestral turtle from the late Triassic of southwestern China. *Nature* **456**: 497–501.

Li J. 2001. The most primitive lower tetrapod fauna in China. *Science in China Series D: Earth Sciences* **44**: 47-51.

Li XW, Liu J. 2013. New specimens of pareisarus from the Upper Permian Sunjiagou Formation of Liulin, Shanxi and their implications for the taxonomy of Chinese pareiasaurs. *Vertebrata PalAsiatica* **51:** 199–204.

Liu J, Li XW, Jia SH, Pu HY, Liu XL. 2014. The Jiyuan tetrapod fauna of the Upper Permian of China–2. Stratigraphy, taxonomical review, and correlation. *Vertebrata PalAsiatica* **52:** 328–339.

Lucas SG. 2001. *Chinese fossil vertebrates*. New York: Columbia University Press, 375 pp.

Menning M, Jin YG. 1998. Comment on 'Permo-Triassic magnetostratigraphy in China: the type section near Taiyuan, Shanxi Province, North China' by B. J. J. Embleton, M. W. McElhinny, X. Ma, Z. Zhang and Z. X. Li. *Geophysical Journal International* **133:** 213–216.

Mueller JF, Rogers JJW, Jin YG, Wang HY, Li WG, Chronic J, Mueller JF. 1991. Late Carboniferous to Permian sedimentation in Inner Mongolia, China, and tectonic relationships between North China and Siberia. *Journal of Geology* **99:** 251–263.

Norin E. 1922. The late Palaeozoic and early Mesozoic sediments of central Shansi. *Bulletin of the Geological Survey of China* **4**: 1–79.

Rieppel O. 1994. Osteology of *Simosaurus gaillardoti*, and the phylogenetic interrelationships of stemgroup Sauropterygia. *Fieldiana (Geology) N.S.* **28**: 1–85.

Rieppel O. 2000. *Paraplacodus* and the phylogeny of the Placodontia (Reptilia: Sauropterygia). *Zoological Journal of the Linnean Society* **130**: 635-659.

Rieppel O, deBraga M. 1996. Turtles as diapsid reptiles. *Nature* **384:** 453–455.

Rieppel O, Reisz R. 1999. The origin and evolution of turtles. *Annual Review of Ecology and Systematics* **30**: 1–22.

Rubidge BS, Erwin DH, Ramezani J, Bowring SA, de Klerk, WJ. 2013. High-precision temporal calibration of Late Permian vertebrate biostratigraphy: U-Pb zircon constraints from the Karoo Supergroup, South Africa. *Geology* **41:** 363–366.

Schoch RR, Sues H-D. 2015. A Middle Triassic stem-turtle and the evolution of the turtle body plan. *Nature* **253:** 584–587.

Seeley HG. 1888. Researches on the structure, organization, and classification of the fossil Reptilia. VI. On the anomodont Reptilia and their allies. *Philosophical Transactions of the Royal Society of London, Series B (Biological Sciences)* 44: 381–383

Seeley HG. 1892. Researches on the structure, organization, and classification of the fossil Reptilia. VII. Further observations on *Pareiasaurus*. *Philosophical Transactions of the Royal Society of London, Series B (Biological Sciences)* **183:** 311–370.

Shen SZ, Crowley JL, Wang Y, Bowring SA, Erwin DH, Sadler PM, Cao CQ, Rothman DH, Henderson CM, Ramezani J, Zhang H, Shen Y, Wang XD, Wang W, Mu L, Li WZ, Tang YG, Liu XL, Liu LJ, Zeng Y, Jiang YF, Jin YG. 2011. Calibrating the end Permian mass extinction. *Science* **334**: 1367-1372.

Stevens LG, Hilton J, Bond DPG, Glasspool IJ, Jardine PE. 2011. Radiation and extinction patterns in Permian floras from North China as indicators for environmental and climate change. *Journal of the Geological Society* **168**: 607-619.

Sun A, Li J, Ye XK, Dong Z, Hou L. 1992. The Chinese fossil reptiles and their kins. Beijing: Science Press, 260 pp.

Tsuji LA. 2013. Anatomy, cranial ontogeny and phylogenetic relationships of the pareiasaur *Deltavjatia rossicus* from the Late Permian of central Russia. *Earth & Environmental Science Transactions of the Royal Society of Edinburgh* **104:** 81–122.

Tsuji LA, Müller J. 2008. A reevaluation of *Parasaurus geinitzi,* the first named pareiasaur (Amniota, Parareptilia). *Canadian Journal of Earth Sciences* **45:** 1111–1121.

Tsuji LA. Sidor CA, Steyer JS, Smith RMH, Tabor NL, Ide O. 2013. The vertebrate fauna of the Upper Permian of Niger–VII. Cranial anatomy and relationhips of *Bunostegos akokanensis* (Pareiasauruia). *Journal of Vertebrate Paleontology* **33:** 747–763.

Vickaryous MK, Hall BK. 2006. Homology of the reptilian coracoid and a reappraisal of the evolution and development of the amniote pectoral apparatus. *Journal of Anatomy* **208**: 263-285.

Wang ZQ. 1993. Evolutionary ecosystem of Permian-Triassic redbeds in North China: a historical record of global desertification. In: Lucas, SG, Morales, M, eds. *The Nonmarine Triassic*. Albuquerque: New Mexico Museum of Natural History & Science, 471-476.

Wang ZQ, Chen AS. 2001. Traces of arborescent lycopsids and dieback of the forest vegetation in relation to the terminal Permian mass extinction in North China. *Review of Palaeobotany and Palynology* **117**: 217–243.

Wang ZQ, Wang LX. 1986. Late Permian fossil plants from the lower part of the Shiqeunfeng (Shihshoenfeng) group in North China. *Bulletin of the Tianjin Institute of Geology and Mineral Resources* **15**: 1–80 [in Chinese with English abstract].

Xu L, Li XW, Jia SH, Liu J. 2015. The Jiyaun tetrapod fauna of the Upper Permian of China. New pareiasaur material and the reestablishment of *Honania complicidentata*. *Acta Palaeontologica Polonica* 60: 689-700.

Young CC. 1979. A Late Permian fauna from Jiyuan, Henan. *Vertebrata PalAsiatica* **1979**: 17: 99-113. [In Chinese.]

Young CC, Yeh HK. 1983. On a new pareiasaur from the Upper Permian of Shansi, China. *Vertebrata PalAsiatica* **17:** 195–214.

Zhang Y, Zheng SL, Naugolnykh SV. 2012. A new species of *Lepidopteris* discovered from the Upper Permian of China with its stratigraphic and biologic implications. *Chinese Science Bulletin* **57:** 3603–3609.

Figure 1. Locality map of western Shanxi Province, showing the principal pareiasaur localities, at Baode, on the banks of the Yellow River, and at Xuecun, and other localities in Liujin, on the Sanchuan River. The base map (from Google Maps) shows topography and main roads and towns, and the Lower and Middle-Upper Permian (LP, M-UP) outcrop, is marked, showing continuity of occurrences in the Upper Permian from Baode to Luliang.

Figure 2. Summary stratigraphic chart of the Middle and Late Permian, showing the international marine stratigraphic epochs and stages, the magnetostratigraphic pattern and key zones, the Russian stages, gorizonts, tetrapod zones, and faunal complexes, the South Afican tetrapod assemblage zones, and the North Chinese formations and tetrapod faunas. The outlines of the diagram are from Benton (2012) and Benton *et al*. (2013), with revisions of the Karoo boundaries, and radiometric dates (indicated by solid circles) from Rubidge *et al*. (2012). The Chinese horizons and correlations are discussed in the text, and are based mainly on Stevens *et al*. (2011).

Figure 3. Teeth of *Honania complicidentata* Young, 1979. A, Isolated tooth, IVPP V4015.1. B, Isolated tooth, IVPP V4015.3. C, Original image from Young (1979, fig. 4), showing the *Honania* type series, teeth IVPP V4015.1 (two views), V4015.2, and V4015.3 (two views). D, Original image from Young (1979, fig. 5), showing the *Tsiyuania* type series, teeth IVPP V4016.1 (two views) and V4016.2 (two views). Abbreviation: ci, cingulum.

Figure 4. Right maxilla of *Sanchuansaurus pygmaeus* Gao, 1989 (IVPP V6723), in lateral (A), medial (B), and dorsal (C) views. Abbreviations: a.p., antorbital process; io.c., infraorbital canal; p.s., palatal shelf; 1–15, tooth numbers.

Figure 5. Hindlimb elements of *Sanchuansaurus pygmaeus* Gao, 1989. (A–D) left femur (IVPP V6724), in dorsal (A), posterior (B), ventral (C), and anterior (D) views. (E–H) left fibula (IVPP V6725) in dorsal (E), posterior (F), ventral (G), and anterior (H) views. Abbreviations: a.t., anterior trochanter; fib., facet for articulation with fibulare; fi.c., fibular condyle of femur; int., facet for articulation with intermedium; i.s., intercondylar sulcus; p.f., posterior flange; ti.c., tibial condyle of femur.

Figure 6. Putative left jugal (IVPP V6722-3) of *Shihtienfenia permica* Young and Yeh, 1963, originally ascribed to *Huanghesaurus*, in lateral (A) and medial (B) views.

Figure 8. Mandible elements of *Shihtienfenia permica* Young and Yeh, 1963, originally ascribed to *Huanghesaurus*. (A, B) portion of left dentary (IVPP unnumbered) in lateral (A) and medial (B) views. (C–E) details of the dentary dentition (IVPP V6722-1) in lateral (C) and medial (D) views, and close-up of dentary teeth 11 and 12 (E). Abbreviations: ci, cingulum; ri, ridge.

Figure 9. Posterior cervical vertebrae of *Shihtienfenia permica* Young and Yeh, 1963. (A) Posterior cervical vertebra (IVPP V2717) in anterior view. (B) Posterior cervical vertebrae, , originally ascribed to *Huanghesaurus* (IVPP V6722-4 to 7), in lateral view. Abbreviations: ce., centrum; dp., diapophysis; n.a., neural arch; n.c., neural canal; n.sp., neural spine; poz., postzygapophysis; pp., parapophysis; prz., prezygapophysis; t.p., transverse process.

Figure 10. Posterior dorsal vertebrae of *Shihtienfenia permica* Young and Yeh, 1963. (A–C) Posterior dorsal vertebrae (IVPP V2717; presacrals 16-20?) in dorsal (A~), left lateral (B), and ventral (C) views. Abbreviations: n.c., neural canal; n.sp., neural spine; poz., postzygapophysis; prz., prezygapophysis; t.p., transverse process; 16–20, estimated numbers of dorsal vertebrae.

Figure 11. Sacral vertebrae and first caudal vertebra of *Shihtienfenia permica* Young and Yeh, 1963 (IVPP V2717), in right lateral (A), left lateral (B), near-dorsal (C(), and ventral (D) views. Abbreviations: ca.v.1, caudal vertebra 1; n.sp., neural spine; poz., postzygapophysis; prz., prezygapophysis; s.r.1, sacral rib 1; 1–5, sacral vertebrae 1–5.

Figure 12. Isolated ribs of *Shihtienfenia permica* Young and Yeh, 1963, originally ascribed to *Huanghesaurus*, in lateral (above) and medial (below) views. (A) cervical rib (IVPP V6722-18), (B, C) anterior dorsal ribs (IVPP V6722-20, 21), and (D) mid-dorsal rib (IVPP V6722-22). Abbreviations: ca., capitulum; tu., tuberculum).

Figure 13. Right scapula of *Shihtienfenia permica* Young and Yeh, 1963 (IVPP V2717), in lateral (A), anterior (B), medial (C) and posterior (D) views. Abbreviations: acr., acromion process; gl., glenoid; int.pr., internal process.

Figure 14. Left shoulder girdle of *Shihtienfenia permica* Young and Yeh, 1963 (IVPP V2717), in lateral (A) and medial (B) views, comprising scapula, coracoid, and clavicle, partly held together by a metal armature used when the specimen was displayed in the IVPP public museum. Abbreviations: acr., acromion process; cl., clavicle; co., coracoid; co.f., coracoid foramen; gl., glenoid; sc., scapula.

Figure 15. Various scapulocoracoid remains of *Shihtienfenia permica* Young and Yeh, 1963. (A–D) Left scapulocoracoid, originally ascribed to *Huanghesaurus* (IVPP V6722-22), in lateral (A, B) and medial (C, D) views, showing ths specimen and a sketch interpretation. (E, F) Left scapulocoracoid originally assigned to *Shansisaurus* sp. (IVPP V6727), in lateral (E) and medial (F) views. (G, H) Left scapula originally assigned to 'Pareiasauride sp.' (IVPP V8533), in lateral (E) and medial (F) views. Abbreviations: aco., anterior coracoid; acr., acromion process; co.f., coracoid foramen; gl., glenoid; pco., posterior coracoid; pr., process; sc., scapula; s.s.f., subscapular fossa.

Figure 16. Dermal shoulder girdle of *Shihtienfenia permica* Young and Yeh, 1963. (A) Left side of shoulder girdle (IVPP V2717), showing clavicle in place. (B–E) Right and left clavicles originally ascribed to *Huanghesaurus* (IVPP V6722-22) in anterior (B), external (C), posterior (D), and internal (E) views. (F, G) Interclavicle originally ascribed to *Huanghesaurus* (IVPP V6722-22) in external/ ventral (F) and internal/ dorsal (G) views, the latter showing the proximal part of the left clavicle in position. (H, I) Sketch reconstructions of the shoulder girdle of IVPP V2717, and anterior (H) and left lateral (I) views. Abbreviations: cl., clavicle; cl.f., clavicular facet; co., coracoid; h, humerus; icl,pr., interclavicle process; p.fl., posterior flange; p.pr., posterior process; R, right-hand side; sc., scapula.

Figure 17. Humerus of *Shihtienfenia permica* Young and Yeh, 1963. (A–D) Left humerus of *Shihtienfenia* (IVPP V2717) in ventral (A), anterior (B), dorsal (C), and posterior (D) views. (E, F) Left humerus of *Huanghesaurus* (IVPP V6722-26) in dorsal (E) and ventral (F) views. (G) Left humerus of 'Pareiasauridae indet.' (IVPP V8534) in ventral view. Abbreviations: a.d.v.l., anterior dorso-ventral line; a.f., articular facet; dpc, deltopectoral crest; ect., ectepicondyle; ent, entepicondyle; ent.f., entepicondylar foramen; ic.f., intercondylar fossa; p.a.f., posterior articular facet; sup., supinator process.

Figure 18. Ulna and radius of *Shihtienfenia permica* Young and Yeh, 1963. (A. B) Left ulna of *Huanghesaurus* (IVPP V6722-27) in lateral (A) and medial (B) views. (C, D) Left radius of *Huanghesaurus* (IVPP V6722-28) om lateral (C) and medial (D) views. Abbreviations: ole., olecranon; sig.n., sigmoid notch; sig. p., sigmoid process.

Figure 19. Pelvis and hindlimb of *Shihtienfenia permica* Young and Yeh, 1963. (A, B) Left side of pelvis of *Shihtienfenis* (IVPP V2727), in lateral (A) and medial (B) views. (C, D) Right side of pelvis of *Shihtienfenis* (IVPP V2727), in lateral (C) and medial (D) views. (E, F) Left femur of *Shansisaurus* (CAGS V301), in dorsal (E) and ventral (B) views. (G–H) Ankle bones of *Huanghesaurus* (IVPP V6722): possible astragalocalcaneum (G), unidentified ankle bone (H), and possible tarsal or carpal (I). (J) Dermal plates of *Huanghesaurus* (IVPP V6722). Abbreviations: ac., acetabulum; ant.pr., anterior process; cr.sac., crista sacralis; fi.c., fibular condyle; i.tr., internal trochanter; ic.f., intercondylar foramen; il., ilium; is., ischium; pu., pubis; sa.r.4, sacral rib 4; ti.c., tibial condyle; tr.m., trochanter major.

Figure 20. Reconstruction of *Shihtienfenia permica* Young and Yeh, 1963, based on preserved elements, photographs of the whole-skeleton mount (Young and Yeh 1963, pls. 1, 2), and broad comparability with *Scutosaurus*, as reconstructed in Ziska in Gregory (1946).

Figure 21. Strict consensus cladogram of relationships among pareiasaurs, with the four named Chinese taxa highlighted in bold. Bootstrap values are 100% throughout, except for the two values shown (51%, 52%).

Table 1. Basic measurements of the crowns of Chinese pareiasaur teeth. Explanation of measurements: breadth, maximum anteroposterior width of the crown, measured on the medial (lingual) face, in mm; height, maximum dorsoventral measurement from tooth tip to cenre of cingulum, measured on medial (lingual) face, in mm; cingulum and marginal denticles represent totals. Position in tooth row is indicated for teeth of *Sanchuansaurus* and *Huanghesaurus*, in parentheses after the repository number; abbreviation: R, replacement.

Genus	Specimen	Height	Breadth	Cingulum denticles	Marginal denticles
Honania	IVPP V4015.1	13	10	c. 12	16
Honania	IVPP V4015.2	-	10	-	15-17
Honania	IVPP V4015.3	11.5	9.5	c. 12	12-14
Tsiyuania	IVPP V4016.1	13.5+	14	c. 15	8+
Tsiyuania	IVPP V4016.2	12+	12+	-	-
Sanchuansaurus	IVPP V6723 (4)	5.5	8	10-12	c. 10
Sanchuansaurus	IVPP V6723 (7)	c. 8	9	10-12	9-10
Sanchuansaurus	IVPP V6723 (8R)	9	c. 9	-	c. 10
Sanchuansaurus	IVPP V6723 (9)	8.5	9	10-12	c. 10
Sanchuansaurus	IVPP V6723 (11)	8+	10	10-12	c. 9
Sanchuansaurus	IVPP V6723 (13)	10+	11	c. 12	c. 10
Huanghesaurus	IVPP V6722-1 (1)	12.5+	c. 12	-	-
Huanghesaurus	IVPP V6722-1 (3)	14	12	-	15-16
Huanghesaurus	IVPP V6722-1 (5)	19	12	5-6	15-16
Huanghesaurus	IVPP V6722-1 (10)	15	11-12	5-6	15-17
Huanghesaurus	IVPP V6722-1 (12)	14	12	5-6	13-15

Table 2. Measurements of the vertebrae of *Shihtienfenia* (IVPP V2717). Individual specimens are not numbered separately, so references to figures in Yang and Yeh (1963) are given, together with their identifications.

1. Height from base of centrum in posterior view to top of neural spine.
2. Maximum width across distal tips of transverse processes.
3. Height of anterior articular face of centrum
4. Width of anterior articular face of centrum
5. Height of posterior articular face of centrum
6. Width of posterior articular face of centrum
7. Maximum length of centrum from anterior to posterior face.

Number	Identity	1	2	3	4	5	6	7
Fig. 5, lower left	Posterior cervical	-	?280	90	74	110	70	82
Fig. 5, upper left	?Presacral 11	-	230	c. 130	75	c. 130	c. 70	90
Fig. 5, upper left	?Presacral 12	-	230	c. 130	c. 75	c. 120	-	90
Fig. 5, upper right	?Presacral 13	-	-	c. 110	c. 65	-	-	80
Fig. 5, upper right	?Presacral 14	-	c. 220	c. 95	c. 70	-	-	c.70
Fig. 2.	?Presacral 16	-	190	77	105	-	-	88
Fig. 2.	?Presacral 17	-	220	-	-	-	-	90
Fig. 2.	?Presacral 18	-	220	-	-	-	-	90
Fig. 2.	?Presacral 19	-	220	-	-	-	-	95
Fig. 2.	?Presacral 20	-	-	-	-	-	-	-
Fig. 3.	Sacral 1	-	c. 170	-	-	-	-	-
Fig. 3.	Sacral 2	c. 240	c. 160	-	c. 65	-	-	85
Fig. 3.	Sacral 3	180+	c. 180	-	-	-	-	85
Fig. 3.	Sacral 4	180+	c. 170	-	-	-	-	87
Fig. 3.	Sacral 5	-	c. 130	-	-	-	-	87
Fig. 3.	Caudal 1	-	c. 100	-	-	-	c. 55	c.80

Table 3. Measurements of the vertebrae of *Huanghesaurus* (IVPP V6722).

1. Height from base of centrum in posterior view to top of neural spine.
2. Maximum width across distal tips of transverse processes.
3. Height of anterior articular face of centrum
4. Width of anterior articular face of centrum
5. Height of posterior articular face of centrum
6. Width of posterior articular face of centrum
7. Maximum length of centrum from anterior to posterior face.

Number	Identity	1	2	3	4	5	6	7
IVPP V6722-4	Posterior cervical	-	-	-	-	87	72	80
IVPP V6722-5	Posterior cervical	-	-	78	c. 75	80	82	80
IVPP V6722-6	Posterior cervical	200	-	c. 90	82	90	90	80
IVPP V6722-7	Posterior cervical	220	c. 140	-	-	c. 95	-	c.75
IVPP V6722-8	Posterior dorsal	265	245	110	115	95	110	65
IVPP V6722-9	Posterior dorsal	-	-	110	110	95	110	60
IVPP V6722-10	Posterior dorsal							
IVPP V6722-11	Posterior dorsal	-	-	110	105	-	-	-
IVPP V6722-12	*Posterior dorsal	-	-	90	77	98	85	64
IVPP V6722-13	*Posterior dorsal	322	-	95	70	90	70	80
IVPP V6722-14	Posterior dorsal	-	-	117	102	94	102	62
IVPP V6722-15	Posterior dorsal	293	255	90	86	85	80	58
IVPP V6722-16	Posterior dorsal	-	252	-	-	-	-	-

*crushed and distorted

Table 4. Character codings for the Chinese pareiasaurs, listed according to the original designations of the taxa. Character numbering follows Lee (1997) and Tsuji (2013). Character absences are coded '?'.

Taxon	Character number
	11 11-11 1-1-1 12222 22333 33-33 44444
[Lee 1997]	23456 78901 23-45 6-7-- 89013 56012 36-78 13567
	1 11111 11112 22222 22223 33333 33334
[Tsuji 2013]	12345 67890 12345 67890 12345 67890 12345 67890
Shihtienfenia	????? ????? ????? ????? ????? ????? ????? ?????
Shansisaurus	????? ????? ????? ????? ????? ????? ????? ?????
Huanghesaurus	????? ????? ????? ????? ????? ????? ????? ?????
Sanchuansaurus	????? ????? ????? ????? ????1 1???? ????? ?????
	---4- 555-2 55656 66666 -6977 77777 78888 88888
[Lee 1997]	---9- 124-7 58190 34567 -8301 23457 91234 56789
	44444 44445 55555 55556 66666 66667 77777 77778
[Tsuji 2013]	12345 67890 12345 67890 12345 67890 12345 67890
Shihtienfenia	????? ????? ????? ????? ?03?? ??120 11111 11011
Shansisaurus	????? ????? ????? ????? ????? ??120 1???? ?????
Huanghesaurus	????? 1110? ?11?4 11??? ?0??? ??120 11111 01???
Sanchuansaurus	????? ????1 0113? ?1??? ????? ????? ????? ?????
	1 11111 11111 11111 11111 1---- -----
	99999 99990 00000 01111 11222 22222 2---- -----
[Lee 1997]	01245 67890 13457 92456 89012 34567 8---- -----
	1 11111 11111 11111 11111
	88888 88889 99999 99990 00000 00001 11111 11112
[Tsuji 2013]	12345 67890 12345 67890 12345 67890 12345 67890
Shihtienfenia	0??01 11211 0???? ????? ????? ????? ????? ????1
Shansisaurus	????? ????? ????1 111?? ????? ????? ????? ?????
Huanghesaurus	?0??? ????? ????? ????1 ????1 120?? ????? ?????
Sanchuansaurus	????? ????? ????1 ?1??? ????? ????? ????? ????1
	----- -
	----- -
[Lee 1997]	----- -
	11111 1
	22222 2
[Tsuji 2013]	12345 6
Shihtienfenia	????? ?
Shansisaurus	????? ?
Huanghesaurus	????? ?
Sanchuansaurus	????? ?

M-UP

LP

Baode

Yellow River

G65

G65

Yulin
榆林市

G210

G307

G209

Xuecunzhen;
Liulin

Lvliang
吕梁市

Sanchuan River

20 km

M-UP

LP

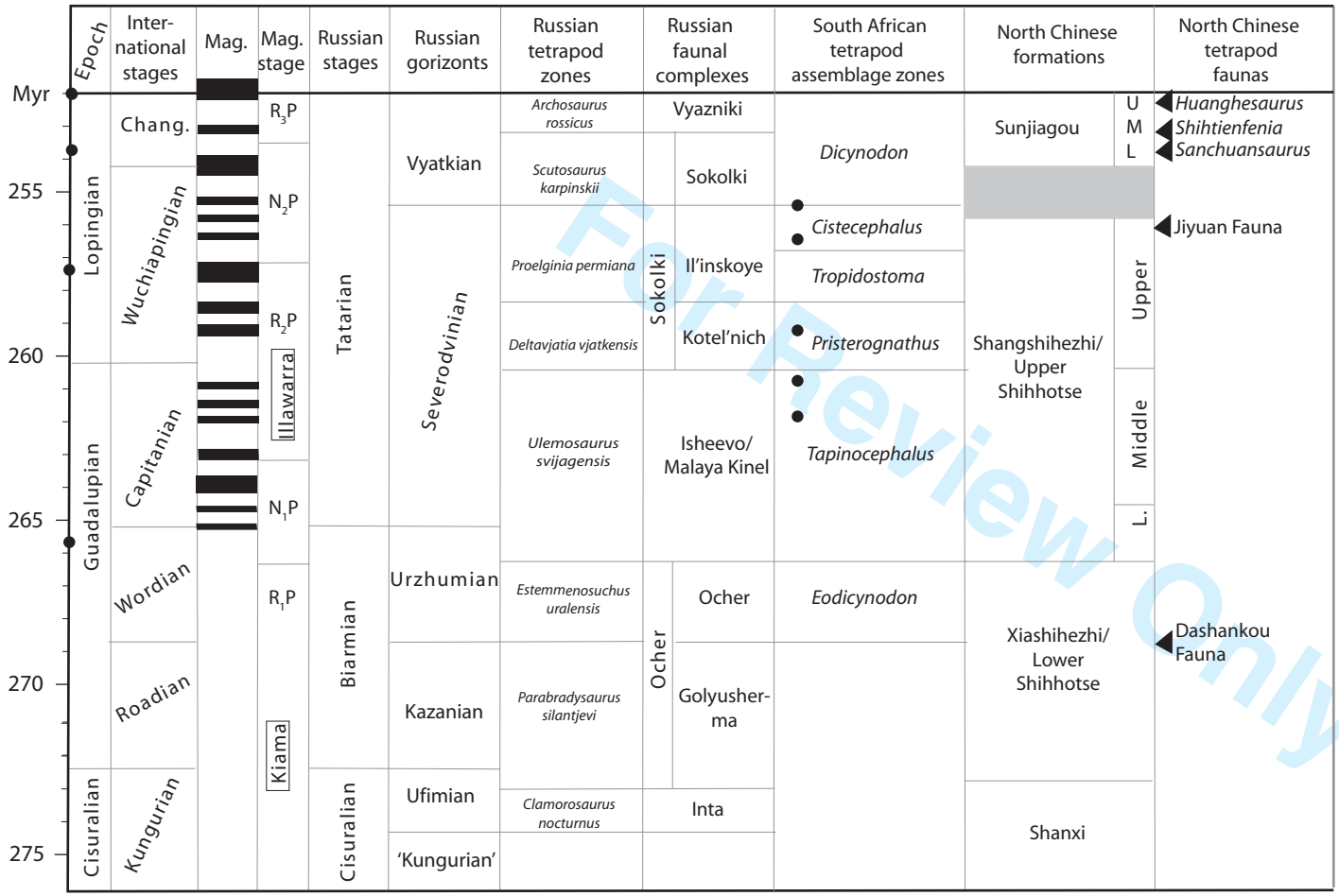

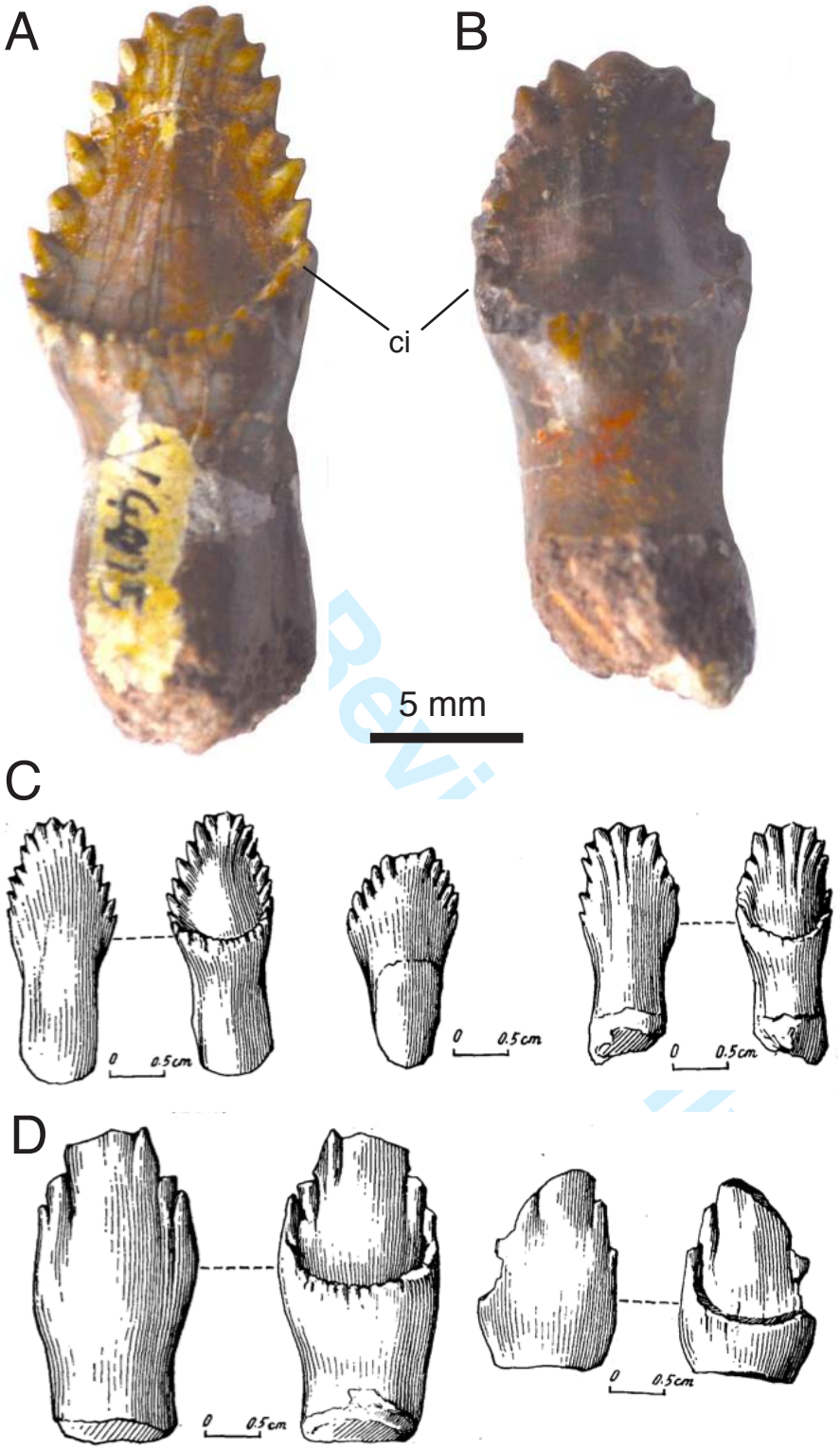
A
B
ci
5 mm
C
0 0.5cm
0 0.5cm
0 0.5cm
D
0 0.5cm
0 0.5cm

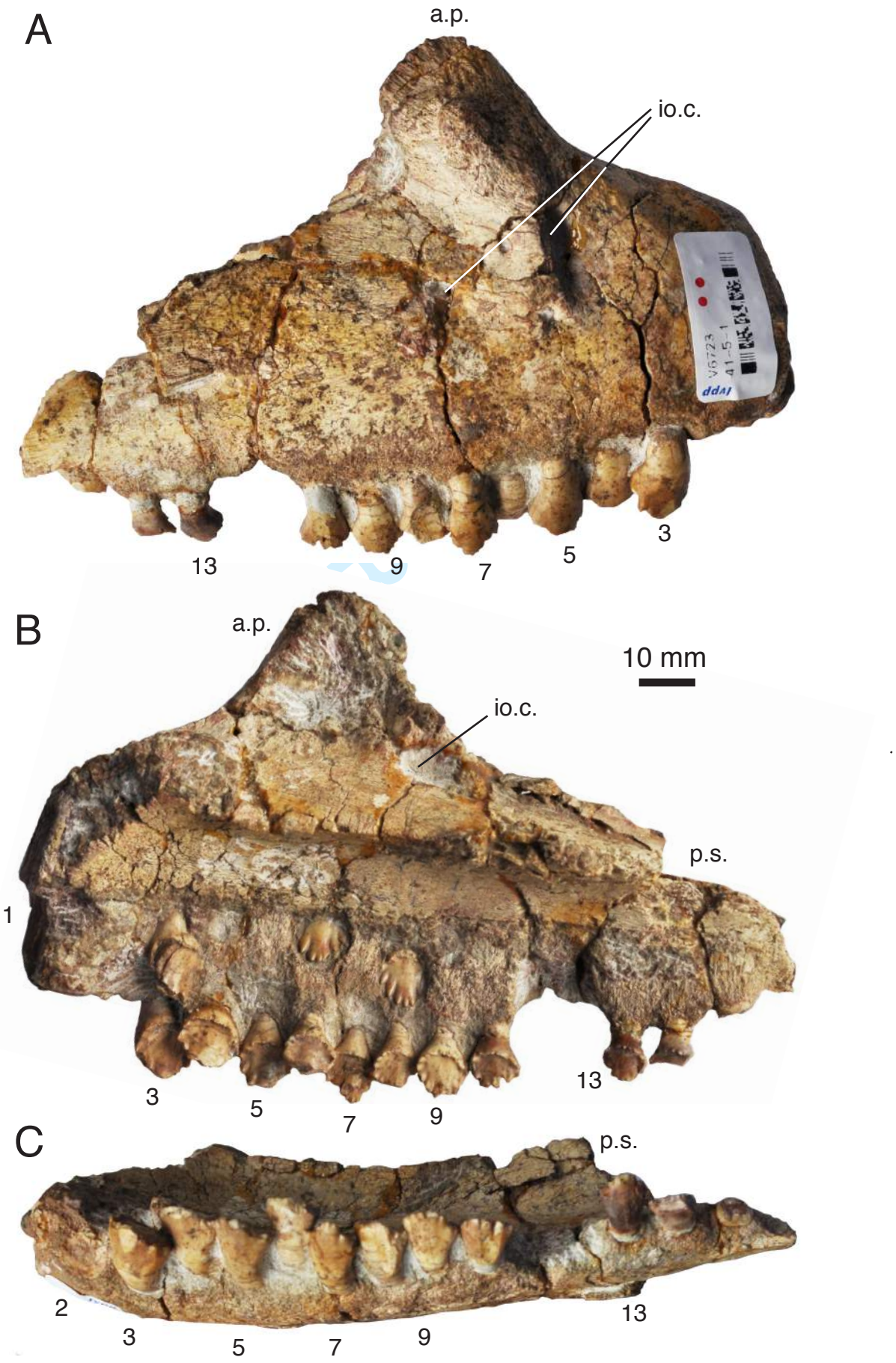
A
a.p.
io.c.
13
9
7
5
3
B
a.p.
10 mm
io.c.
p.s.
1
3
5
7
9
13
C
p.s.
2
3
5
7
9
13


A
B
C
D
p.f.
i.s.
ti.c.
fi.c.
50 mm
E
F
G
H
a.t.
fib.
int.

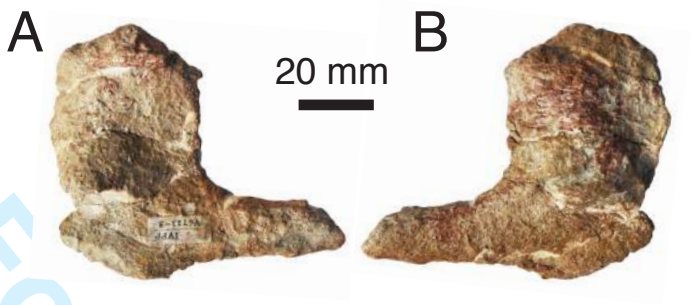

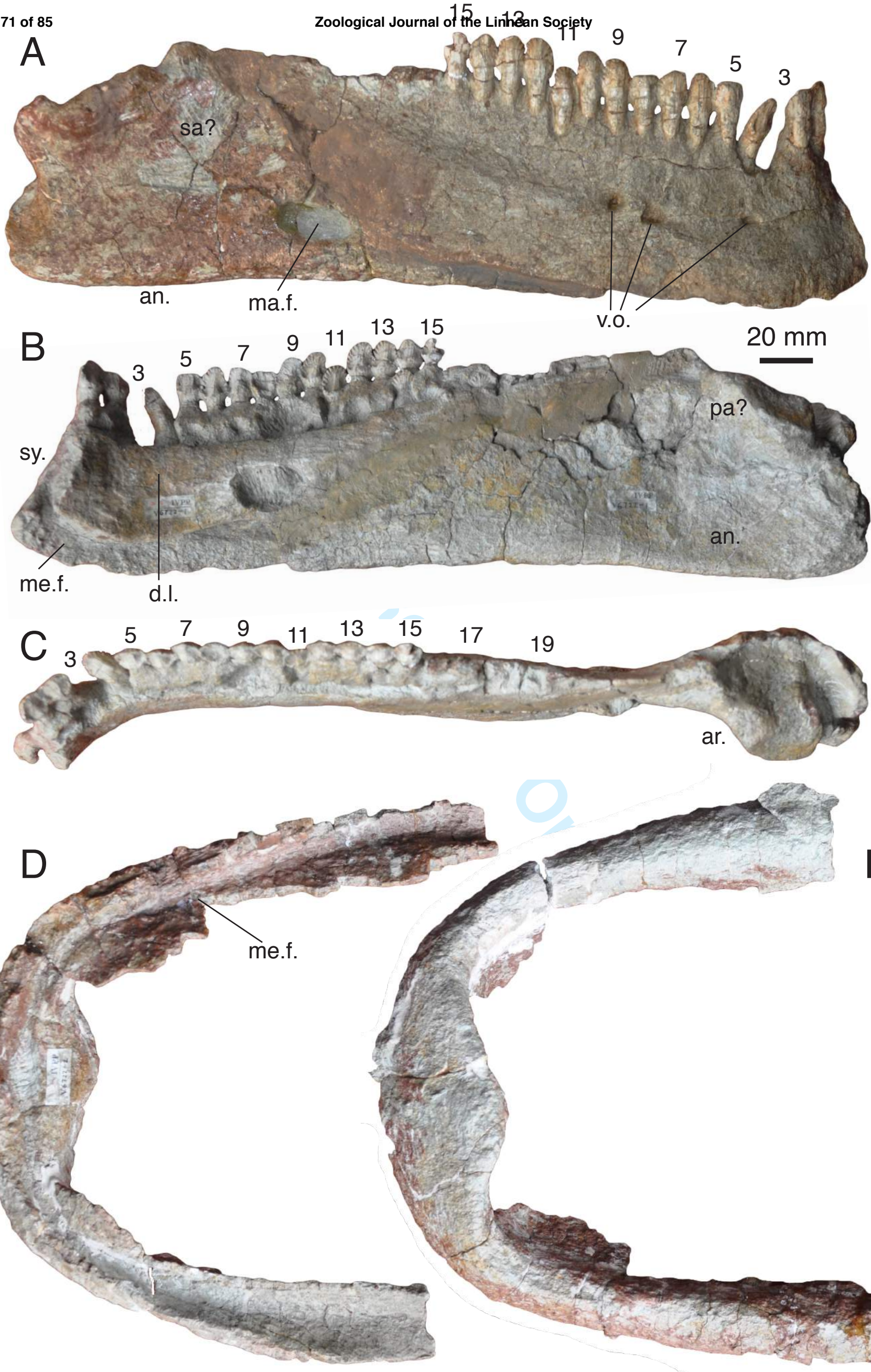
A
15
13
11
9
7
5
3
sa?
an.
ma.f.
v.o.
B
3
5
7
9
11
13
15
20 mm
pa?
sy.
an.
me.f.
d.l.
C
3
5
7
9
11
13
15
17
19
ar.
D
me.f.
E

A

20 mm

B

C

15

13

11

9

7

5

3

E

ri

ci

10 mm

20 mm

D

13

15

9

11

7

5

3

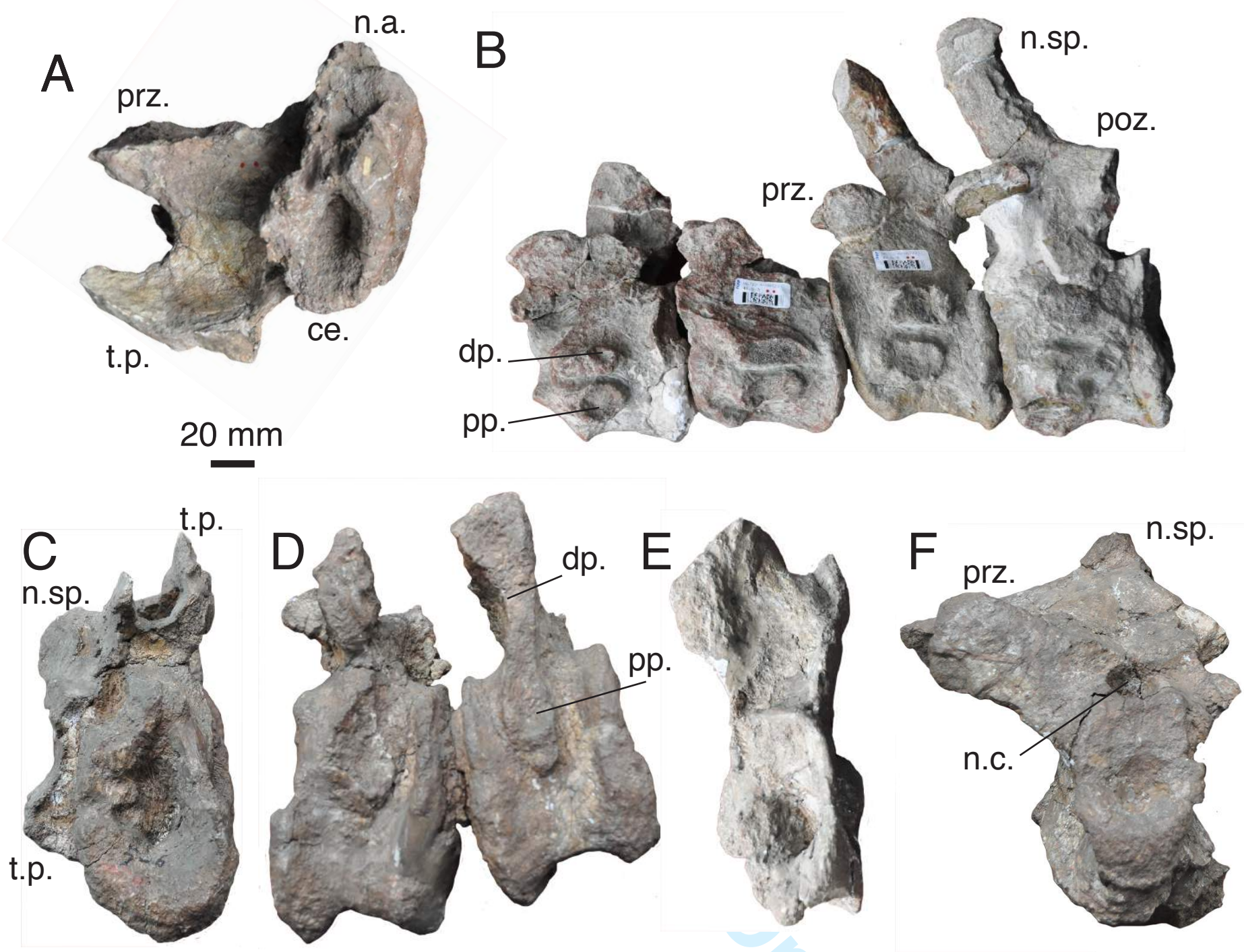

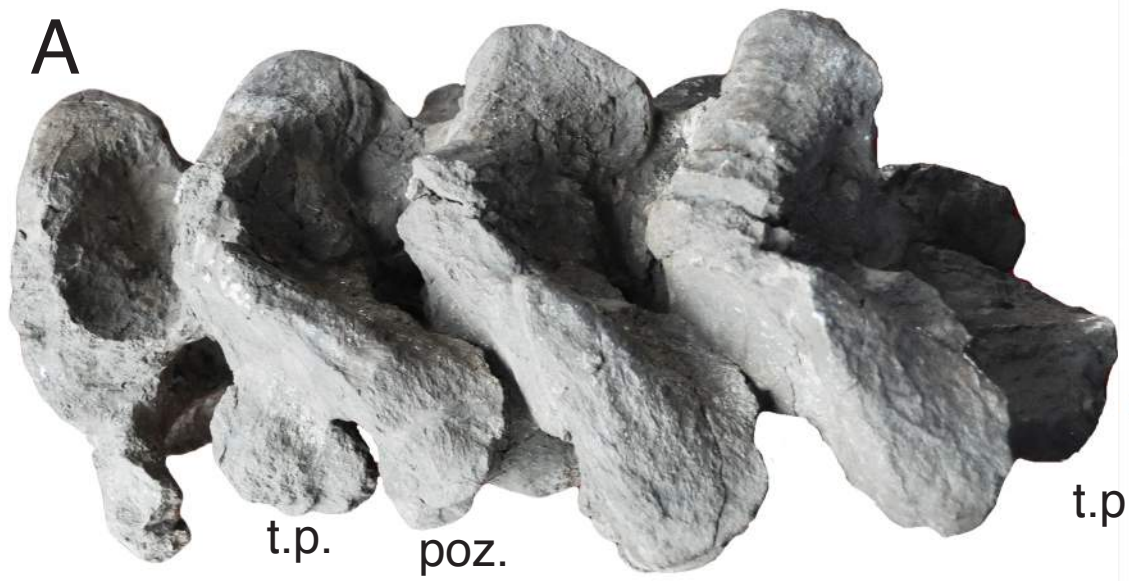
A
t.p.
poz.

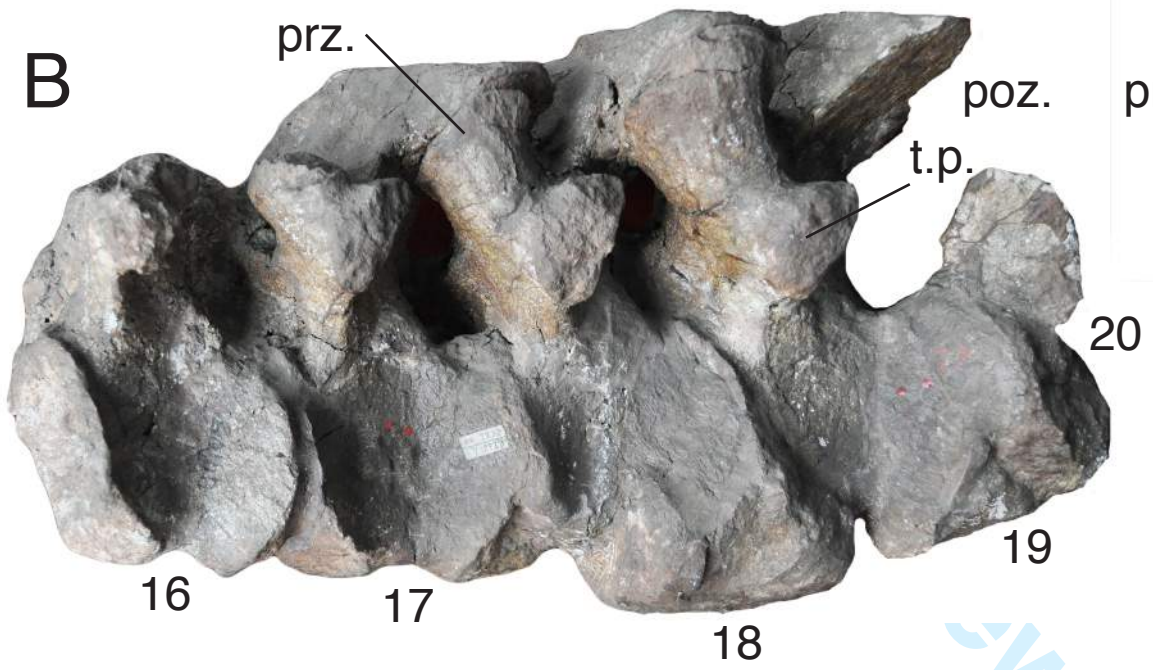
B
prz.
poz.
t.p.
20
19
16
17
18

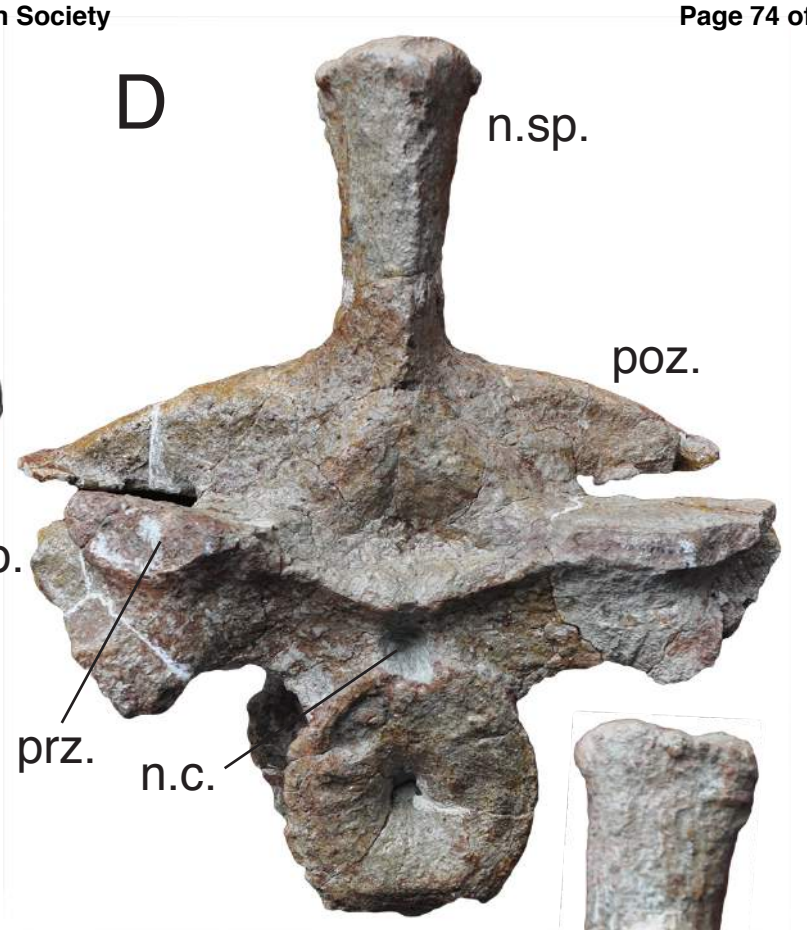
D
n.sp.
poz.
t.p.
prz.
n.c.

20 mm


E
poz.
prz.
r.f.


C
t.p.

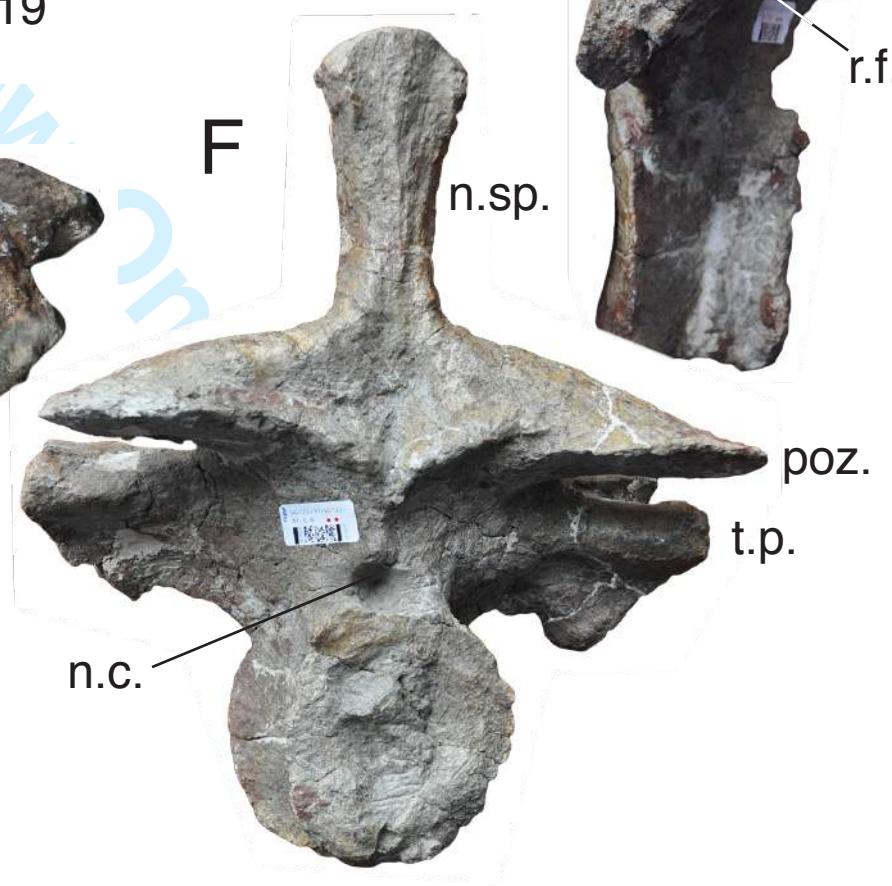
F
n.sp.
poz.
t.p.
n.c.

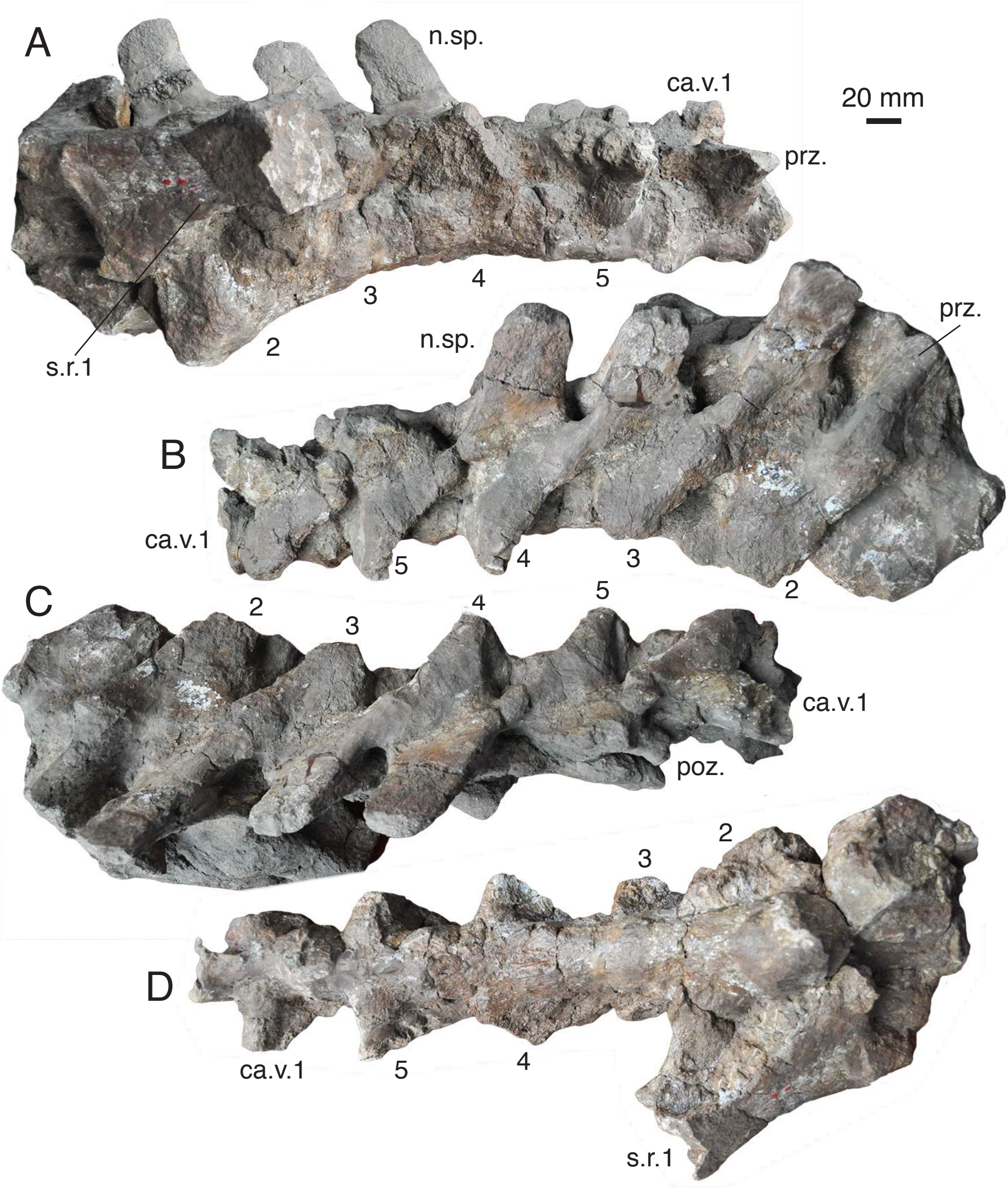
A
n.sp.
ca.v.1
20 mm
prz.
3
4
5
2
s.r.1
B
prz.
n.sp.
ca.v.1
5
4
3
2
C
2
3
4
5
ca.v.1
poz.
D
2
3
ca.v.1
5
4
s.r.1

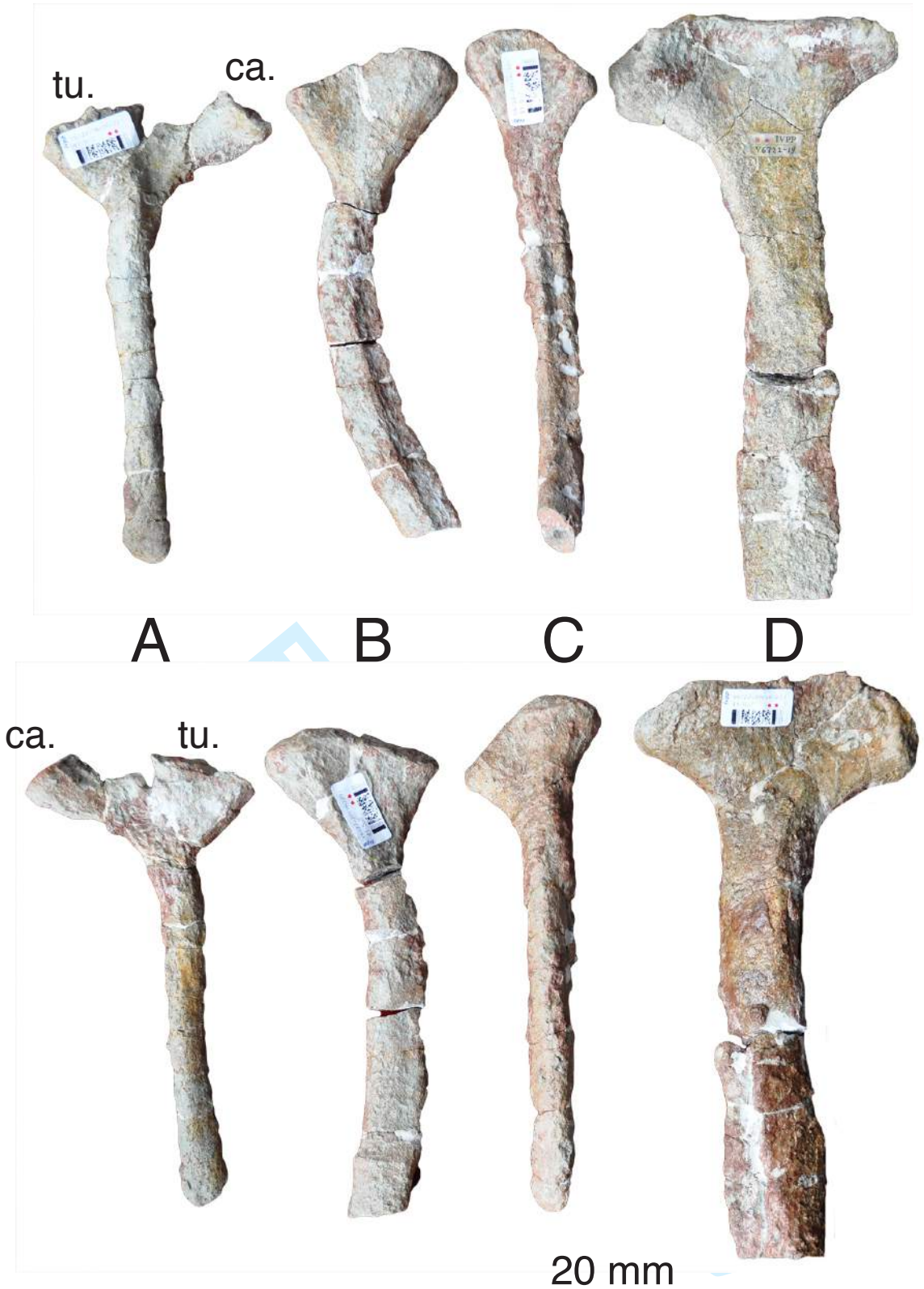
tu.
ca.
A
B
C
D
ca.
tu.
20 mm

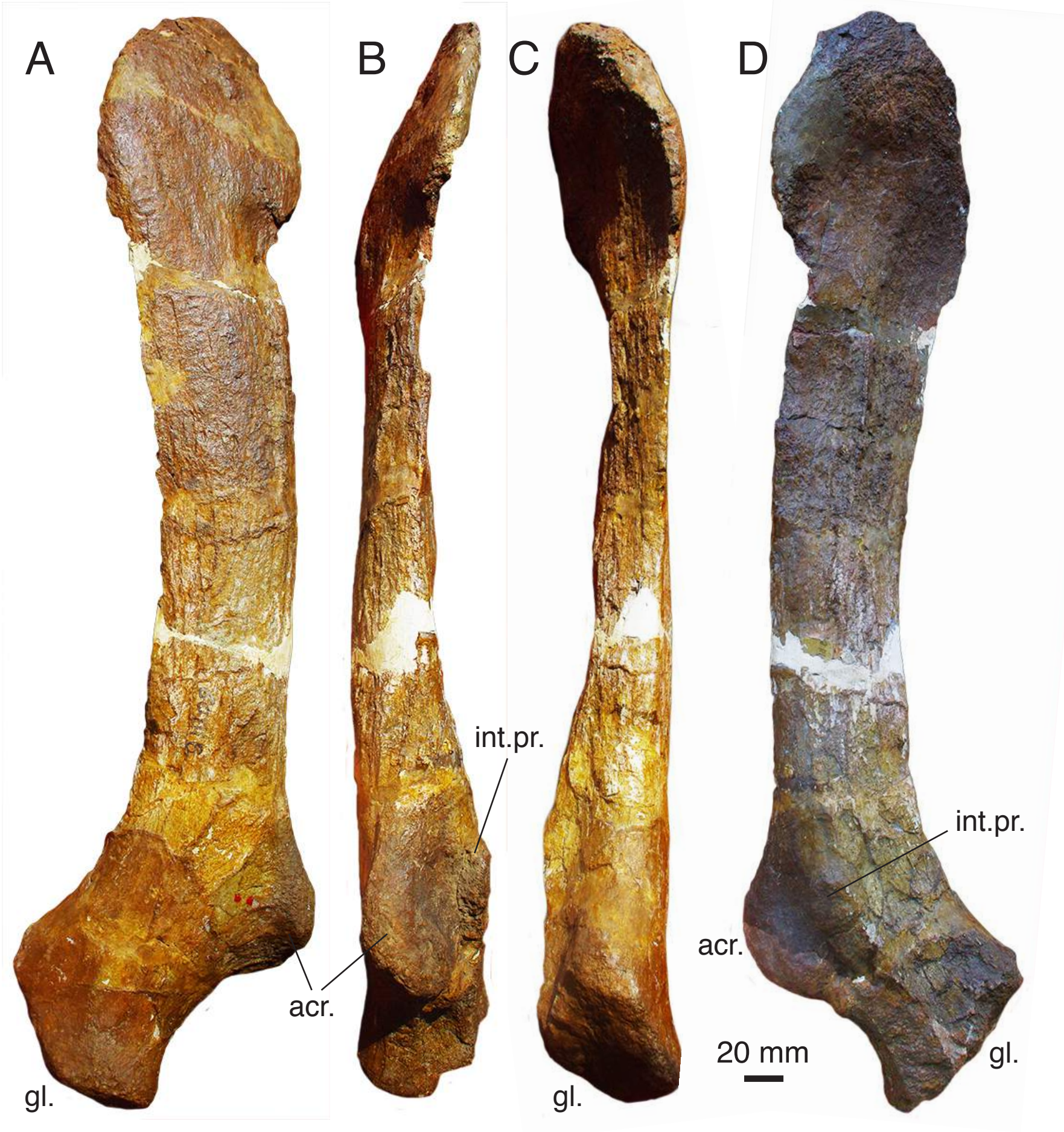
A
B
C
D
int.pr.
acr.
gl.
gl.
int.pr.
acr.
20 mm
gl.

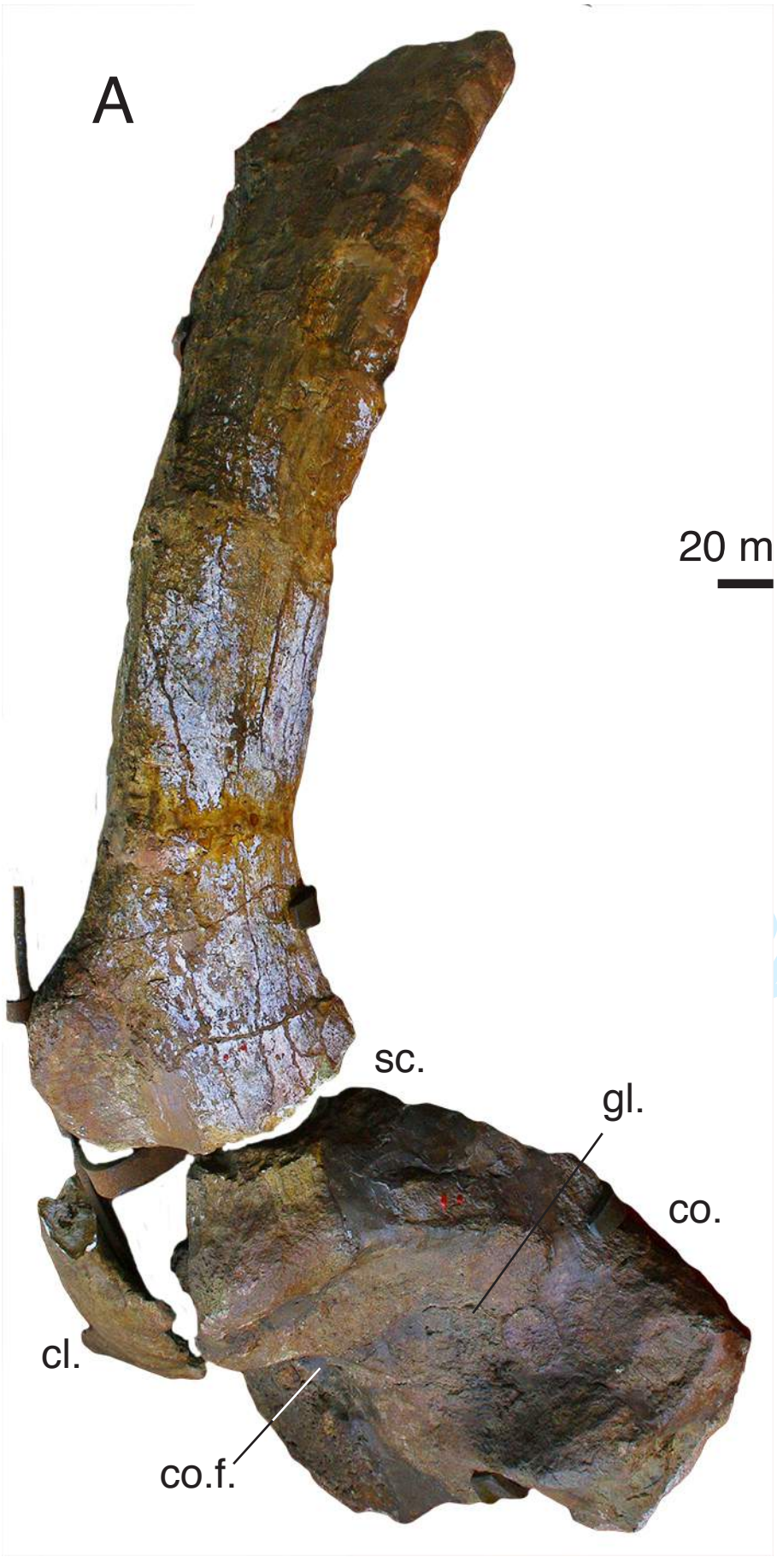

20 mm

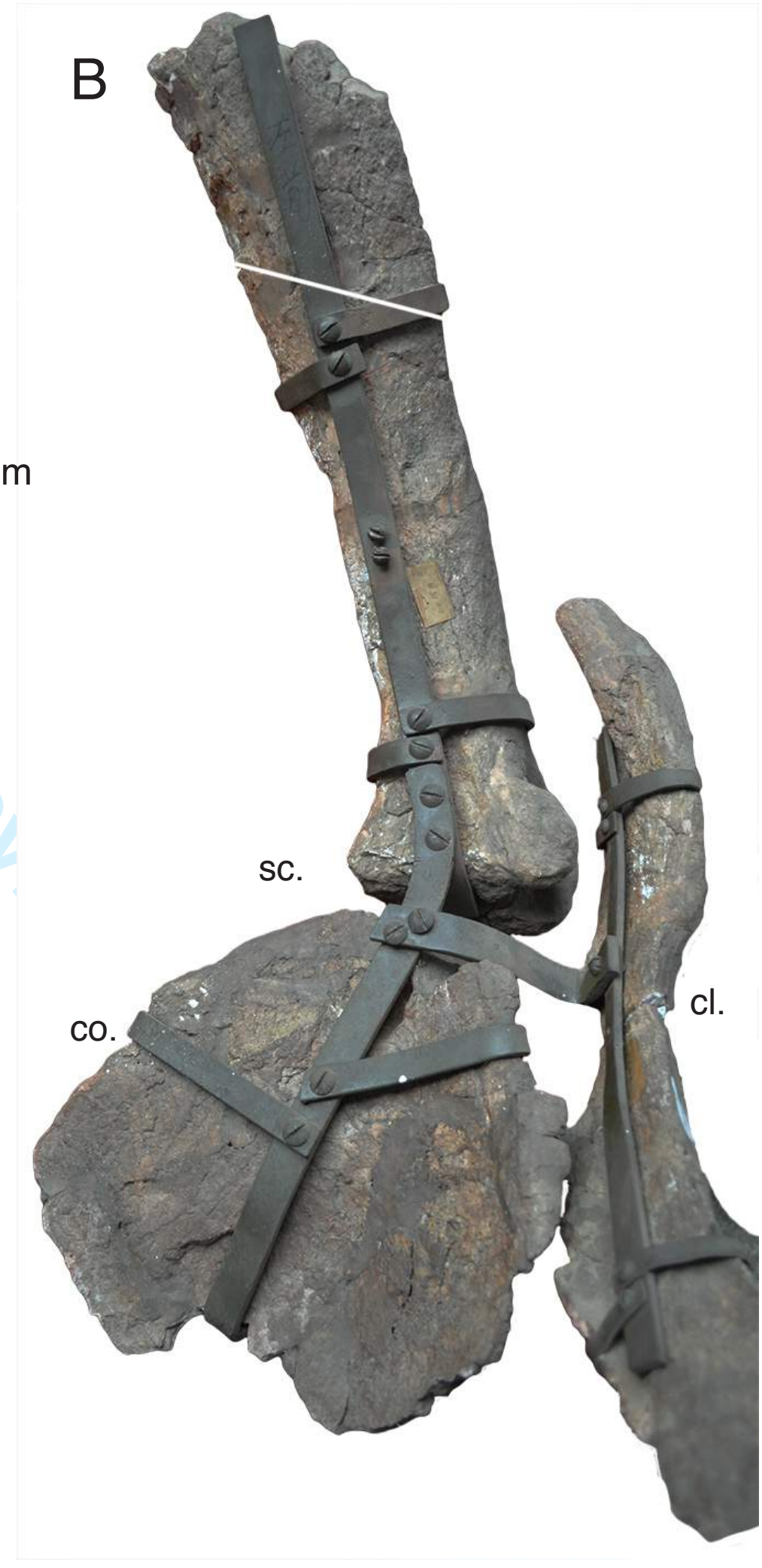

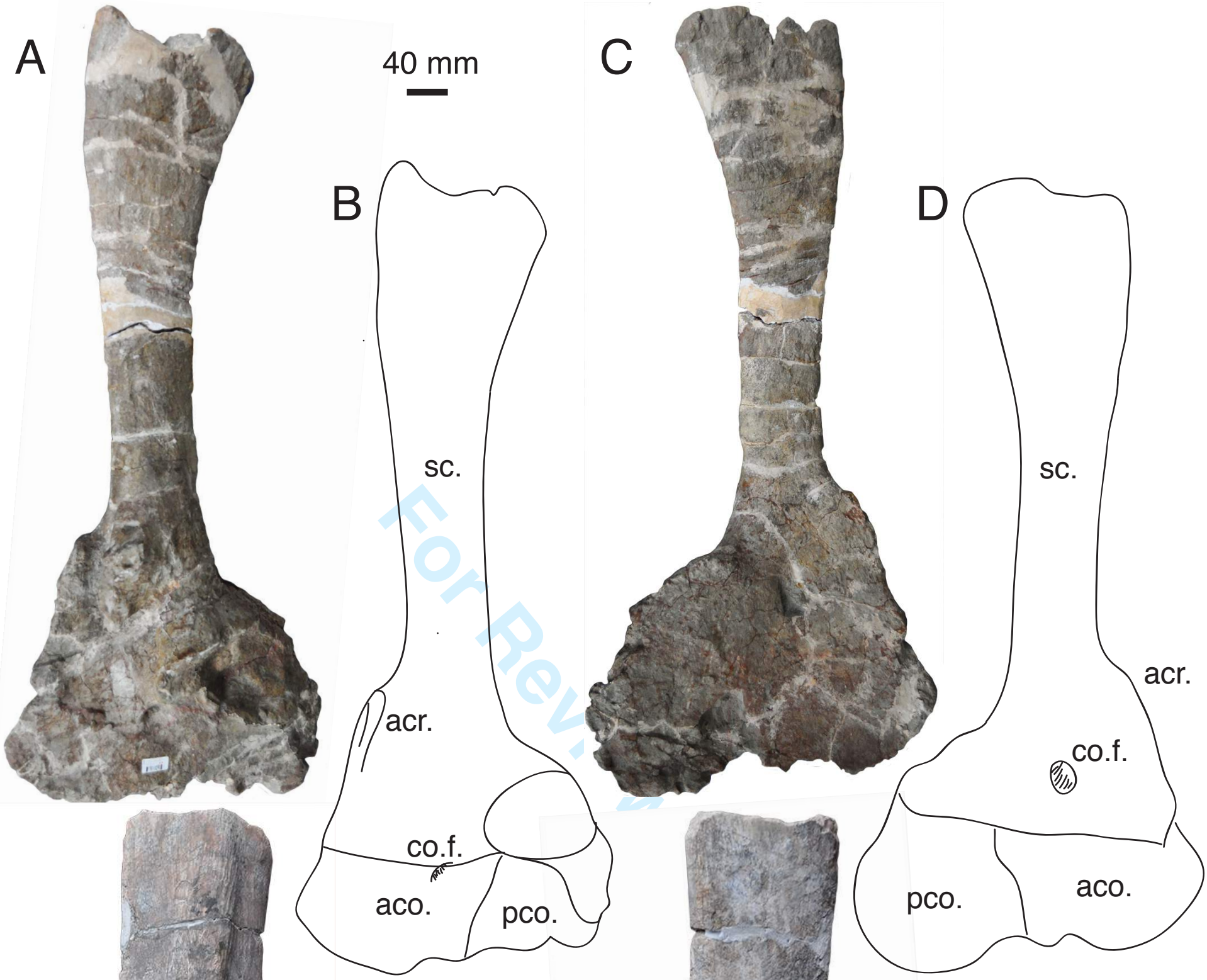
A
40 mm
B
C
D
sc.
acr.
co.f.
aco.
pco.
sc.
acr.
co.f.
pco.
aco.

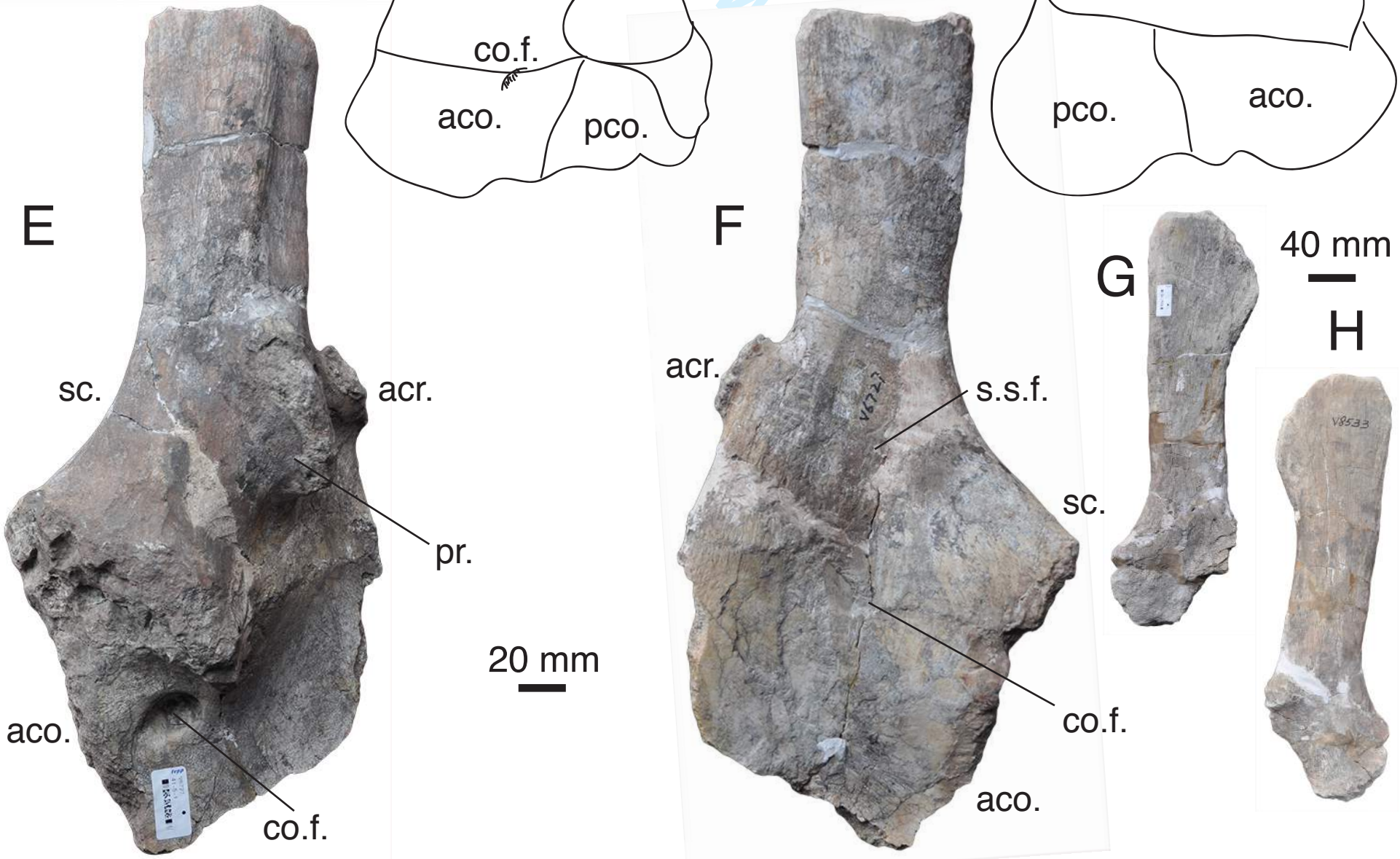
E
sc.
acr.
pr.
aco.
co.f.
20 mm
F
acr.
s.s.f.
sc.
co.f.
aco.
G
40 mm
H

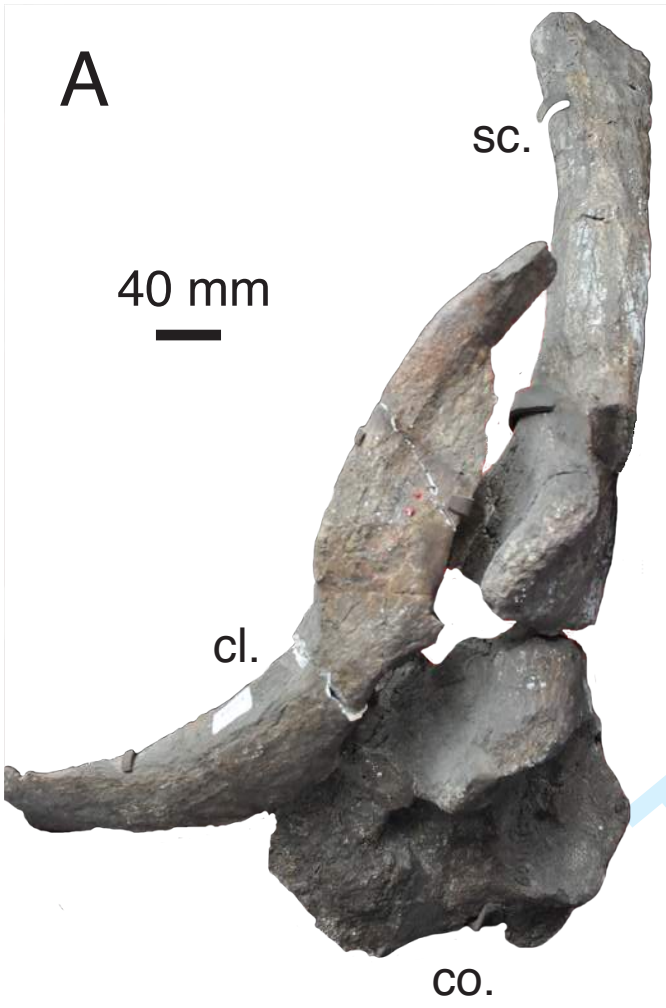
A
sc.
40 mm
cl.
co.


B
R.


C
R.


D
icl.pr.
R.

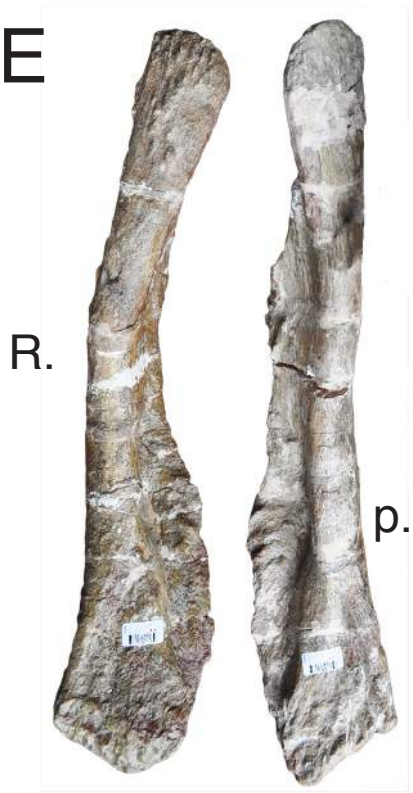
E
R.
p.fl.

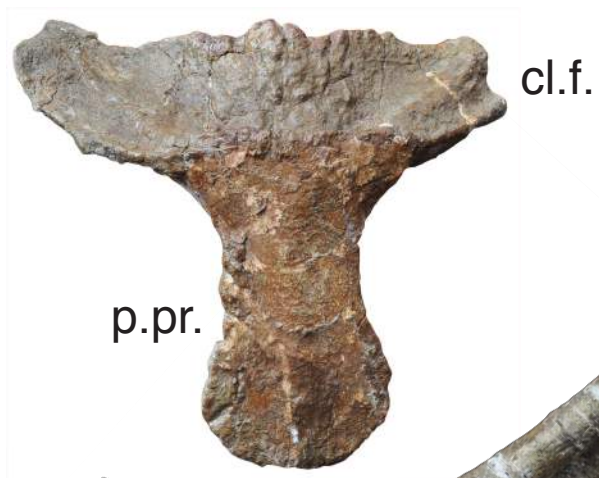
F
cl.f.
p.pr.

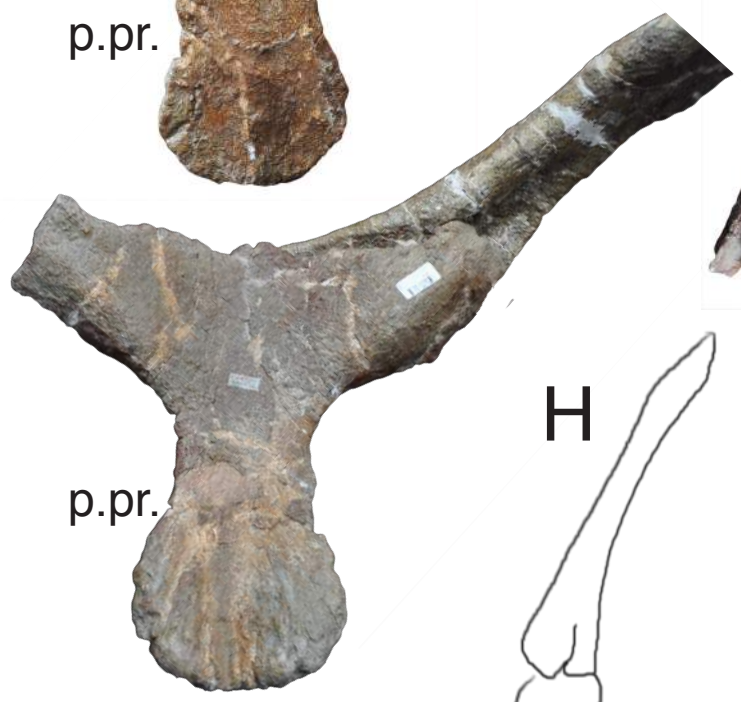
G
p.pr.

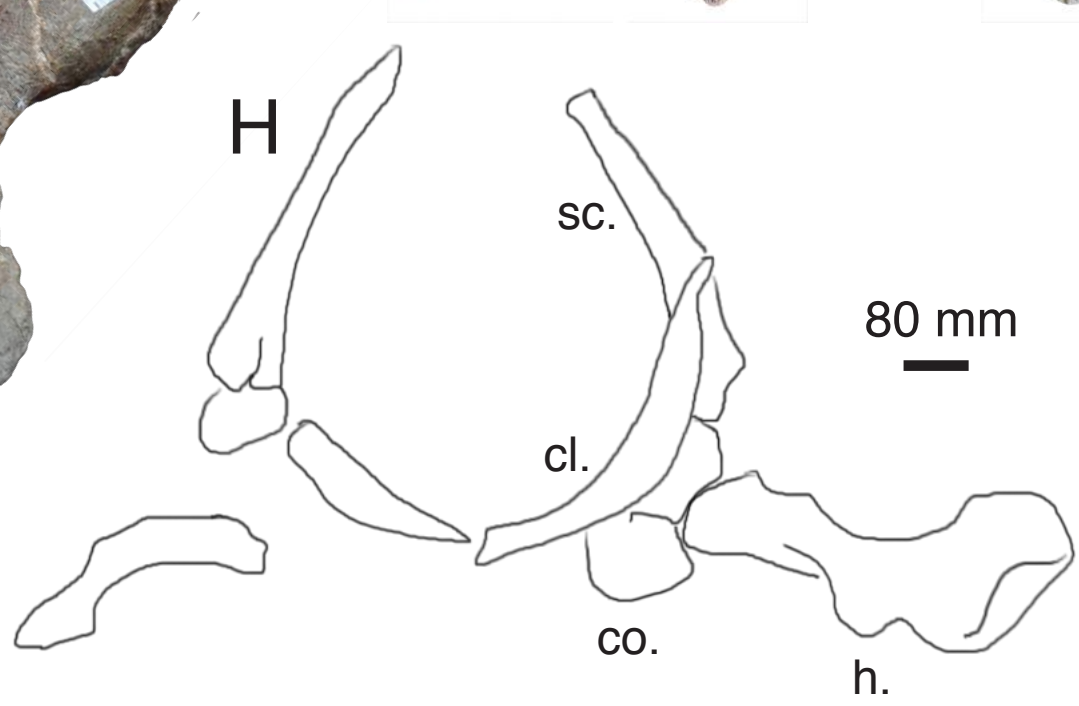
H
sc.
80 mm
cl.
co.
h.

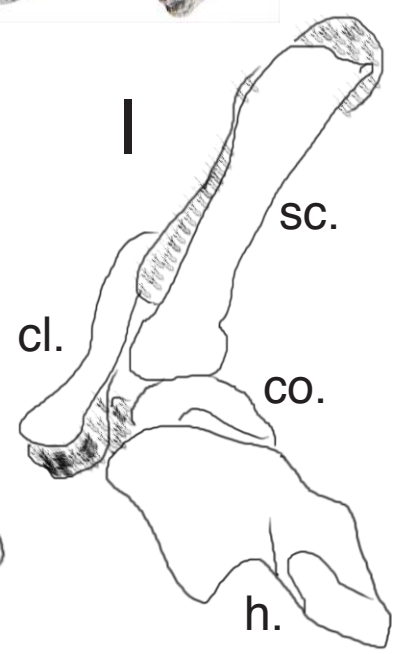
I
sc.
cl.
co.
h.

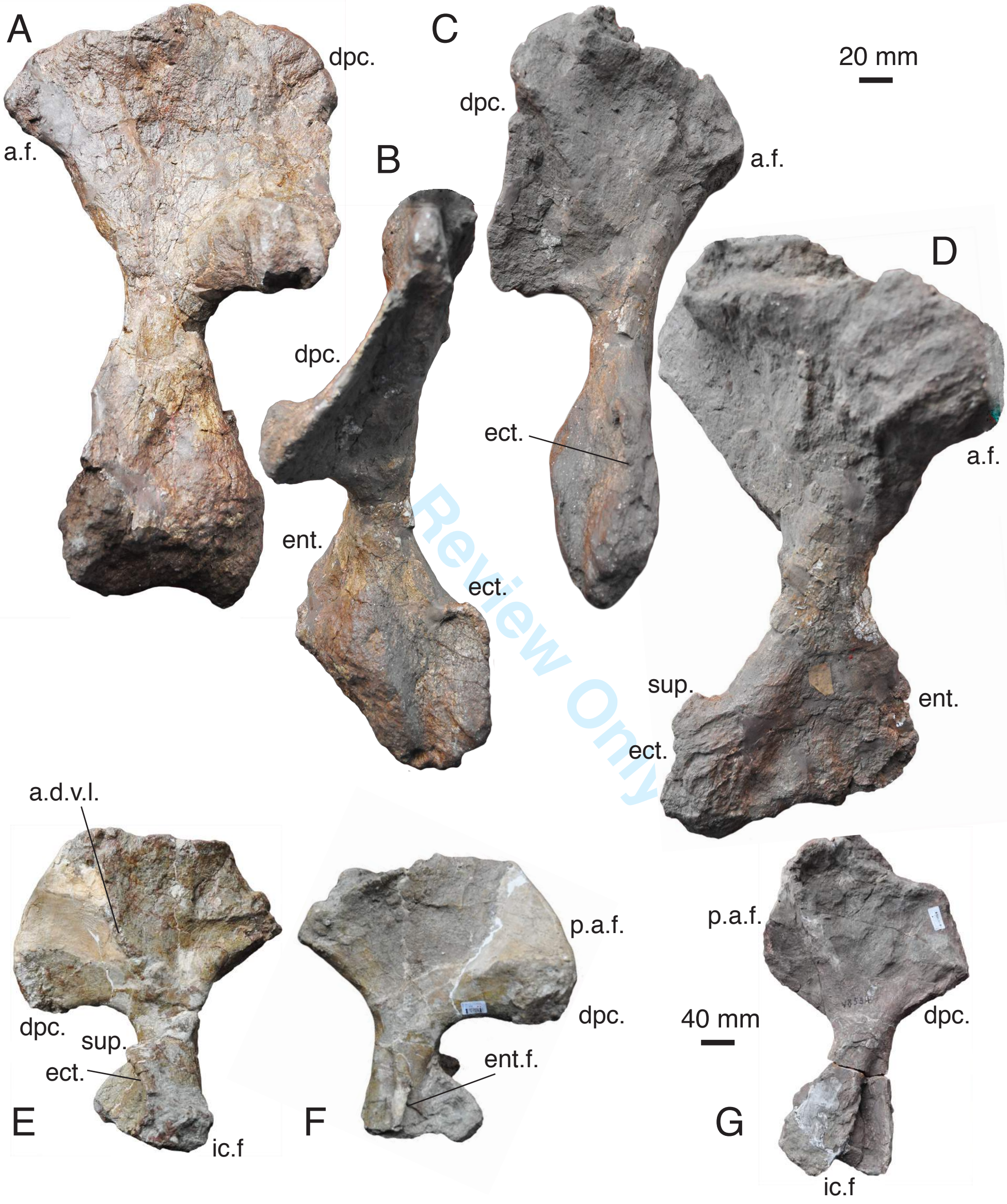

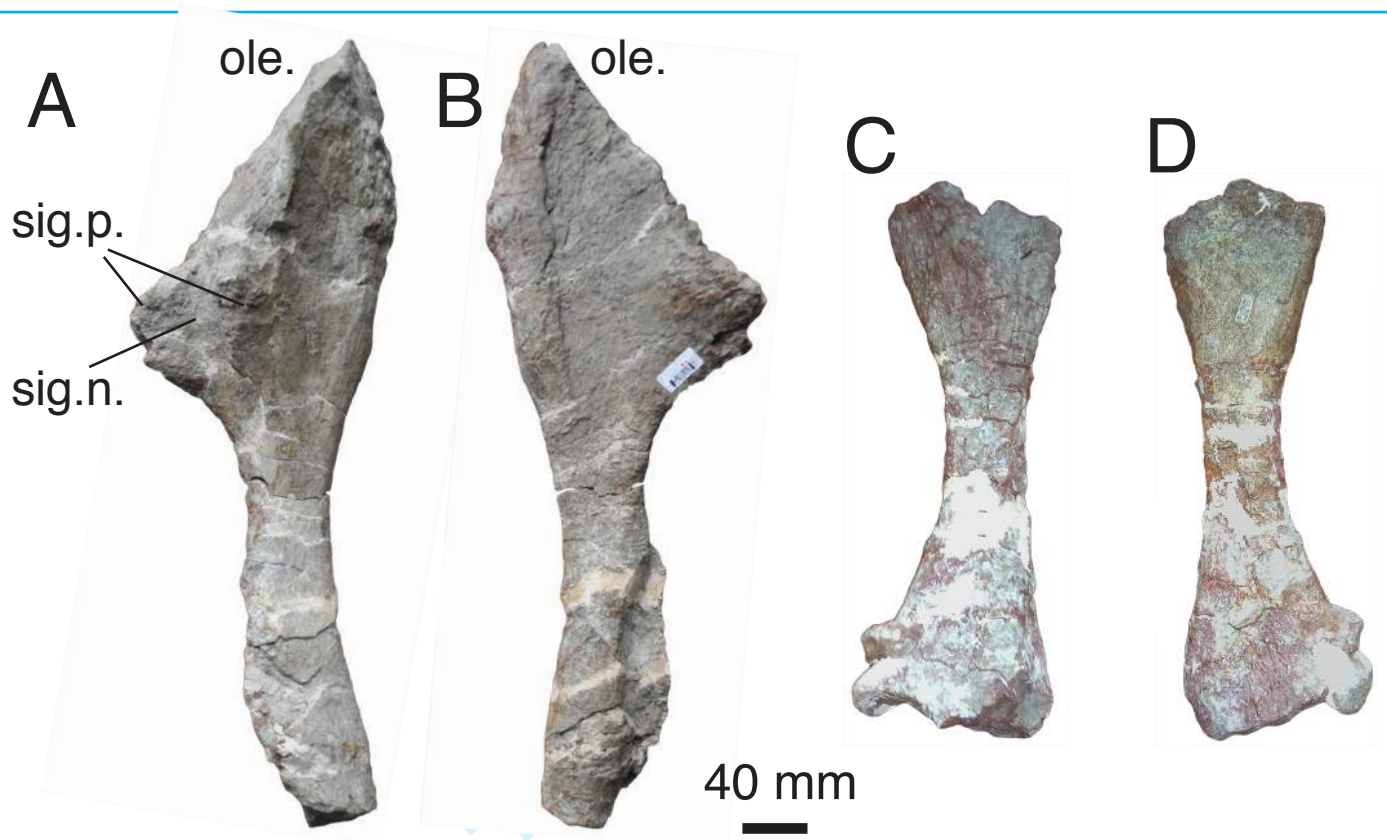

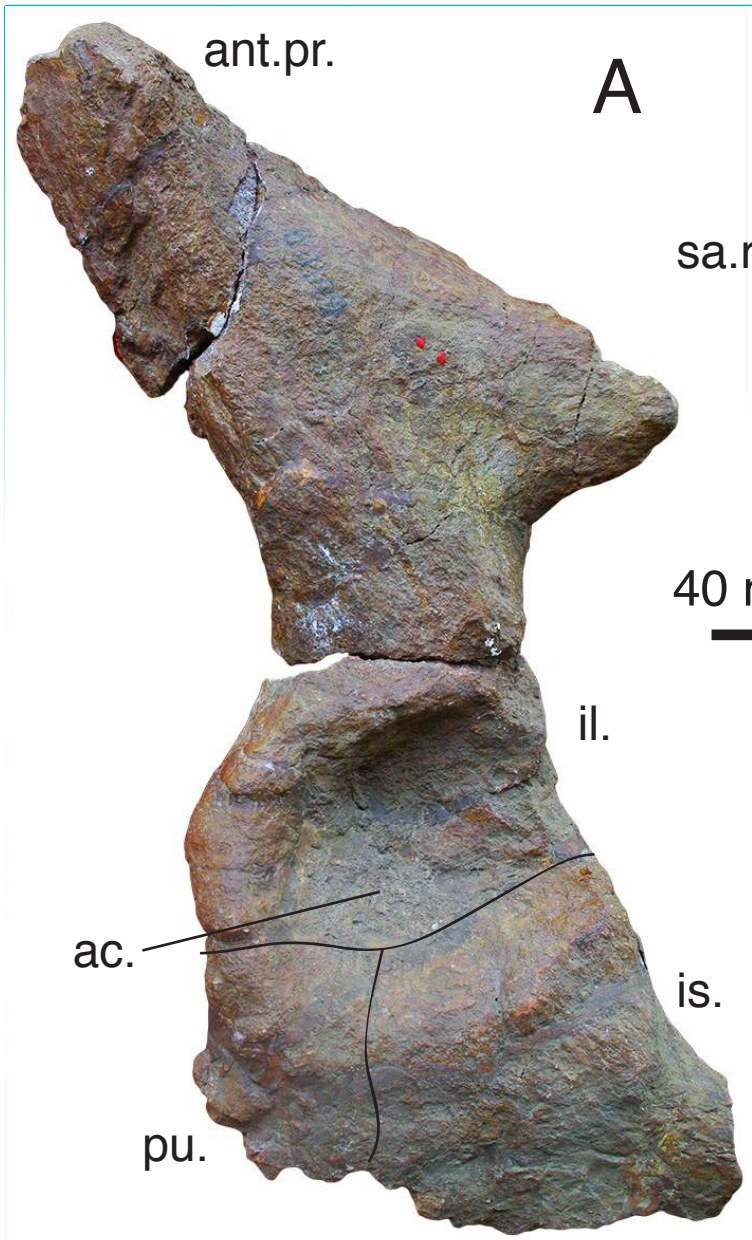
ant.pr.
A
il.
ac.
is.
pu.


ant.pr.
B
cr.sac.
sa.r.4

40 mm

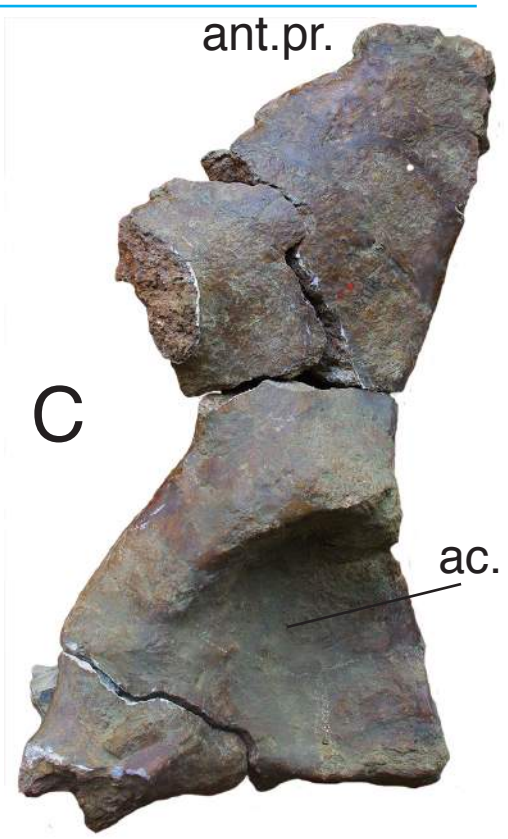
ant.pr.
C
ac.


ant.pr.
D

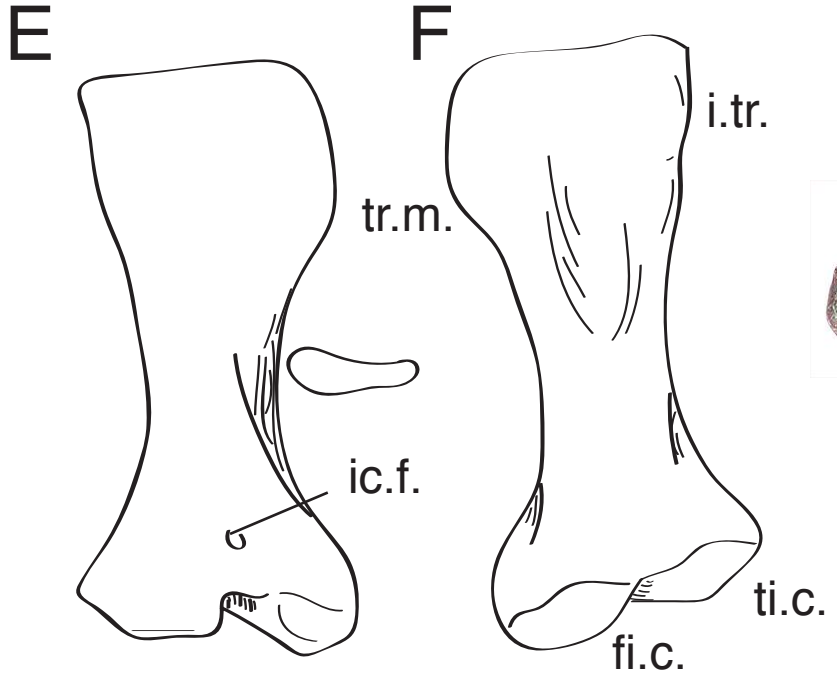
E
F
i.tr.
tr.m.
ic.f.
ti.c.
fi.c.


G
H
I

20 mm


J